

Design and Development of an Auto-Steering System Control for Off-Road Vehicles

Ehsan Kiani

Submitted to the
Institute of Graduate Studies and Research
in partial fulfillment of the requirements for the Degree of

Doctor of Philosophy
in
Mechanical Engineering

Eastern Mediterranean University
September 2012
Gazimağusa, North Cyprus

Approval of the Institute of Graduate Studies and Research

Prof. Dr. Elvan Yılmaz
Director

I certify that this thesis satisfies the requirements as a thesis for the degree of Doctor of Philosophy in Mechanical Engineering.

Assoc. Prof. Dr. Ugur Atikol
Chair, Department of Mechanical Engineering

We certify that we have read this thesis and that in our opinion it is fully adequate in scope and quality as a thesis for the degree of Doctor of Philosophy in Mechanical Engineering.

Asst. Prof. Dr. Mehmet Bodur
Co-Supervisor

Asst. Prof. Dr. Hasan Hacisevki
Supervisor

Examining Committee

1. Prof. Dr. Majid Hashemipour

2. Asst. Prof. Dr. Mehmet Bodur

3. Asst. Prof. Dr. Neriman Özada

4. Asst. Prof. Dr. Selim Solmaz

5. Asst. Prof. Dr. Hasan Hacışevki

ABSTRACT

In this thesis, a control method is developed to enhance the path tracking accuracy of an agricultural vehicle steering system. Therefore, in order to boost the mean error value, the lateral error of a farm tractor at the curvature transitions is minimized by introducing a second look-ahead reference point (LARP) to the conventional lateral deviation controller. Since automation and precision have been significant objectives in the recent studies of land vehicle guidance controllers, a reasonable trade-off has been sought to come up with a steering control system approach with respect to the modern farming operation needs, recent industrial developments, sophistication degree of the approach, reliability, manoeuvrability, accuracy, computational cost, implementation feasibility and sensitivity to variation of system parameters.

Present study develops a simple automatic path tracking system to satisfy the typical requirements of an unmanned agricultural tractor application based on properties of two look-ahead reference points (LARPs) on the desired path. The main objective of the proposed control system is to track the desired path within reasonable tolerances of a typical farming process including considerable slippage.

Since the path shape of the farm field depends strongly on the terrain and surrounding environment such as crop rows pattern, the curvature of the reference path is subject to change. Thus, the employed look-ahead reference points provide compensation for centrifugal forces and reduction of the peak lateral deviation due to curvature transition, using only simple arithmetic operations.

Extensive numerical tests were carried out on the computer simulation of the system dynamics driven by the proposed control method. Simulation results indicate enhancements in vehicle manoeuvrability and reduction of peak lateral displacement error at the curvature transitions to one fifth of single LARP error.

The proposed 2-LARP control strategy performs exactly same as the conventional lateral deviation controller on the linear and circular paths but it outperforms the conventional controller at the curvature transitions where the second LARP behaves independent to the first LARP.

Keywords: look-ahead reference point (LARP) control, path tracking, automatic steering agricultural vehicle, curvature transition.

ÖZ

Bu çalışmada dairesel dönüş yapan tarımsal traktör aracının yanal hatalarının ikinci ileri görüş referans noktasının (LARP) konvansiyonel yatay sapma kontrolörüne ilave edilmesi ile en aza indirilmesi sağlanmıştır. Otomasyon ve hassasiyet son zamanlarda arazi araçları kontrolünde önemini artırdığından direksiyon kontrolünde hatırı sayılır ticari değer artışları gözlemlenmiştir. Modern tarım operasyonları olaya yaklaşım derecesi ve endüstrideki son gelişmeler da dikkate alınarak dayanıklılık, manevra kabiliyeti, doğruluk, bilgisayar fiyatı, uygulanabilirlik fizibilitesi, ve hassasiyet parametrelerinin değişim derecesi bunu daha önemli kılmaktadır.

Bu çalışmada insansız tarım aracından beklenen tipik uygulamaları sağlamak için iki ileri görüş referans noktasını (LARP) özelliklerini kullanarak basit otomatik yol takip sistemi geliştirilmiştir. Önerilen control sisteminin ana konusu, tipik tarımsal prosesler için arzu edilen yolun makul kaymalar ve kabul edilebilir toleranslar dahilinde alınmasıdır.

Bir tarım arazisinin yol şekli kuvvetle tarım arazisinin bölge ve çevresine bağlıdır, örneğin ürün sıra şekline, bu yüzden referans noktasın kavisi her harekette değişime uğramaktadır. Sadece basit aritmetik operasyonlar kullanarak atanmış ileri bakış referans noktalarının merkezkaç kuvvetlerin dengelenmesi ve pik yatay sapmaların azalması kavis geçiş ile sağlanmaktadır.

System dinamikleri simülasyonu üzerine önerilen control metodu ile ilgili olarak çok miktarda bilgisayar destekli numerik çalışma yapılmıştır. Simülasyon neticeleri araç manevra kabiliyetinde artış olduğunu göstermiştir. Testler araç yanal kayma hata miktarının kavis taşınması sırasında tek ileri bakış açısına göre beş kez daha az olduğunu göstermiştir.

Önerilen çift ileri bakış referans noktası (2-LARP) control stratejisi kullanılan konvansiyonel yatay sapmalı kontroler ile düz ve virajlı yollarda tamamen aynı neticeyi vermiştir, fakat konvansiyonel kontroler kavis geçişlerinde daha az başarılıdır, ikinci ileri bakış referans noktası birinci ileri bakış referans noktasına göre daha bağımsız davranmaktadır.

Anahtar Kelimeler: ileriye bakış referans noktası (LARP) kontrolü, yol takibi, otomatik direksiyon tarımsal araç, eğrilik geçiş.

ACKNOWLEDGMENT

First of all I thank God for giving the strength and potential, guidance opportunity to pursue the present study up to a certain level. I should thank my parents for growing the science passion as well as their sacrifice and pushing me whenever disappointed. “Son! No guts no glory” my parents often remind me. Moreover, Uncle Mick for his generous supports.

I should thank many people without whom I could not progress this project; first, my supervisors, Asst. Prof. Dr Mehmet Bodur to his guidelines, technical ideas and scientific helps and also Asst. Prof. Dr. Hasan Hacısevki for his continuous encouragements.

TABLE OF CONTENTS

ABSTRACT	iii
ÖZ.....	v
ACKNOWLEDGMENT.....	vii
LIST OF TABLES.....	xii
LIST OF FIGURES	xiii
LIST OF SYMBOLS	xvii
1. INTRODUCTION	1
1.1 Automation Significance in Modern Off-Road Operations.....	1
1.2 Overview of the Problem and the Proposed Solution.....	3
1.3 Contributions of the Present Study to Science and Industry.....	3
2. LITERATURE REVIEW	5
2.1 Automatic Off-Road Vehicle Guidance	5
2.2 Feasibility Evaluation and Foundation	16
2.3 Numerical Tests and Software Simulation; Aspects and Benefits in Off-Road Operations	18
2.4 Previous Significant Methods of Agricultural Vehicle Path Tracking Control	21
2.5 Drawbacks of the Previously Presented Agricultural Tracking Control Strategies.....	23
2.6 Objective of This Study	25
3. MODELLING APPROACHES.....	28
3.1 Modelling Preliminaries.....	28

3.2	Model of Vehicle Kinematics and Dynamics	30
3.3	Tyre model for vehicle dynamics.....	32
3.4	Modelling of the steering system	40
3.5	Required sensors for simulation test bed	42
3.6	Modelling of the soil disturbance.....	43
3.7	Amplitude determination of Disturbance functions	43
3.8	Determination of disturbance function	44
3.9	Measurement and actuation.....	46
4.	LARP CONTROL METHOD	47
4.1	Look-ahead Reference Point Control	47
4.2	Proposed LARP control structure in application.....	47
4.3	Similarity of the proposed control and local-error feedback	51
4.4	Controller gains relation with the LARP distances	54
4.5	Open loop transfer function on linear paths.....	55
5.1	Modern off-road operation and automation	58
5.2	Simulation Platform and Agricultural Vehicle Parameters	58
5.3	Test Path.....	59
5.4	System Identification for the Dynamic Simulations.....	60
5.5	Optimization Method.....	60
6.	APPLICATIONS, RESULTS AND VALIDATION	69
6.1	Overview	69
6.2	Verification of the dynamic simulation platform.....	70
6.3	Nonlinearity Comparison in Controller Parameters Formulation	73
6.4	Evaluation of Step Responses of the system.....	77

6.5	Steer-Ability Evaluation for a Typical Farm Application	79
6.6	Frequency Response Analysis.....	80
6.7	Steering Angle Outcomes and Steer-Ability.....	82
6.8	Tracking Accuracy performance comparison	83
6.9	Lateral Motion Enhancements	84
6.10	Manoeuvrability Evaluation.....	86
6.11	Seeding, Spraying and Fertiliser-Spreading Efficiency.....	89
6.12	Overall Evaluation of the System Attributes	91
7.	DISCUSSION.....	93
7.1	Overview of 2-LARP Controller Significance Evaluation.....	93
7.2	Discussion of Results.....	94
8.	CONCLUSION AND FUTURE WORKS.....	101
8.1	Concluding Remarks	101
8.2	Future works.....	102
	REFERENCES	104
	APPENDICES.....	104
	Appendix A: Optimization algorithm flowchart	113
	Appendix B: Simulation Program	115
	Appendix C: Program Code of 2-LARP Control law.....	119
	Appendix D: Control Loop Used in Simulations	121
	Appendix E: Dynamics Modelling in Simulation Software	122
	E.1 Simulink Configuration of Two DOF Model Equations	122
	E.2 Modelling of Y-Coordinate Dynamics.....	123
	E.3 Modelling of ψ -Coordinate Dynamics	124

E.4 Modelling of Side Slip Angle (β) 125

E.5 A Model of Actuator Used for Simulation Tests 126

LIST OF TABLES

Table 1: Verification parameters of CLAAS Renault ARES 640.....	71
Table 2: Simulation Parameters of John Deere 8420	71
Table 3: Optimization conditions, optimum parameters, and resulted errors.....	80
Table 4. Overall system characteristics and evaluation.....	92

LIST OF FIGURES

Figure 1. Side view of a typical agricultural vehicle with implement for material spreading dynamics having controller and position-sensor unit	32
Figure 2. Top view of a typical agricultural vehicle showing the symbols related to the vehicle kinematics	36
Figure 3. Bike model of vehicle as three degrees of freedom (3DOF) model with its definition of symbols	37
Figure 4. Definition of symbols on a) The 3-DOF vehicle model, and b) The front tyre.	38
Figure 5. Architecture of the simulation platform for the automatic tracking control system and vehicle dynamics.	41
Figure 6. Block diagram of 2-LARP Control Unit.....	42
Figure 7. Source of a disturbance force while a tyre passes over a slope. Front view of vehicle.	44
Figure 8. Source of a disturbance force while a tyre passes over a slope. Front view of tyre on the soil clod.....	45
Figure 9: Schematic model of the actuator used for this study.....	46
Figure 10. Path tracking specifications.....	48
Figure 11: The relation between K_I and L_I with RMS error values	55
Figure 12: The relation between K_I and L_I with peak error values	55
Figure 13. Top view of the test path to observe the performance of the controller.....	59
Figure 14. The overall algorithm of the optimization.....	61

Figure 15. Step response of lateral error control for minimum $d_{N, RMSE}$ case without using LARP. The amplitude of the applied step is 0.1 m. The peak and opposite peak points are marked by a and b.	62
Figure 16. Root locus plot for the overall system. The circle marks the zero, and the crosses are the poles of the system with the minimum $d_{N, RMSE}$ along a 0.1 m step response.....	62
Figure 17. Root locus plot of the poles caused by the controller parameters found in the third step, non-constrained search for best peak lateral error.	64
Figure 18. Step response of the linear system from the controller parameters found in the third step, non-constrained search for best peak lateral error.	64
Figure 19. Schematic flowchart of the third and forth steps of optimization algorithm .	66
Figure 20. Lateral displacements of the systems with the best parameters for case b (dotted line) and for case (d) along the test path with 7 m circular section from s=10 to s=32. The peak and opposite peak points are marked by a and b.	68
Figure 21. Comparison of the lateral errors.	72
Figure 22. Relation between lateral deviation and orientation deviation gains with peak value of the lateral error.	73
Figure 23. Relation between lateral deviation and orientation deviation gains with RMSE value of the lateral error.....	74
Figure 24. Relation between look ahead point distances, l_1 and l_2 with peak values of the lateral error, while $k_d = k_N = k_l = k_2 = 1$	75
Figure 25. Relation between look ahead point distances, l_1 and l_2 with RMSE values of the lateral error, while $k_d = k_N = k_l = k_2 = 1$	75

Figure 26. Centrifugal force compensation tests on a circular path of $\rho= 7$ m, with $K_I= 0$, $K_d = 0.6$, and $K_0 = 2 - K_2^c$, for four cases of K_2^c , (a) $K_2^c = 0$, (b) $K_2^c = 0.5$, (c) $K_2^c = 0.8$, (d) $K_2^c = 1.0$ 76

Figure 27. Effect of second LARP distance on the peak lateral deviation $d_{N, peak}$; the solid curve is for 8 kmh^{-1} and the dashed curve is for 11 kmh^{-1} forward speeds. 77

Figure 28. Effect of second LARP distance on the mean lateral deviation, $d_{N, RMSE}$; the solid line is for 8 kmh^{-1} , and the dashed line is for 11 kmh^{-1} forward speed. 77

Figure 29. Step response of the disturbance-free system to 2.5 m initial deviation, travelling over soil profiles with different grip conditions. 78

Figure 30. Step response of the closed loop system with $d_N= 1$ m initial lateral deviation for controller settings $K_N^l= 2.0$, ($K_I= K_2= 0$) and (a) $K_d^l= 0.4$, (b) $K_d^l= 0.6$ (c) $K_d^l= 0.8$ 79

Figure 31. Schematic illustration for frequency response of lateral deviation in linear system transfer function..... 81

Figure 32. Schematic illustration for frequency response of orientation deviation in linear system transfer function 81

Figure 33. Root locus plot for lateral deviation gain variation along the linear path with $K_N= 1$ 82

Figure 34. Steering angle δ (solid line), δ_{des} (dashed line), δ_{dis} (dotted line). Dotted lines are obtained with disturbance parameters used in the verification tests..... 83

Figure 35. Lateral deviation d_N (solid line), $d_{N, dis}$ (dotted line) measured at 8 km h^{-1} . Dotted lines are obtained with disturbance parameters used in the verification tests. 84

Figure 36. Tracking accuracy comparison of the Proposed 2-LARP method and results reported by Lenain et al. (2006). 84

Figure 37. Vehicle side slip angle.	85
Figure 38. Front tyre slip angles α_f (solid) without disturbances, and $\alpha_{f,dis}$ (dotted) with disturbances.	86
Figure 39. Lateral deviation, d_N , for velocities 5, 6.5 and 8 km h ⁻¹	87
Figure 40. Lateral deviation error cause by change in second LARP distance having constant velocity of 8 km/h.....	88
Figure 41. Lateral deviation error cause by change in second LARP distance having constant velocity of 11 km/h.....	88
Figure 42. Lateral deviation error cause by change in 2-LARP forward velocity	89
Figure 43. Centrifugal Force versus second LARP distance variation.....	89
Figure 44. Graphical demonstration for estimated agricultural performance comparison.....	91

LIST OF SYMBOLS

α_f, α_r (rad)	Front and rear tyre slip angles	N_G	zero-mean unity-variance Gaussian distributed random number
β (rad)	Vehicle side slip angle	I_Z (kg m)	Vehicle mass moment of inertia
Δs_{po} (m)	Curvilinear distance between $d_{N,peak}$ and opposite $d_{N,peak}$.	K_1, K_2	Controller coefficients for LARP tangent deviation
δ (rad)	Front tyre steer angle	K_d, K_N	Controller coefficient for lateral and tangent angle deviation
ψ (rad)	Vehicle heading angle	l (m)	Wheel-base ($=l_f + l_r$)
ψ_i (rad)	Tangential direction of path point P_i	l_f, l_r (m)	Distances from vehicle centre of mass
ρ (m)	Curved path radius	L_1, L_2 (m)	Distances of look ahead reference points
θ_i (rad)	Angular deviation from vehicle heading	LARP	Look ahead reference point
$a_{F,dis}$	Extent of force disturbance	LQR	Linear Quadratic Regulator
$a_{M,dis}$	Extent of moment disturbance	m_{veh} (kg)	Vehicle mass
CG	Vehicle centre of gravity	M_{dis} (N m)	Disturbance moment
C_f, C_r (N/rad)	Cornering stiffness	P_W	Mid-point of rear wheels
d_N (m)	Lateral deviation error	P_{L1}, P_{L2}	Look ahead reference points
DOF	Degree of freedom	P_N	Nearest point on the reference path to P_W
EH	Electro-hydraulic	R (N)	Rolling resistance
F_C (N)	Centrifugal force	RMSE	Root Mean Squared Error
F_D (N)	Propulsion force	s (m)	Curvilinear abscissa
F_{dis} (N)	Amplitude of disturbance force	v (m s ⁻¹)	Vehicle actual velocity
F_f, F_r (N)	Cornering forces	X, Y (m)	Global reference frame coordinates
F_y (N)	Lateral Force	X_w, Y_w (m)	Coordinates of P_W
h	Vehicle orientation vector	h_{dis} (m)	soil clod height

Chapter 1

INTRODUCTION

1.1 Automation Significance in Modern Off-Road Operations

Modern off-road vehicle operations such as agricultural field tasks require modern techniques and technologies. By the advent of modern technologies into the engineering practice, the advanced methods are implementable to enhance the efficiency of the field operation. Moreover, the efficiency of each farming task has been broken down into more precise divisions containing more details.

Modern agriculture requires advanced autonomous methods to augment productivity both quantitatively and qualitatively. To accomplish the farming tasks on a field with high efficiency many technologies must be incorporated. In addition, for the sake of energy and environment saving even a few percentages enhancement in efficiency can result in remarkable financial benefits.

Careful usage of new technologies in sensors, actuators and processors boosts efficiency and reliability by integration of the scientific developments into agricultural applications.

The automatic control of ground vehicle steering system typically requires integration of five different technologies as path planning, medium recognition, sensing and actuation intercourse, path tracking and obstacle avoidance. In the present study, a problem is

addressed to be solved as follows. A given predefined path is assumed to be accurately followed subject to an unpaved terrain conditions. Admittedly, the materials developed within the present study will be used for further advancements in controller and modelling to boost the provided performance according to the research and industry realms tendencies. Therefore, the core of this dissertation is focused on the proposed controller and evaluation of its performance. In addition each part of the project concept is broken down into simple description in order to pave the way of future advancements and further utilizations for any interested reader.

Indeed, a farm vehicle must operate even more accurately than a mars rover because if a mars rover path following tasks results in 20 cm error, it might not be considered as a failure while the same error of a farm vehicle tire might damage the whole crop row, that is an absolute failure. In addition, using technologies such as sensors in the agriculture vehicle has more advantages compared with passenger car. First, an agricultural vehicle is usually very heavy and hence additional weight of a sensor setup can be considered negligible. Secondly, an agricultural vehicle is often a large machine compared to a typical passenger car and can provide power for external implements. Therefore, implementation of sensor or processing setup, does not affect the overall system. Thirdly, the price of an agricultural vehicle is typically higher than that of a passenger car, in as much as, implementation of technologies will not increase its overall price remarkably.

1.2 Overview of the Problem and the Proposed Solution

Since the field for off-road operation varies according to the local climate and soil condition, etc., the shape of the off-road pattern can be irregular. Therefore, the geometric curve which represents the path to be followed may change several times during the operation. This study proposes a simple method to reduce the lateral deviation error at the aforementioned curvature transitions to boost the tracking accuracy.

1.3 Contributions of the Present Study to Science and Industry

- A novel control method is developed for automatic guidance of a typical agricultural vehicle. The proposed 2-LARP control was extended from the idea of look ahead guidance of mobile robots to satisfy the typical requirements of an off-road vehicle such as an agricultural tractor.
- The introduced control law for 2-LARP strategy employs simple arithmetic operations.
- Peak lateral error at curvature transitions is reduced by five times as compared to the results reported in the literature by a lateral deviation controller (Derrick and Bevely, 2008).
- The presented system serves the purpose of precision needed in agricultural harvesting as well as for farm automation which have been hot topics in the last three decades.
- Performance is enhanced to millimetres tracking accuracy so that the system outperforms a human driver to facilitate both farm automation and precision.

- A software code has been generated (Appendix B) simulating real applications such as tracking a given desired path through a control method integrated into the steering dynamics and kinematics of an agricultural vehicle.
- Extensive numerical simulations were carried out to evaluate the system performance. The evaluation results of the overall system indicates stability and manoeuvrability enhancements.
- The introduced second LARP reduces the peak lateral error at curvature transitions to one fifth of to 1-LARP and thus it indicates the independent effect of each LARP on lateral and consequently nonexistence of an equilibrium point.
- The computational cost of the second LARP injection in the conventional lateral control law is sufficiently low. Indeed, computational times of 1-LARP and 2-LARP systems are almost the same.
- The proposed method performs the agricultural application such as spreading insecticides more satisfactory than the ones previously presented in the literature. It is mostly because of the error reduction at curvature transitions and simplicity of the control structure in response to the precision and agility advantages of the recent actuation and measurement technology.
- The presented system can be used for dead reckoning of an automatically steered land vehicle with low forward velocities with high capability of oscillation rejection. Hence, the developed method facilitates the automation and precision in off-road operations.

Chapter 2

LITERATURE REVIEW

2.1 Automatic Off-Road Vehicle Guidance

The trend towards using accurate and safe methods for agricultural automatic guidance systems has led to numerous researches since the 1920s. Indeed, a proper Automatic Guidance Control approach optimizes the use of water, land, fertilizer and seed (Aghkhani and Abbaspour Fard 2009).

Agricultural tasks in the field are often accomplished while travelling along a path. Therefore, path tracking for agricultural purpose is often carried out as a tedious work for labour since the driver must repeatedly do the same task. Moreover, spreading fertilizer and poison in the field is hazardous for the farmer. Besides, cost of labour is getting more expensive so the use of automatic systems may be preferable. Hence, efforts have been dedicated to improve the performance of unmanned vehicles in path tracking tasks and various automatic methods and system descriptions have been presented thus far. In recent two decades, research efforts in the agricultural vehicle automation field were enriched by Owen since 1982. The dynamics of a tractor for the handling purpose was extensively studied and used in the later research in this area. The foundation was sufficiently to define a handling analysis framework of a mobile robot moving on an unpaved surface with non-severe manoeuvre. Although the focus of the aforementioned research was on the motion analysis of the farm vehicle, rather than the

controller or guidance method evaluation, yet, the formulations have been used several times thus far and it has been benefitted the research on the farm machinery motion analysis. One may notice that, in the control of an agricultural vehicle the interests of farmers must be accounted and hence in the following, their main desirable aspects of agricultural vehicle controller will be enlisted as studied by Reid et al. (2000) and Li et al. (2009);

1- The agricultural environment is a biosystem with considerable degree of sensitivity to changes. The tasks with minimal damaging to the environment are seriously recommended. In other words, an agricultural background consists of parts such as soft and moist material over the ground surface, crop rows, hill-hole profiles and large sands or clods as well as soft tyre contact patches. In addition, the tyre air pressure is adjusted in such a way that it can pass smoothly over the surface irregularities. Indeed, it is strictly forbidden to have tyres sinkage into the soil or overlap with crops lanes.

2- Rather than the speed of operatio, the quality of work is on priority. The products of farming often will be eaten by people directly or indirectly after some food processing so that the farm products must be carefully seeded, harvested and treated. Indeed, high speed working on farm has no room of consideration whereas it is risky to harm the machine or the surrounding. The restrictions on farming are:

a. The high chassis of tractor that is prone to turn over by some sharp turns which are not unsafe for passenger cars.

b. Beating the fruits, seeds or other usable parts of plants by the implement beyond the range of safety is likely undesired because it changes the product quality. Therefore, the speed of operation should be well set to have minimum unwanted damages.

c. Soil texture particles are the essential elements to form the plants bed. Fast travel on the soil by a heavy vehicle and dealing with by an implement is counterproductive.

d. Indeed, since in the automation of agricultural operation, the performance is evaluated according to the quality of the operation, poor outcomes will easily hardly damage the entire performance and even may fail it. The precision in agriculture is one the concepts that is recently received heavy attention by several authors, research institutes and farm machinery manufacturers, to provide the brief goals of precision farming in the industry, techniques and tools (Li et al. 2009).

3- Spreading of materials such as fertilizer as well as spraying insecticide liquids in a hasty fashion causes overlaps over uncovered surfaces on the farm field and it seriously reduces the efficiency. Whereas these years the environment saving carries high weight especially for the annual approval of the machinery company, time, price and efforts that has been dedicated to the precision and automatic farming is justifiable. Several authors and institutions have been joint and collaborated to put these concepts and techniques some steps forward (Bevly and Cobb 2010, Lenain 2007, Zhang 2004, Rovira Mas et al. 2010, Hellstrom and Ringdahl 2006, and Eaton et al. 2008).

Apart from what a farm vehicle driver aims while working on the field, the farmer prefers not to face the matters and situations in which the followings may exist:

1- Spreading herbicide and fertiliser, generates an unhealthy atmosphere around the distributor for at least some minutes so that human working beside those are harmful (O'Conner 1997). Moreover, agricultural vehicle works over a surface full of irregularities. Farm tractor can easily turn over and this is often due to wrong prediction of the driver for future state of tractor motion. Statistically speaking, several reports were broadcasted regarding death of driver specially in the busy, hot, cold or frustrating situations.

2- Driver supposed to carry out the agricultural job for a certain amount of time consists of divisions which are very similar to each other. This phenomenon is so called "driver fatigue" is very common particularly in large field in the agricultural friendly lands of states in North America and Australia. Getting tired is the first step towards loss of accuracy as well as danger to crop products, fatal turn over which remarkably damages the machine, operator and surrounding (Rovira Mas et al. 2010).

3- The cost of the recruitment of labour is getting higher. In other words, employment of human elements has its own concerns that it not desirable such as salary, insurance and some official job which are tedious and costly procedures [Rovira 2010]. In addition, rollover of a tractor has caused the driver's death. Hence, development of technologies and techniques to plan, design and manufacturing towards safe, reliable, cost-effective and accurate or in general an efficient configuration can substitute the

traditional way of human operation especially for the operations which are recursive or repetitive. On the other hand, expertise and moral of human driver may affect the operation efficiency on the field where the reprocess of the farming is not feasible most likely.

4- Advancement of technologies needs corresponding compatible and robust efficient approaches particularly land vehicle guidance controllers to cooperate well with the computerized facilities. The life is getting computerized these days more and more and gradually it is handling even personal matters and farming is not an exception. Therefore, authors have been through new and more accurate strategies which are implementable since the required facilities are on the way with quite close to what is needed to have the maximum possible efficiency. Actually, in large fields with financially sufficient infrastructure, human operators are reduced unless for the supervisory of the operation and also keeping the margins of safety within an agricultural task (Lenain et al. 2007, and Zhang and Qiu 2004).

5- Last but not least, the degree of preciseness of a computerized machine is far better than human operator, if the enough underlying tools and data are provided. On the other hand, machine does not get frustrated and exhausted and thus the field job can be pursued in the conditions which might not be desired most probably e.g. dusty, foggy or herbicide spread area (Bevly 2001). Therefore, automatic methods are so much beneficial even though still farmers who have been used to conventional farming especially on the small lands. Consequently, the cost of auto-farming must be dealt besides the reliability and precision concerns.

6- Advent of newly developed integrated methods such as real time kinematic global positioning system (RTK-GPS) and carrier phase differential global positioning system (CD-GPS) which provide centimetre accuracy as well as actuator advancements to carry out the controller actions over the machine and terrain (Fang et al. 2011).

The research on the agricultural robotics is kind of multidisciplinary channelling task whereas it deals with biosystems via a dynamic behaviour and mechanical aspects. Therefore, spectrum of research are widely varied from agricultural studies to electrical analysis. In the following it is tried to cover the major works which have been provide the foundation for the further studies on the agricultural robotics with concentration on the tracking control of the vehicle utilizing computerized methods.

This underlying structure that was built by O'Conner in Stanford University and were further developed through three other PhD projects. O'Connor research focused on the feasibility of CDGPS implementation on land vehicle for the purpose of a precise guidance on a perfect land (O'Conner 1997). For a centimetre level accuracy the overall experimental system performance was satisfactory inasmuch as to be adopted for real-time application. This work was almost the first extensive study towards the practical analysis of technology integration for the purpose of auto-farming as well as evaluation and estimation for feasibility of controller, sensor and actuator utilization in the land vehicle guidance in which precision and efficiency were addressed. On this basis, Bell commenced a study over auto-farming concept towards high-precision. Indeed, precision criterion has been altered within last decade whereas measurement devices were developed and communication technology has been advanced to provide higher

precision and less inaccuracy. The sensor characteristics and noise plays very significant role in the navigation and in turn, affect the controller performance because decision making in presence of lag and disturbance is close to the unstable and poor response margins (Lenain, et al. 2007 and Bell, 2000). Bell, (2000) proved that an automatic system facilitated by electronic processor and data collector can work more precise than an expert human driver on straight line route. The system identification used of this study was the main platform for future modelling of non-severe manoeuvre of farm tractor. For GPS sensor outage and control of the yaw motion of a tractor with a towed implement for slightly higher velocities and larger bandwidth, an approach was presented through dead reckoning of automatically steered farm vehicle. The fundamentals presented in this study paved the way for further research for real system parameter variation and estimation techniques (Bevly, 2001). The system identification of the aforementioned system and the obtained preliminary modelling restrictions paved the way for the future studies on the automatic farm tractor path tracking in presence and absence of both high irregularities and towed implements. The extensive modelling studies and analysis in this research has been used thus far for online estimation and predictive control action for automatic trajectory and path following. Also the concepts of lateral local error feedback were detailed. Indeed, for online or offline satisfactory path tracking performance, efforts must be dedicated to virtually execute the control action on the simulation test bed up to the end of the route to observe the performance along the entire path. On the other hand, in the Bevly's research the effect of yaw motion and yaw rate were highlighted and formulated to some extent. Although as it is mentioned before, the problem statements has been altered since the difficulties of the modern technology implementation has been resolved over last few years. Specifically

speaking, thanks to the advancement via research endeavours deficiencies such as actuator preciseness and control GPS uncertainties, high lag, outage and noise has been treated (Rovira Mas, et al. 2008, and Fang, et al. 2011). Gartley, (2005) established a cascaded system to have online estimation by determining an adaptation gain. Single input single output (SISO) control configuration presented in this study attempted to well define the relations between different parameters of the tracking system, however the focus was on the yaw stabilizing the system especially in the presence of hitch loading and unknown disturbances. The frequency domain representation clearly shows some margins for the stability and verifies the correlations among system major input and output variables such as transfer functions of steer angle actuation and desired steer angle requested by controller, lateral local error and yaw rate as well as lateral velocities. The prediction calculations were pursued along the straight lines and still there were room for curved path tracking control problem. Derrick (2008), followed the previously mentioned study to get more precise and detailed results and continued the adaptation gain evaluation of a towed implement effect on the modelling and found deterministic ratios on the almost the same cascaded system configuration. One significant aspect of his work is that the actuator effect the system is precisely modelled by accurate closed loop system and indeed it shows how the system performance is restricted in the simulations. In other words, the actuator saturation can damage the optimum pre-set controller design by avoiding the simulation to reach a certain and negligible error whether as lateral or heading deviation (Derrick and Bevly, 2008). Step responses presented by implement applied and implement free vehicle systems on the actual agricultural field showed a more than conventional second order system response with

satisfactory error convergence and minimal steady state error along the straight line tracking.

Another avenue of research which is still under development is commenced in the Lasmea University by a team of research with an integration of expertise in agriculture, mechatronics and electronics disciplines. The idea of the current research was inspired by the aforementioned study from kinematic and path planning point of view since it is progressing over a strong kinematic modelling and verification foundation (Lenain et al., 2005). The sliding parameters which are the essential element for vehicle motion is extensively studied and the stream of the above research can be straightforwardly observed via the materials they have published. Indeed, to come up with the idea of accurate control of a mobile robot system, they focused on the sliding phenomenon which was dealt since the linear and nonlinear regions cause remarkable discrepancies especially for an off-road vehicle that is moving over an unpaved terrain since an agricultural vehicle does not travel by severe manoeuvre since it must move in a careful fashion not to harm the surroundings. The flow of research in the latest years is focused on the feasibility of high precision tracking control of an agricultural vehicle while it move over the special conditions such as a path with curvature transition as well as a terrain having constant slope. In addition, it has been tried to construct a model predictive control that is to provide the future states of the vehicle having motion over a predefined path. Moreover, the automation was kept as a priority to prove that the effort has practical application and financial benefits for farmers and manufacturers. As a matter of fact, prediction is a key feature of simulation and, in order to create a good model for control prediction concerns, parameter identification is required. Thus, many

studies thanks are carried out by authors and research institutes and manufacturer. The mentioned French team have been developing their studies beyond the conventional ranges of vehicle linearity and gradually attempted to find the a simple method to bring the traditional modelling in validity with the semi-steady cornering of an agricultural vehicle manoeuvre simply via the correction factors respectively on the corresponding circumstances such as path shapes or terrain change divisions. Furthermore, since the agricultural task on the field is a repetitive kind of task on the straight lines followed typically by a circular curve path to turn the back to the field at the field margins so that the U-turn definition presented in the aforementioned research as one the main research challenge for evaluation of the control response quality, stability and error zero-convergence. In the present study it was observed that tracking along a path with curvature transition introduces large peak deviation errors that in some special cases it might result in the system performance failure by divergence if the straight line controller design is applied. For resolving of the problem one may suggest to have variable control parameter that is possible for an intelligent system. The point is in the agricultural robotics the simple design is preferred since complex systems may require large computer capacities such as memory or high power processor (Rovira Mas et al. 2010). Polar kinematics used in mentioned French team's works is beneficial and precise though the system complexity is high to some extent. Besides, the controller may require strong embedded processor and in many farm lands it is not reasonable since the facilities for some farmers are poor and limited such as having computer administrator to fix the processor in the case of hot working shut down due to high load computational tasks. In general, that research jobs presents a good understanding of orientation and lateral error along path with a shape changes that is typical for an agricultural

application on the farm field with sufficient simulation and actual field experimental tests that verify the validity of their virtual modelling. Although the disturbances on the field might be troublesome while an accurate model of the system is sought, recently it is tried to have the field well ploughed in such a way that travel of the vehicle tyres besides the furrow traces is a sort of moving over a semi-smooth surface (Behrouzi Lar, 2006). There are some other significant research efforts towards the farm tractor automatic and precise path or trajectory tracking. In brief, Zhang and Qiu (2004) tried to not only model the system but also come with the new idea of the controlling the system by simple and practical method by using middle points of the pre-defined path that is discretely dictated by the remote sensor such as GPS. Another independent research is dedicated to the actuator behaviour analysis that is one the main characters to modify the agricultural behaviour.

Within the aforementioned studies the tracking performance has been improved and some more characteristics and aspects of vehicle modelling and guidance have been taken into account for different manoeuvres and path and terrain specifications.

In most predictive path tracking control algorithms, a look-ahead point is employed to describe the position and orientation of a vehicle at a future time instant (Ozguner et al., 1995; Hellstrom and Ringdahl, 2006; Zhang and Qiu, 2004). The work done by Ozguner, et al. (1995) is the preliminary step towards path preview information usage for outdoor non-holonomic mobile robots. What has been carried out within last two decade in which modern technology such as computer is invented and implemented in the industrial products has been robust and safe automation and enhancement in the

operation precision (Reid, et al., 2000). Precision improvement has been of priority besides stability guarantee however still there is a room for more precise data collection and actuation. Indeed there are bunch of approaches for controlling the guidance of vehicle on the off-road terrain. Furthermore, using remote sensors serve the purpose of automatic path tracking quite satisfactory because off-road operation is being pursued while the weather is fine (not rainy or too much windy), especially agricultural operation is not allowed in the conditions which are not appropriate which means that the soil or crop might be deformed or damaged. Therefore, farm land offers a good environment or background for path tracking control whereas clear and open farm land in which a few machines transmit communication waves for position and orientation data.

The follow-the-carrot method is simple to apply to a human driver; however, it has several drawbacks in automatic path tracking, such as oscillatory behaviour with insufficient LARP distances and undesired corner cutting with longer LARP distances (Barton, 2001; Lundgren, 2003).

2.2 Feasibility Evaluation and Foundation

By the advancement of modern facilities, the tractor subsystems such as sensor and actuator were studied to drive a reliable model for off line system. An analytical representation was provided and also the characteristics of electro-hydraulic actuator were discussed (Rovira-Mas 2008). A model of an electro-hydraulic actuator is presented and the adaptation gain is obtained to adjust the modelling with the tractor real time dynamics and kinematics such as lateral tire force and lateral/yaw errors (Derrick, 2008). Some researches were dedicated to stereo-vision camera and laser scanner to

localize the vehicle position and attitude with respect to the crop rows (Wang 2011, and Oscar, et al. 2007). The experiment with these systems were satisfactory ran however, certain circumstances were maintained such the field conditions to have a clear vision and it is not surely available in the actual situation in the farm environment. Integration of different approaches into GPS systems has improved the accuracy of position and attitude measurement of outdoor vehicles. Indeed an agricultural vehicle is aimed to pursue an operation over the field rather solely to successfully pass a division of a road. Therefore, even centimetre accuracy is significant for farmers, especially when during the operation, sensor outage takes place or uniform lines are sought for seeder rows (Lenain, et al. 2006). In the open lands like an agricultural field, using integrated GPS sensor has been prevalent because the shortcomings such as connection interruption are rare. Real time kinematic global positioning system is one of the most reliable and commonly-used sensor types that for precise tracking controls of out-door robots have been widely adopted. In one of the most recent research, Fang, et al. 2011, employed GPS dual frequency EPOCH 25 RTK GPS, with 710 mm accuracy and 10 Hz sampling frequency (Fang, et al. 2011). For this study, it has been assumed that the proposed method is implemented into the setup with commonly used subsystems and it is already considered that sensor and actuator properties can affect the system performance. Hence, for development of the simulation test bed, and use it as a platform for semi-experimental tests to evaluate the system performance, these characteristics are taken into account.

2.3 Numerical Tests and Software Simulation; Aspects and Benefits in Off-Road Operations

Iterative experimental work on the outdoor mobile robot and off-road terrain has special characters. First, it needs to take into account the controller aims to solve the tracking problem so that restrictions must be well identified and comprehended as well as the risks or failure-producing actions. In addition, characters of highly nonlinear systems cannot be straightforwardly predicted or it will be formulated with infinite number of iterations to find the actual optimum design of a controller. Moreover, the characteristics of the terrain likely varies as long as the experiment is being carried out several rounds so that either the system design or the surrounding surface (terrain soil surface) will be heavily deformed and this is a critical point which must not occur since the soil deformation damages the performance by compaction that results in closing of the water passages inasmuch as the water penetration takes longer than one hour (Behrouzi Lar, 2006) and it ruins the plant roots which in turn drastically damages the farming efficiency. Apart from that, if the surface characteristics are altered then the next experiment will not be on the same foundation as the previous one and hence a claim based on each specifications alters experimental set-up so that it is not very reliable though it might give satisfactory results in practice since there might be better setting or design if the same characters is kept.

In general, empirical field tests on farm applications are tedious, hazardous, and cost-ineffective. Simulation tests are not only cost-effective but also precisely observable, and they provide rapid estimation of the efficiency of proposed methods. Computer-based approaches are proper choices, even to estimate the economical returns to the

farmers. In contrast to the passenger car driver, the objective of the agricultural vehicle driver is not only to stay in a lane but to also accurately track a desired path because the overall efficiency of farming depends on the tracking accuracy. Consequently, a series of experimental simulations can be carried out to verify the feasibility of a proposed system as well as to evaluate its performance.

Review of the previously studied related papers which are focused on the precise tracking control of an autonomous off-road vehicle indicates that before the real field experimental tests, a set of numerical iteration for the purpose of motion and state analysis were carried out to first crosscheck the feasibility and overall performance of designed system as well as estimation prior to field tests (Lenain et al. 2006, Bevly and Cobb 2010). Indeed, combination of simulation and real time tests saves the resources and reduces the costs of controller design (Lenain 2010 however the financial supports of the internationally well known research groups are sufficiently high for even prone to damage experiments since development of a system that is reliable and helps the universal move towards environment saving draws so much attention and encouragement (Aghkhani and Abbaspour Fard 2009). Nonetheless, it has been common to use the real field parameter values of the system which were previously obtained carefully in which same system characters existed or preliminary parameter tests were performed to search for the certain parameter values and their corresponding circumstances (Lenain et al. 2006 and 2007, Gartley 2005, Derrick 2008, Zhang and Qiu 2004, Fang et al. 2011). Nevertheless, the vehicle specifications such as tyre properties and wheel distances from the vehicle centre of gravity (*CG*), are significant in overall system performance evaluation, since manufacturers do not produce agricultural

vehicles with broad range of specifications, the terrain characteristics effects in system responses carried more weights than tyre properties and wheel distances from the vehicle centre of gravity *CG*, in system parameter identification and system formulation (Bevly 2001, Zhang and Qiu 2004). Hence, the common practice for commencement of a project towards tracking control system design and development which is funded by a factory to manufacture a real prototype has been terrain parameters identification so that the soil surface was already addressed (Fang, 2011). Derrick (2008) and Lenain, et al. (2007) performed their tests in such a way that simulation tests and the real experiments executed close together and therefore, a comparison between them gives the correction gain to be applied in the simulations tests and bring the results closer to the actual tests. It should be noted that in the modelling of the system, the expected but unknown disturbances will be present and they affect the performance evaluation particularly if the results being compared to the disturbance and noise free test inasmuch as those unwanted inputs dominate the overall outcomes of the system and re-evaluation must be of high necessity (Chapters 3 and 4). Those simulations have been a computerized method to determine the expected results specially position and orientation errors as well as lateral acceleration and yaw rate (Fang et al. 2011, Bevly 2001, Gartley 2008). Simulation offers free tests to even visualize the probable outcomes of the vehicle states subject to the certain external loads and under specific circumstances. In this study it has been tried to use the simulation test environment to search for the optimum parameters since each test for track a pre-defined path does not take more than a fraction of a second using a conventional personal computer.

As a matter of fact, although to obtain the precise values there is often a need for actual field experimental tests, to verify the performance of a proposed approach there is a solution as integration of both methods on the same simulation test platform.

The idea of peak lateral error reduction at curvature transition was suggested Lenain, et al. (2006). Within their experimentations they observed large peak error at curvature transition and suggested to improve the tracking accuracy of automatic agricultural vehicle guidance by reducing this error. Since the human driver looks for a distance ahead of the car and adjusts the steer angle according to the future desired steer angle on the reference path. Similar path preview approach of deviation angle was used by Lenain, et al (2006). Intuitively speaking, using human intention method within the context of control practice helps the stability even if it does provide high accuracy. This later issue was discussed in details in controller method chapter.

Furthermore, the pattern of the waypoint is often known in advance, from a top view image. Therefore, within this study it is assumed that the path is given and planned by a higher level controller.

2.4 Previous Significant Methods of Agricultural Vehicle Path Tracking Control

Various automatic methods and system descriptions have been presented thus far to serve the purpose of following a reference trajectory keeping a desired behaviour as the criterion for performance evaluation. These methods enriched and guided the present

study by inspiration of the idea of the proposed control strategy as well as providing a benchmark for the performance comparison.

One of the major streams of research on agricultural automatic guidance was based on sensor communication effects and feasibility of the guidance automation of land vehicles since 1995 by O'Connor at Stanford University. The research of O'Connor (1997), Bell (1999), Reid (2000) and Bevly (2001) were all devoted to the feasibility of a simple lateral deviation controller for autonomous agricultural tractor. Vehicle, sensor and actuation models were presented and circumstances were discussed. In addition the footsteps for controller development were taken by extensive research on automation of agricultural vehicle in North America (Reid et al., 2000), Japan (Torii, 2000) and Europe (Keicher and Seufert, 2000).

Many controller aspects were covered such as vehicle modelling, estimation, manoeuvrability and stability (Derrick and Bevly, 2009; Bell, 1999; O'Connor 1997). The focus has been on the lateral position and attitude control and stability specification of the system.

Zhang and Qiu (2004) presented a method as a basis for path preview information usage, in which look ahead point was addressed to be used for steering angle command. An intelligent navigation plan was designed and implemented on the real tractor and sufficient accuracy was obtained. The idea of path tracking control of an autonomous vehicle was inspired by the approach presented by Zhang and Qui (2004) in which for simulation real time kinematic (RTK) GPS is assumed for simulation and used in

practice. In addition, navigation control along both straight and curved paths was aimed to achieve peak lateral error of 10 cm.

Structurally similar approaches were presented such as look-ahead point strategy for forest autonomous vehicle (Hellstrom and Ringdahl, 2006) predictive, smart and precise experimental approaches (Lenain et al., 2006), intelligent off-road systems (Rovira-Mas et al., 2010), prompt control using electro-hydraulic steering (Wu et al. 2001), farm tractor dynamics estimation (Gartley and Bevly, 2008) and stereovision-based off-set measurements (Wang et al., 2011).

The lateral peak error reduction at curvature transitions was suggested by Lenain, et al. (2006). They came up with a robust and precise system however experienced poor performance at curvature transition. This weakness motivated the present study to develop a method with less computational complexity and better behaviour whenever changes in curves occur.

2.5 Drawbacks of the Previously Presented Agricultural Tracking Control Strategies

In the previous presented methods (section 2.4), several drawbacks were noticed as follows;

- Although fuzzy control is a good alternative for the human operator (by deriving his intention), it is prone to instability. A jump between two neighbour rule functions can destabilize the tracking behaviour presented in Moustris and Tzafestas (2005), and Wang, et al. (2011).

- Actuator non-linear behaviour has been a complicated problem. Servo-feedback can solve this drawback however; on the other hand, a transfer function model is required to represent the possible outcomes in response to desired values (Rovira-Mas and Zhang, 2008).
- Surface laid cable, proposed by Aghkhani and Abbaspour-Far (2009) is an expensive approach and hence it lacks many advantages of cost-effectiveness and applicability for a large farm field.
- Laser scanner resolution at night or in dusty fields is poor and can result in fatal tracking errors (Wang et al. 2011).
- GPS sensor communication outage is very common in off-road practice (Bevly, 2001) and thus an automatic simulation method is required.
- The degree of complexities in the structure of controllers as well as the computational inefficiency may make these methods inefficient for agricultural tasks.
- Large lateral peak errors at curvature transitions have been reported by the results of the previous studies. Even advanced control methods have produced high overshoots in response to reference path shape change. In my knowledge, the effects of waypoint shape variation on an agricultural tracking behaviour have not been studied.

The fuzzy control instability and structure complexity problems have been solved by employing a look-ahead strategy (Zhang and Qiu, 2004), while stereovision-based (e.g., laser scanner, camera) drawbacks have been addressed via a CDGPS-based approach (Thuilot et al., 2002).

Automatic guidance of an agricultural vehicle requires a combination of technologies, such as electro-hydraulic actuation, DGPS sensors, and embedded controller techniques. The main aim of such mechanisms is to facilitate high manoeuvrability and accurate localization of a farm tractor. An electro-hydraulic (EH) actuator is highly nonlinear, but linearization of the servo control loop is possible and improves the actuator accuracy. Therefore, both of these techniques have been taken into account when developing the proposed system. On the other hand, for path tracking on a variable shape route such as a U-turn, the error in the shape transition needs to be reduced.

2.6 Objective of This Study

2.6.1 Problem Statement

Reference path shape in the off-road applications depends on a pattern provided by the terrain conditions and environment surroundings. As an example, the crop rows of agricultural field may have irregular shape since they planned to be next to the watering canal or against the local slope of a hilly surface. Subsequently, the curve type of the reference path changes several times and curvature transitions will produce large peak lateral errors during vehicle path tracking mission. Even existing advanced control methods produce large peak error at curvature transitions.

2.6.2 Proposed Solution

The lateral peak error will be sufficiently reduced if a farther point ahead of the vehicle on the reference path provides advanced information of curvature transitions. In addition, a closer look ahead reference point is required to compensate the centrifugal forces as well as a lateral deviation controller to guarantee the tracking preciseness.

This study offers a simple method that improves stability and provides sufficient tracking accuracy to prevent the above-mentioned drawbacks.

The underlying foundation for modelling is built on previous studies (e.g. Bell, 1999; Bevely, 2001; Gartley, 2005). The goal of the proposed method is to track a reference path at a sufficiently high accuracy so that the distance between the middle of the rear wheels and the reference path always remains within the typical required tolerances of agricultural applications. It was assumed that a curvilinear reference path is planned by a higher level navigation planner, and the vehicle is equipped with proper instruments to determine its position and orientation with respect to the reference path frame. Thus, the controller on the vehicle can search the nearest point on the path and determine the lateral deviation of the vehicle from the path. A look-ahead reference point (LARP) is a point on the reference path at a specified curvilinear distance from the nearest point. The proposed LARP control method simply emulates natural actions of three virtual drivers over the nearest point and two look-ahead points on the desired path. The difference between the direction vectors of a look-ahead reference point and the nearest point mainly provides the curvature of the path in advance, and also provides correction for the centrifugal forces along the circular paths. Using multiple LARPs provides smoothness of the driving actions, and reduces the peak errors at the transition of partitions. The output of the LARP control is applied to the steer angle employing an EH-actuator which is linearised by a servo control loop.

Among the advantages of the proposed system are i) simple reference path representation, ii) computational simplicity, e.g., no integral, and iii) fewer position data

requirements compared to the other methods. Further development is feasible to reach a certain level of maturity for a more detailed system. The goal is an approach that is convenient for agricultural applications such as spraying and seeding, and has a sufficient level of safety for travelling between crop rows.

Chapter 3

MODELLING APPROACHES

3.1 Modelling Preliminaries

In order to predict and analyse the future states of the real system there is an absolute need for mathematical modelling. A proper model of the system can express the relations and behaviour in the system and the interactions between the sub-systems. Hence, this section introduces the fundamental relations and formulations needed to build a dynamic model of a vehicle in agricultural working conditions that have considerable skid and slip.

To form a structure for the sake of analysis and evaluation, first, each system must be analyzed independently to take into account the details which have significant effect on the behaviour of the system when the kinematics and kinetics of the whole system is considered (Senatore and Sandu, 2011).

For modelling the whole system four main sub-systems must be taken into account; the vehicle (upper moving body), tyre and tyre contact patch, sensor noise and delay, actuator saturation and lag as well as terrain irregularities. These are the least for the modelling of a vehicle tracking while in some research the controller act as a dynamic behaviour regulator to track the desired route while towed implement or trailer is attached and also the obstacles are assumed to be available and must be passed such that no crush or turn over occur.

Although, vehicle behaviour can be controlled to behave in the region that formulation is straightforward and can be held in the linear region; the tyre interactions with the terrain surface is not that much routine to be modelled via a simple and short formula, especially when the slip and skid occur. In such cases the experiments must be carried out to determine the model that can well predict the effect of the travel on the unpaved road and give the required involved parameters within the system functionality. Wheel interaction with the soil that hardly behaves like a homogenous material has been a field of interest and has been studied in details since 1987 (Bakker et al. 1987) up to 2011 (Senatore and Sandu, 2011). Moreover, in the field there are unknown disturbances. In the present study the soil disturbance to be model and applied on the system is a load that acts in the modelling as a special mathematical function. Indeed, disturbance on the field is whatever that was not already taken into account and might alter the vehicle's behaviour for tracking a desired route (Bell 1999).

A model that deliberately takes into account all the circumstances and forces is impossible (Bevly and Cobb 2010).

An accurate model of a steering system is expected to generate the same outcomes as the real vehicle on the actual field so that the conditions of the real system must be well perceived. On the other hand, in the majority of previous well known studies, it has been tried to come up with a system that is relatively simple and sufficiently precise (Bevly and Cobb 2010, Bakker et al 1987, Gartley 2005, Zhang and Qiu 2004, Fang et al. 2011)]. The last two terms introduce ambiguity that is undesirable for a systematic

research. By simplifying the system for specific applications, minimal computational effort will be produced as was done by Senatore and Sandu (2011).

Furthermore, accuracy also indicates a proposed controller system, works at least in the same level as a human operator. The designed system might perform better than the previous proposed systems but an overview of the previous studies on the off-road automatic vehicle steering system denotes that each proposed method thus far stands for special conditions and limited range of parameter variations (Li. Et al 2009, and Reid et al. 2000). Although this study attempts to show the effectiveness of the proposed controller by means of evaluation over the same foundation leading to performance comparison regardless of whatever the outcome might be, rather than the prediction of the exact effects on the real set up since some processes on the real setup is not determined beforehand, however it is possible to have close results to the real set up via some correction gains (Derrick 2008) or some parameter modifications (Lenain et al. 2006).

A detailed description and discussion of the vehicle and terrain modelling will follow this section including the circumstances assumed prior to modelling.

3.2 Model of Vehicle Kinematics and Dynamics

An accurate model of the vehicle steering system represents all motions on the vehicle body. The model of a steering system without towed implement is quite straightforward since the perturbations on the system are less whereas they have serious impact on the system inasmuch as the response type of the system might easily change (Derrick,

2008). Most likely they affect the vehicle body side slip angle which in turn alters the vehicle states to display inaccurate outcomes (Fang, et al. 2011)

A model that has been broadly used by the researchers is an 8 degree of freedom model of the vehicle that is designed to show the lateral, longitudinal, bounce, roll, pitch and yaw which are all assumed on the vehicle centre of gravity. Although the control point might be assumed elsewhere on the vehicle or the whole system body, the computational efficiency will not be affected by simple arithmetic that will be used for control point position determination.

One may notice that in off road vehicle steering analysis some variables such as aerodynamic (wind) force or suspension effect have no significance or involves fewer effects (Bell, 2000, and Kiencke and Nielsen, 2005).

A typical four wheel active front tyre steering vehicle may be accurately modelled by an 8 DOF model, but in almost all previous research studies, it has been common to simplify the 8 DOF model into 3 DOF to reduce system complexity without losing the main characteristics of the dynamic system (Bell, 1999; Bevly, 2001; Gartley, 2005; Derrick and Bevly, 2008; Fang, et al., 2011; Zhang and Qiu, 2004). The side view of the system is shown in Figure 1.

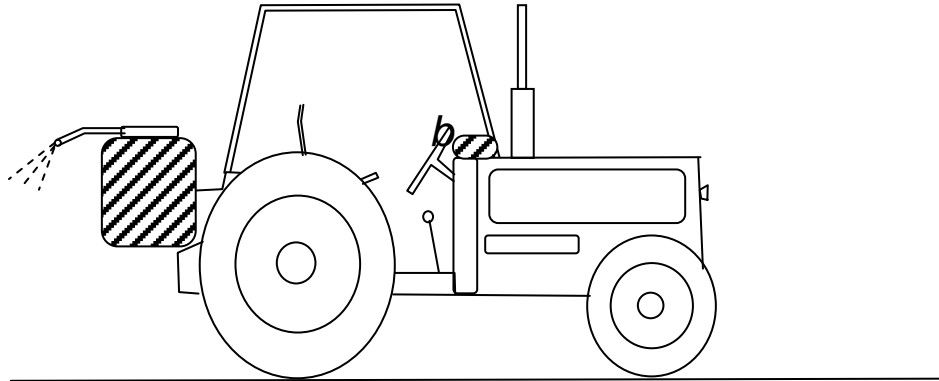


Figure 1. Side view of a typical agricultural vehicle with implement for material spreading dynamics having controller and position-sensor unit

3.3 Tyre model for vehicle dynamics

The main effective parameters within the steering system analysis and evaluation are the tyre interaction with the terrain surface. Indeed the friction coefficient between the tyre treads and the soil surface produces the force to act as a major quantity to govern the motion of the vehicle (Karkee, 2010). The mismatch between the simulation of a steering model and the actual test is caused by the fact that the tyre is not as circular as it is assumed. Besides, the faulty assumption regarding suspension and symmetric body motion pre-considerations such as roll and pitch motion neglecting load transfer discarding can be another reason to observe discrepancies between simulation and real experiment tests. Apart from that, the tire deforms in such a way that it adjusts itself to the terrain bed and therefore, the lower part of the tire becomes flat. This is the reason why the relaxation length was introduced by Senatore and Sandu (2011) to correct the previous formulation over the unpaved and paved road surfaces. Although a widely accepted tire model cannot be found in the literature (Karkee and Steward, 2010) and most likely it is due to the circumstances and application of the tyre study, it is possible to work in the region that has been commonly used in the controller design task in the

land vehicle navigation operation analysis. As a matter of fact the soil conditions or the quality of the terrain while having interaction with the tyre via contact patch is case study dependent and needs real experimental determination in such a way that it must be computed carefully right before the simulation since the soil condition changes and the coefficient assumed for the interaction effects will alter. As an example, the humidity of the soil easily changes the soil behaviour while reacting to the normal load of the tyres (Hemmat, et al. 2009). In addition, sinkage and rolling resistance opens another room of discrepancy among the simulation and real experiment. The point is soil compaction is of high avoidance in the agricultural studies and technically speaking some of the methods have been used to work in the condition with minimal compaction such as tandem or double wheels.

The tractor tyres are expected to work on sandy loam soil whose characteristics are presented in Wong (2001) and Hemmat et al. (2009). Tyres should not sink deeply into the soil because sinkage compacts the soil and reduces farming productivity. Moreover, sinkage causes a high rolling resistance and a weak propulsion force, which may create unexpected slippage and tracking failure. Usually, those effects are prevented by tandem tyres, which produce a moderate rolling resistance and a sufficient propulsion force on front and rear tyres, respectively. Treads of radial tyres with pressure above 28 psi do not penetrate into the soil surface.

Figure 1, schematically represents a side view of a conventional farm tractor and Figure 2 represents a top view of the vehicle to describe the kinematics symbols in the global

reference frame (X, Y) (Lenain, et al. 2007). In addition, Figure 2 introduces the symbols used for the analysis and modelling of the vehicle and tyres.

The tyre model and vehicle dynamics are inspired by the studies done by Bakker et al. (1987), Zhang and Qiu (2004), Gartley (2005); Derrick and Bevly (2009) and Fang, et al. (2011).

This study takes into account the assumptions made for tyre modelling by Gartley and Bevly (2008). Kienke and Bakker (1987) and Bevly and Cobb (2010) have shown that the force acting on a tyre is caused by friction among tyre and terrain surface and can be broken into two major components as lateral force and longitudinal force. Longitudinal force develops on the tire most likely due to skid phenomenon because the tyre is forced to move longitudinally and turns by the torque applied by the terrain surface so it is non-driving tyre (Wong, 2009). Indeed, this force plays a insignificant role in comparison with the force that develops laterally to the tire direction. For the case of two wheel drive tractors it is exactly the case of application on the both of front tyres. On the other hand, since tyre does not move laterally a resistance force (R) is generated by the soil friction along the wheel axis centre (Wong, 2009). It is experimentally proven that the lateral force is proportional to the angle among the tire direction and its actual velocity (tyre slip angle), while the aforementioned angle is less than four degrees. Therefore, in the present study the case for evaluation of performance and comparison of efficiencies it is tried to operate the system within the linear region by controlling the vehicle manoeuvre in the steady-state motion. Clearly the vehicle is run either on the linear path with the control of behaviour not to cause a driving or highly perturbed behaviour that may

damage the linear relation among the tyre slip angle and tyre lateral force (Bell 1999) as well as the steady state cornering in which very close vicinity is obeyed however in none of the previous research it has been asserted that the modelling used in their study can be validly working in the all conditions especially while travelling having high velocity (sufficiently high to cause nonlinearity in the force angle relation) and curve tracking and curvature transitions (Lenain, et al. 2006).

Furthermore, in order to stay often within the linear region of soil adhesion and slip ratio as well as to prevent tyre saturations, non-severe manoeuvres developed by the proposed controller were tried. On one hand, the forward speed is about 2 m s^{-1} having steady-state cornering via steer angle that is not likely to exceed $\pm 15^\circ$ in smooth driving of farm applications up to the end of the curvature transition phase. On the other hand, since the farming is carried out with linear crop rows, the performance is examined over the linear path segments rather than the curved routes on the headlands. Besides, the meadow is adjusted for farm work with a moderately soft and moist soil (e.g. grass plot terrain).

Top view of the vehicle model and its corresponding symbols and direction are illustrated in Figure 2. It also shows a full vehicle model as well as the longitudinal symmetry required if further simplification of the vehicle model is possible.

Figure 3 illustrates the simplified model which gives the important platform for simulations tests required in comparisons of the results as well as optimizing and determining the parameters to be discussed the optimization Chapter.

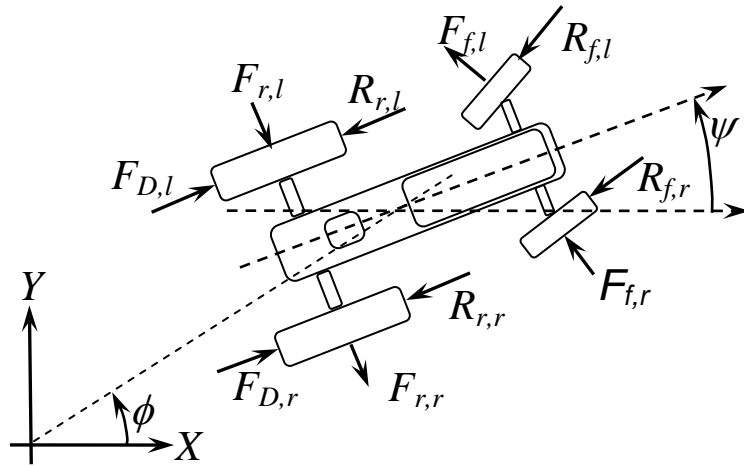


Figure 2. Top view of a typical agricultural vehicle showing the symbols related to the vehicle kinematics

Therefore, three degrees of freedom (3-DOF) vehicle model given in Figure 3, shows how the equation dynamics can be performed and its features are very similar to the previous studies in agricultural vehicle guidance field (Zhang and Qiu, 2004; Gartley, 2005; Derrick and Bevly, 2008).

As a matter of fact, in order to capture the vehicle movement while travelling between crop rows, the full vehicle model shown in Figure 2, is the basis for dynamics analysis. In the simulations of dynamic motion, the pitch and roll motions are bounded not to exceed the boundary values discussed in Day, et al.(2009).

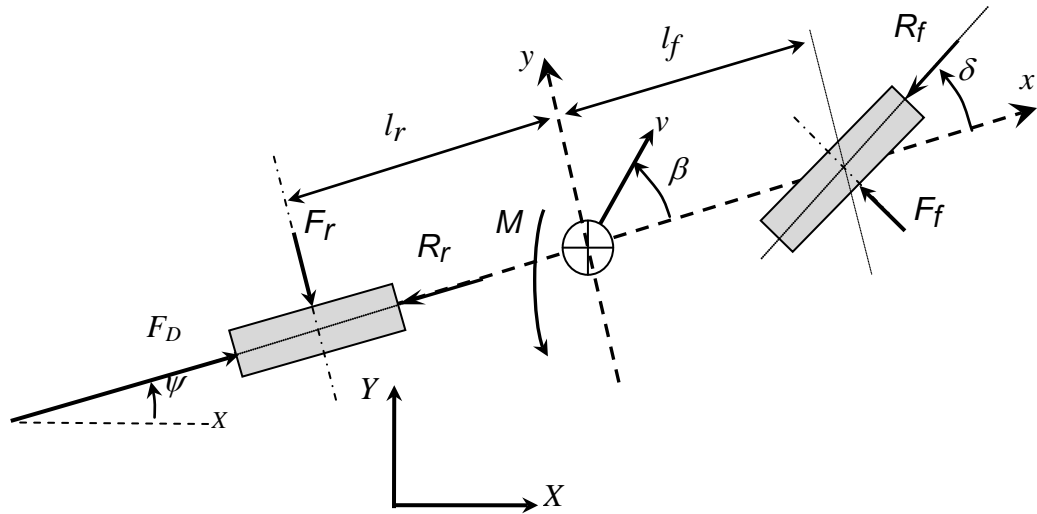


Figure 3. Bike model of vehicle as three degrees of freedom (3DOF) model with its definition of symbols

In order to determine the dynamics of vehicle body or a control point assuming on the vehicle or on the towed implement or elsewhere but fixed with respect to the vehicle horizontal two dimensional coordinates plane, the interaction between the vehicle tyres and terrain surface must be considered. Hence, a tyre model illustrated in Figure 4 is developed and assumed. The tyre model is used in the manoeuvres of linear tyre model regime and close to the boundaries and characteristics discussed by Solmaz and Baslamisli, (2010).

Tyre model is very significant in the off-road vehicle guidance study since it produces the mutual forces in the machine and soil surface interactions which in turn define and manipulate the results obtained from the sensor communications on the vehicle and stations. Moreover, since this study is evaluating the preciseness of a certain path tracker control system, variations in the parameters or models must be carefully preceded.

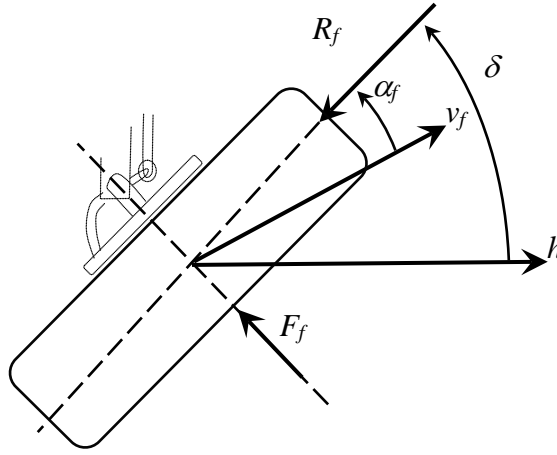


Figure 4. Definition of symbols on a) The 3-DOF vehicle model, and b) The front tyre.

Hence, the lateral acceleration and tyre slip angles do not likely exceed 0.8 m s^{-2} and 4° , respectively, even at curvature transitions. The angle α between the actual velocity of the tyre and the direction of the tyre plays a significant role in producing lateral forces. The modelling principles are similar to Bodur, et al. (2012). Consequently, the relation between the angles α_f and α_r with the lateral forces F_f and F_r on the front and rear tyres are:

$$F_f = C_f \cdot \alpha_f,$$

$$F_r = C_r \cdot \alpha_r, (1)$$

where C_f and C_r are the cornering coefficients of the front and rear tyres. The dynamic equations are derived by applying first principles in the local coordinate axis (x, y) shown in Figure 3.

$$F_D = m_{veh}(\ddot{x} + \dot{y}r) + C_f(\delta - \beta - \frac{\dot{\psi}l_f}{\dot{x}}) + R \quad (2)$$

where F_D provides the propulsion force for velocity control. The propulsion torque required for the propulsion force, F_D , shall be decided by the engine governor. The resistance force R is the product of tyre penetration in the field soil and soil longitudinal compaction in front of the tyre tread. Nevertheless the longitudinal dynamics in the path tracking of a constant forward velocity vehicle has negligible contribution, it is brought to indicate the significance of controlling the forces as propulsion or brake in longitudinal direction required for the system performance improvement. The lateral force, F_y , is derived via

$$F_y = m_{veh}(\ddot{y} - \dot{x}\dot{\psi}) = C_f(\delta - \beta - \frac{\dot{\psi}l_f}{\dot{x}})\cos\delta + C_r(\frac{\dot{\psi}l_r}{\dot{x}} - \beta) + \text{sgn}(\beta)m_{veh}\dot{x}^2 / \rho + F_{dis} \quad (3)$$

where y and \dot{y} indicate the lateral displacement and acceleration, respectively, towards vehicle orientation. F_y includes the centrifugal force, $m\dot{x}^2 / \rho$, which causes undesirable lateral vehicle slippage. The moment, $I_z \dot{\psi}$, required for turning the vehicle is derived via

$$I_z \dot{\psi} = C_f(\delta - \beta - \frac{\dot{\psi}l_f}{\dot{x}})\cos\delta + C_r(\frac{\dot{\psi}l_r}{\dot{x}} - \beta) + \mu N_f l_f \sin\delta + M_{dis} \quad (4)$$

where ψ and $\dot{\psi}$ are the yaw angle and the aligning angular acceleration produced by the tyre cornering force; $\dot{x} = v \cos\beta$ is the forward vehicle speed, and $\beta = \sin^{-1}(\dot{y}/v)$ is the slip angle of the vehicle body, which is expected to give a value so long as the front tyre angle is non-zero. Solely, for linear system construction, assuming that vehicle body slip angle $\beta < 16^\circ$ (Bevly, 2001; Zhang, 2004; Gartley, 2005; and Fang et al. 2011)

then, $\dot{x} = v \cos \beta \approx v$. For simulations, \dot{x} is assumed to be constant as farm tractor driver normally does during the operation. The position of the vehicle in the global reference frame is derived from the following equations:

$$\dot{X} = v \cos(\beta + \psi)$$

$$\dot{Y} = v \sin(\beta + \psi) \tag{5}$$

3.4 Modelling of the steering system

Guidance control of automatic steering equipped vehicles requires an EH-actuator to adjust the front tyre angle, and an engine governor to modify the forward propulsion force. The present study attempts to show the advantages of the LARP controller compared to conventional lateral controller on the systems with same characteristics. Figure 5 shows the block diagram of the simulated closed-loop control system which performs the steering and speed control tasks using a LARP controller, an EH-servo controller, and a speed governor. An embedded controller guides the vehicle by employing LARP control to track the reference path.

The steering servo-actuator used in this study is similar to that presented by Derrick and Bevly (2008), with $\omega_{n,actuator} = 28.425 \text{ rad s}^{-1}$ and $\zeta = 0.633$.

It provides fast and linear operation of the actuator to keep $\delta = \delta_{des}$ with a 0.4 s lag. The actuator outputs $\delta, \dot{\delta}$ are restricted to the ranges of 32° and $20.6^\circ \text{ s}^{-1}$ king-pin angle to

avoid the fatal turnover of the farm tractor. Engine governors regulate the velocity of the vehicle for constant speed operations.

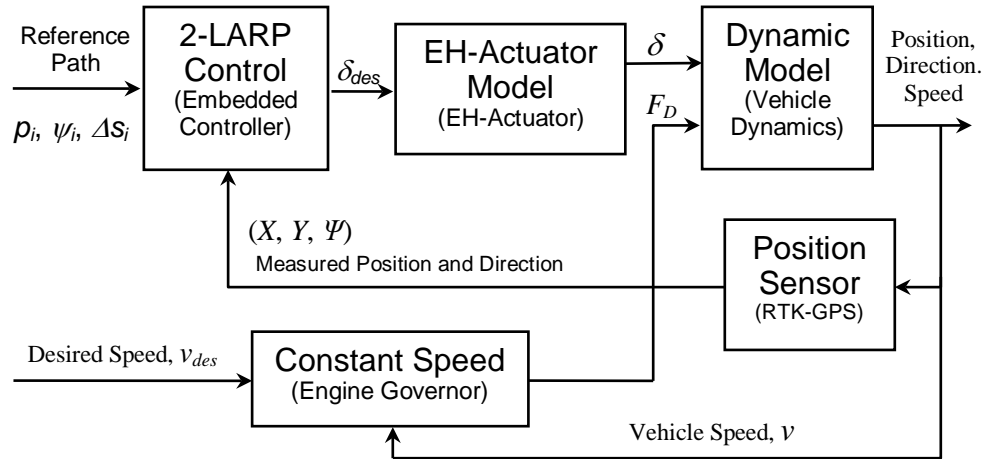


Figure 5. Architecture of the simulation platform for the automatic tracking control system and vehicle dynamics.

The parameters of $p_i, \psi_i,$ and Δs_i are entries of sequence as a given path to be used in the controller algorithm. In brief, since the path is assumed to be given and thus it is planned by a higher level navigator, $p_i, \psi_i,$ and Δs_i are waypoints, desired orientations and reference path segments. The Real time kinematic global positioning system sensor (RTK-GPS) is preferred rather than carrier phase global positioning system sensors because the position measurements of RTK-GPS are more accurate than CD-GPS.

The block diagram of the LARP controller is shown in Figure 6. The proposed localisation process and effects of the control parameters on the steering response are described in detail in the next section.

3.5 Required sensors for simulation test bed

The system simulated in the present study is assumed to work in real time with the electronic devices which have specifications similar to the previous studies in order to observe improvements. By the advent of modern technologies, the accuracies are getting higher and uncertainties are decreasing within the dynamic systems measurements. For displacement measurements e.g. tyre angle, a linear variable differential transducer (LVDT) can serve the purpose of high accuracy from a few nm up to several cm as well as rapid response with an ms delay (Fateh and Alavi, 2009). For positioning measurements, different remote techniques are available and have been used for large fields. Integrated GPS-based approaches such as real time kinematics (RTK-GPS) and carrier phase differential (CD-GPS) techniques provide minimal delay and inaccuracies

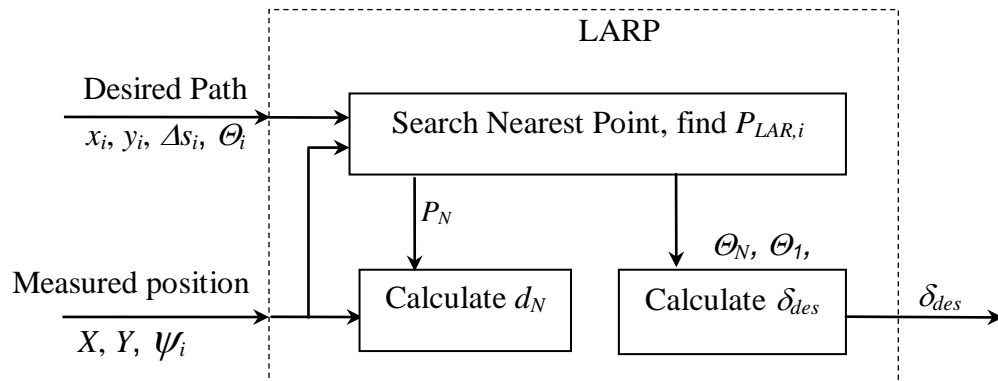


Figure 6. Block diagram of 2-LARP Control Unit

with the velocity and displacement measurements to 5 cm s^{-1} and 2.5 cm , respectively, and frequency to 5 Hz (Daily and Bevly, 2004; Gartley, 2008; Li et al., 2009). In addition, a commercial optical range finder can provide the system with error accuracy of 2.5 mm and response frequency of 770 Hz . Hence, the proposed controller could be applied to a system with the above specification and it was observed that lower equipment accuracy could bring improved results in terms of higher tracking enhancement if LARP controller performances are compared to a conventional lateral controller. Finally, for this study, a EPOCH25 RTK GPS is assumed with $\pm 10 \text{ mm}$ accuracy and 10 Hz sampling frequency (Fang et al. 2011).

3.6 Modelling of the soil disturbance

An agricultural terrain has unevenness that introduces disturbance forces at the tyre soil contact points. A dynamic model that ignores these disturbances might be misleading when predicting the efficiency of the applied control. Indeed, the disturbance varies from terrain to terrain and with degree of unevenness presence and stubble terrain. It also varies within experiment iterations so that a precise specific function cannot represent the field disturbance. Over a large ploughed field it can be assumed that the soil clods are randomly distributed with random shapes and sizes. Notice that the major source of disturbance is the lateral component of the gravitational force on the tyres when they pass over a soil clod.

3.7 Amplitude determination of Disturbance functions

The clods lift up the tyre by h_{dis} and tilt the corresponding tractor axle by λ angle (Figure 7), so that gravity introduces a lateral force F_{dis} and a moment M_{dis} on the *CG* (Figure

8). Assuming the height of the soil clod is 0.2 m and width of tractor is 1.5 m, then

$\lambda \approx \frac{0.2}{1.5} = 0.13$ rad. Accordingly, assuming the half mass over one axle tilts, then

$F_{dis}^{max} = 0.5m_{veh}g \sin \lambda = 0.65m_{veh}$, accelerates the vehicle crabwise. Notice that the

vehicle coordinates plane is tilted so that the actual horizontal acceleration is determined

as $F_{dis}^{max} = 0.5m_{veh}g \sin \lambda \cos \lambda = 0.64m_{veh}$. Moving F_{dis} to CG , a disturbance moment

will be introduced as $M_{dis}^{max} = F_{dis}l_f$. Since $l_f > l_r$ the larger moment gives the worst

case. Therefore, the disturbance angular acceleration applied to the tractor is determined

as $M_{dis}^{max} = F_{dis}l_f = 0.89I_Z$.

3.8 Determination of disturbance function

The disturbance model is completed by assuming that the heights of soil clods have a Gaussian distribution, leading to random changes at regular curvilinear distance steps. Hence, the heights and distances between the soil clods are the parameters to be adjusted according to the terrain conditions. In other words, the amplitude, time step, mean value and seed of the applied disturbance functions should be set. This study assumes an

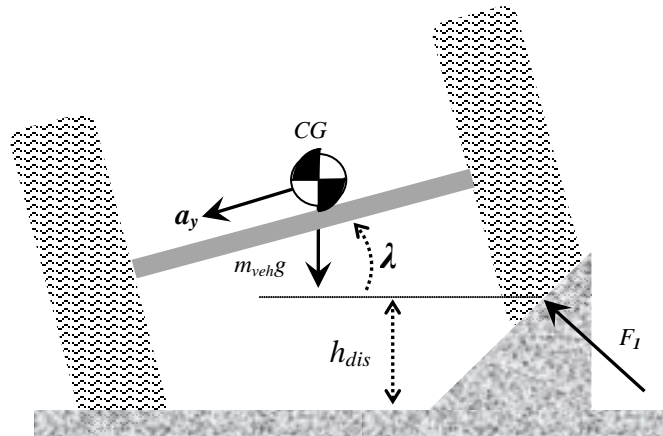


Figure 7. Source of a disturbance force while a tyre passes over a slope. Front view of vehicle.

extent of maximal force and moment ($a_{F,dis}, a_{M,dis}$) to be applied, according to the terrain conditions or say the RMSE value of the disturbances applied to perturb the lateral and angular motions as $0 < a_{F,dis} < 1$ and $0 < a_{M,dis} < 1$. Thus, the disturbance force and moment change at regular intervals

$$F_{dis}(t) = a_{F,dis} 0.65 m_{veh} N_G,$$

$$M_{dis}(t) = a_{M,dis} 0.89 I_Z N_G, \quad (6)$$

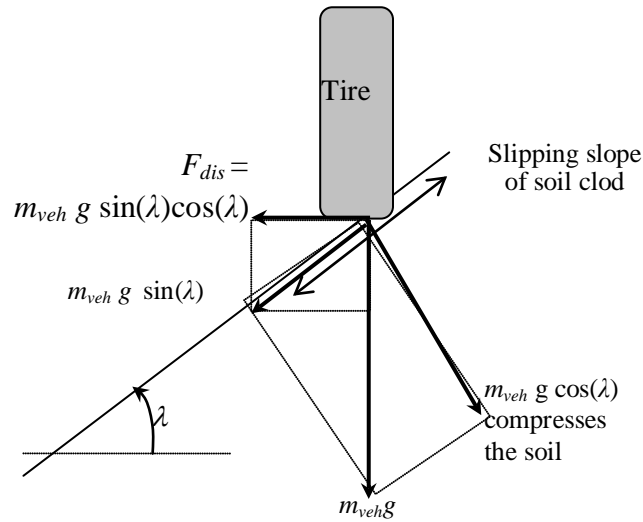


Figure 8. Source of a disturbance force while a tyre passes over a slope. Front view of tyre on the soil clod.

where, N_G stands for the zero-mean unity-variance Gaussian distributed random number. Eventually, in order to find a proper random function, the specifications of seed, variance, and disturbance intervals must be tuned according to the case study e.g. terrain type (grass plot, loamy low moist soil etc.) and vehicle parameters ($C_f, C_r, I_f, I_r, m_{veh}, I_Z$). Section 5.4 contains a tuning example of the above specifications.

3.9 Measurement and actuation

Satisfactory path tracking requires collaboration of all techniques and facilities involved. Accurate measurement of the vehicle position and attitude along with internal variables to be sensed such as tire angle are so significant for the sake of precision tracking (Backman, et al. 2012). Furthermore, sufficient actuation helps the system to produce high quality response (Rovira Mas and Zhang, 2008) with lower order (Derrick, 2008). For this study, the actuators and sensor devices are assumed that are in use currently and referred to in the previous well studies (Fang et al. 2011, and Derrick, 2008). The modelling assumed for these devices will be detailed in the simulation Chapter.

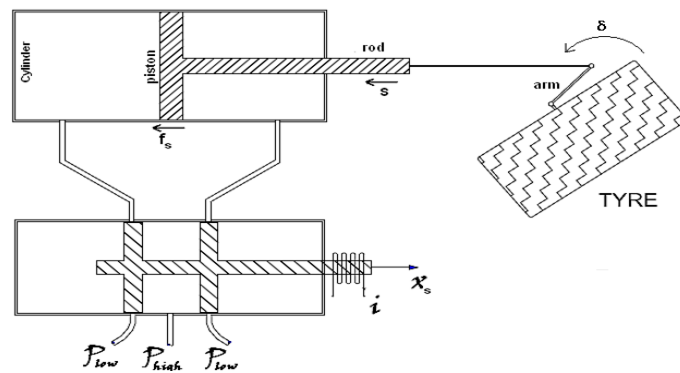


Figure 9: Schematic model of the actuator used for this study

Chapter 4

LARP CONTROL METHOD

4.1 Look-ahead Reference Point Control

This study proposes a control law that determines the steering angle according to three points on the reference path: the nearest point on the path, P_N , and two look-ahead reference points, P_{L1} and P_{L2} .

$$\delta_{des} = K_d d_N + K_N \theta_N + K_1 \theta_1 + K_2 \theta_2, \quad (7)$$

where $\{K_d, K_N, K_1, K_2\}$ are the controller coefficients for corrective actions to reduce the lateral deviation, d_N , in a sufficiently small time period, and $\Theta_i = \psi_i - \psi$ is the angle of the tangent at P_i relative to heading angle, ψ . The feedback gain, K_d , corrects for the lateral deviation, d_N . The sum $(K_N + K_1 + K_2)$ stabilises the sixth order dynamic response of the controlled system by derivative feedback, and the feed-forward action by the coefficients K_1 and K_2 corrects the centrifugal forces proportionally with respect to look-ahead distances. Furthermore, distributing the centrifugal correction to K_1 and K_2 reduces the peak deviation at the curvature transition of the path.

4.2 Proposed LARP control structure in application

Figure 10 shows the vehicle model, the reference path, and the points related to the LARP control law. On a real-time application the positions of P_N , P_{L1} and P_{L2} shall be

determined to obtain the corresponding signed lateral and angular deviations of d_N , Θ_1 , Θ_2 .

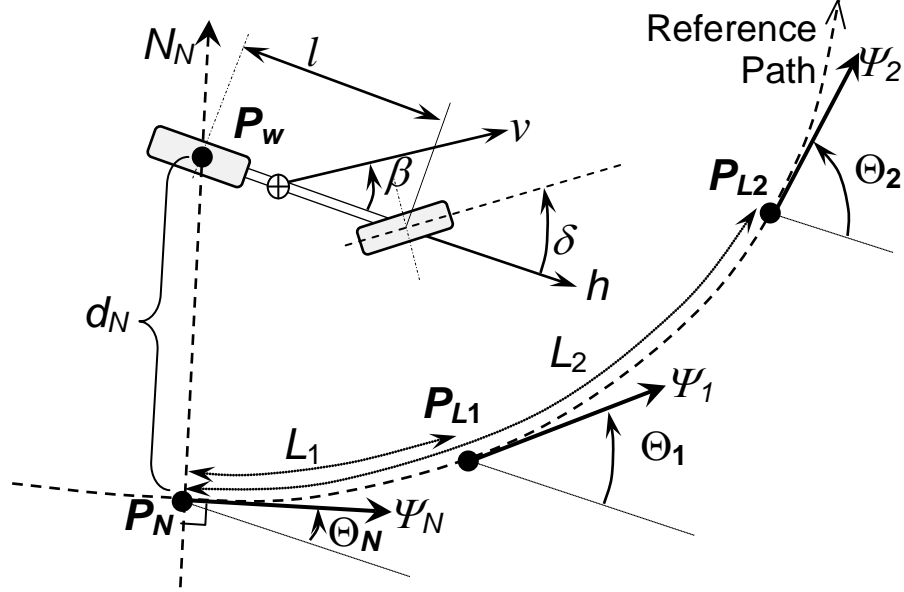


Figure 10. Path tracking specifications

The following path structure and algorithms are proposed to reduce the required operations for the proposed control law to only square root and simple arithmetic operations.

Path Structure: The reference path is assumed to be planned by a higher level intelligent path planning navigator, which also calculates the curvilinear distance from p_{k-1} to p_k , i.e., $\Delta s_k = [(X_{k-1} - X_k)^2 + (Y_{k-1} - Y_k)^2]^{1/2}$, and the direction vector ψ_k for each point p_k . Consequently, the reference path is described by an ordered set of reference points $\{(p_0, \Delta s_0, \psi_0), (p_1, \Delta s_1, \psi_1), \dots, (p_n, \Delta s_n, \psi_n)\}$ on the desired path. The set is ordered to provide path continuity in time and in the curvilinear dimension. Assume that the system dynamics are discretely controlled for time step T , which is about 50 ms. Typically,

passing two or three points per time step might be sufficient. For larger fields, it is possible to describe the reference path with fewer points and interpolate at every time step with spline or cubic interpolation techniques.

Search $P_N(t)$: Assume that at time $t-T$ the nearest point on the path is $P_N(t-T) = p_k$. The nearest point $P_N(t)$ is expected to exist in the set of path points in the neighbourhood of p_k , which is the set of points $\{p_{k-j}, \dots, p_k, \dots, p_{k+j}\}$, where j depends on the number of points passed per time period T . The nearest point $P_N(t)$ is at p_i that satisfies

$$\min_{i=k-j, \dots, k+j} \|p_i - P_w\|,$$

where P_w denotes the midpoint of rear wheels of the vehicle. Let the distance $d = \|d_N\|$ be minimum at index m_{N1} , and next minimum be at index m_{N2} . Then P_N is between the points p_{N1} and p_{N2} , and the lateral distance between P_w and P_N is

$$\|d_N\| = \frac{1}{2} \sqrt{(p_{N2} - P_w)^2 - \frac{[(p_{N1} - P_w)^2 - (p_{N1} - p_{N2})^2]^2}{(p_{N1} - p_{N2})^2}}, \quad (8)$$

The angular deviation Θ_N is calculated by

$$\Theta_N = \psi_{m_{N1}} - \psi.$$

The signed lateral deviation d_N is obtained by a cross product

$$d_N = -\text{sgn}((x_{m_{N1}+1} - x_{m_{N1}})(y_{m_{N1}} - y_w) - (y_{m_{N1}+1} - y_{m_{N1}})(x_{m_{N1}} - x_w)) d. \quad (9)$$

Update $s(t)$: The curvilinear distance s is measured on the desired path by summing the curvilinear distances of path steps. It is possible to calculate $s(t+T)$ iteratively by summing $s(t)$ and the Δs_r of the remaining points taken during the last time step T .

$$s(t) = \sum_{r=1}^k \Delta s_r,$$

$$s(t+T) = \sum_{r=1}^{k'} \Delta s_r = \sum_{r=1}^k \Delta s_r + \sum_{r=k}^{k'} \Delta s_r,$$

$$= s(t) + \sum_{r=k}^{k'} \Delta s_r.$$

Determine Θ_1 and Θ_2 : Indices m_1 and m_2 of the look-ahead reference points P_{L1} and P_{L2} can be simply determined to satisfy the sum of curvilinear distances L_1 and L_2 , respectively, from P_N to P_{L1} and from P_N to P_2 ,

$$L_i = \sum_{r=k'}^{m_i} \Delta s_r; \quad i \in \{1, 2\}, \quad (10)$$

where the curvilinear look-ahead distances L_1 and L_2 are parameters of the control law; their determination is explained in the next subsection. Once m_1 and m_2 are determined, then Θ_1 and Θ_2 are calculated by $\Theta_1 = \psi_{m_1} - \psi$, and $\Theta_2 = \psi_{m_2} - \psi$.

Apply the control law to calculate δ_{des} using (7).

The described path structure and algorithm requires only simple arithmetic operations and a square root function in its implementation. The path may be calculated by a higher

level path planner unit that considers the boundaries of the field and the obstacles in the work area.

4.3 Similarity of the proposed control and local-error feedback

On a linear path, the 3-DOF equation of motion (3) under the local-error feedback has been approximated in the literature by a fourth order linear differential equation (Gartley, 2005). Parameter variation and frequency response analysis of such farm systems using lateral error control based on lateral deviation have previously been presented by Gartley (2005), Derrick and Bevly (2008) and Fang et al. (2011). Local error-based control methods and their stability have been tested on third order models using control gains obtained by root locus and LQR (Bell, 1999, O'Connor, 1997). The local error-based control requires minimal computational effort, however, it has poor performance for the agricultural path tracking requirements especially at curvature transitions (Bell, 1999, pp 129). The simplest path tracking control is obtained by only two control gains, K_d and K_θ , for the local lateral deviation and for local angular deviation, respectively.

$$\delta_{des} = K_d d_y + K_\theta \Theta \quad (11)$$

Values of K_d and K_θ for a stable operation of the system may be obtained by many design methods such as using pole placement techniques, by Root Locus, or using a Linear Quadratic Regulator design technique. Tracking the arcs and curves requires a feedforward correction term that is mainly a function of velocity and path curvature (Bevly 2001).

The proposed control law (7) approximates (11) in tracking a linear desired path, assuming that the heading error $\Theta < 0.28$ rad, since $d_N = \cos(\Theta)d_y$, and $\Theta = \Theta_N = \Theta_1 = \Theta_2$ provided that $K_d = K_N^l = K_N + K_1 + K_2$. In other words, on a linear path, the tangential directions of P_N , P_{L1} , and P_{L2} are equal to each other, and thus, the control effect of the parameters $\{K_N, K_1, K_2\}$ is equivalent to

$$K_N^l = K_N + K_1 + K_2. \quad (12)$$

On an arc, the heading angle of look-ahead point compared to the heading angle of the closest point contains curvature information and it is useful to compensate the centrifugal force along a circular path by optimally distributing the sum among the coefficients $\{K_N, K_1, K_2\}$. The non-holonomic kinematic constraint to track the arc is $\delta = \tan^{-1}(l / \rho)$, where, l is the wheelbase and ρ is radius of the path curvature. Let the system use a 1-LARP, $L_2^c = L_2$, i.e., $L_1=0, K_1=0$. Let the radius of the desired circular path be ρ . Assume that the rear tyre tracks the desired path almost tangentially, which is valid since C_r is much higher than C_f . In Tables 1 and 2 examples of these parameters of corresponding references are given. According to Bevly 2001 (p12), $-C_f \alpha_f - C_r \alpha_r = m(\dot{v}_y + \dot{\psi} v_x)$. For perfect tracking of the arc $d_N = 0$, $\theta_N = 0$, and $\alpha_r = \dot{\psi} l_r / v - \beta = 0$, where $v = v_x / \cos \beta$ and $\dot{\psi} = v_x / \rho$. Therefore $\beta = \tan^{-1}(l_r / \rho)$. The slip angle due to the centrifugal force $F_c = mv^2 / \rho = -C_f(\delta - \beta - \dot{\psi} l_f / v) \cos \delta$ is compensated by the control term $\delta^c = K_2^c \theta_2$, where $\theta_2 = L_2^c / \rho$. Consequently, the sum of the slip angle and the kinematic constraint of vehicle movement is balanced by

the feed-forward action of the control law when the control parameters satisfy the constraint (13).

$$K_2^c L_2^c = \cos(\tan^{-1}(l_r / \rho))l - \frac{m_{veh} v_x^2}{C_f \cos(\tan^{-1}(l / \rho)) \cos^2(\tan^{-1}(l_r / \rho))}. \quad (13)$$

In a 2-LARP system, the effects of both the first and the second look-ahead points are similar and additive, and therefore their cumulative effects are,

$$K_2^c L_2^c = K_1 L_1 + K_2 L_2. \quad (14)$$

to compensate the steer angle deviation for a perfect tracking condition. Equation (13) indicates that only a 1-LARP is sufficient to compensate the steer deviation due to the lateral centrifugal forces and resulting side slip angle.

In the proposed control law, the second look-ahead point is introduced to compensate for lateral positional deviations at the curvature transition sections. Let the look-ahead distance L_2^c be partially in the arc with length L_c . Then, $L_2^c - L_c$ remains in the linear part. At this instant the control law applies a compensation for the circular path proportional to L_c . The full compensation is developed when the rear axis passes to the circular section. For the 2-LARP case, since $L_1 < L_2$ the compensation effect of L_2 starts at a different time instant compared to L_1 , but their full effect starts after the nearest point P_N and both look-ahead points P_{L1} and P_{L2} enter the circular path. That is, the effect of each look-ahead point appears different in phase at the curvature transitions, and therefore their compensative effects at the transition are independent. Consequently

the controller gains K_1 and K_2 can be optimized to reduce the peak deviations which are observed at the curvature transitions.

4.4 Controller gains relation with the LARP distances

In order to come up with an enhanced controller the values of its parameters must well set. Since change in one parameter must done carefully with respect to change in others and whereas the linear relation can be obtained thus iterations can take over. In other words, the whole system has four controller gains and two distance parameters thus totally six variables. The objective is determine the minimum error because the main purpose of the steering control system within the present study is the path tracking which most likely deals with the accuracy of the tracking. Therefore two cost functions will be developed as root mean square error (RMS) and peak error (lateral deviation).

The sequence is in such a way that first the minimum RMS error must be found and on top of that the second cost function as the minimum peak error should be satisfied. It was observed during the simulation iterations on a U-turn that possesses three constant radius parts and acts over time as a pulse function, the error is generated as an off-set along the arc and overshoots on curvature transitions. The characteristics of the transition error and the analysis as well the treatments which are the main target of the proposed path tracking controller will be discussed in details within the upcoming sections. Subsequently, here it is intended to demonstrate the system parameters relations via simple illustrations. By setting the $(K_d, K_N, K_2) = (1, 1, 0)$ it is possible to display the relations among the RMS and peak errors with K_I and L_I via three dimensional plots as shown in Figure 11 and Figure 12, respectively.

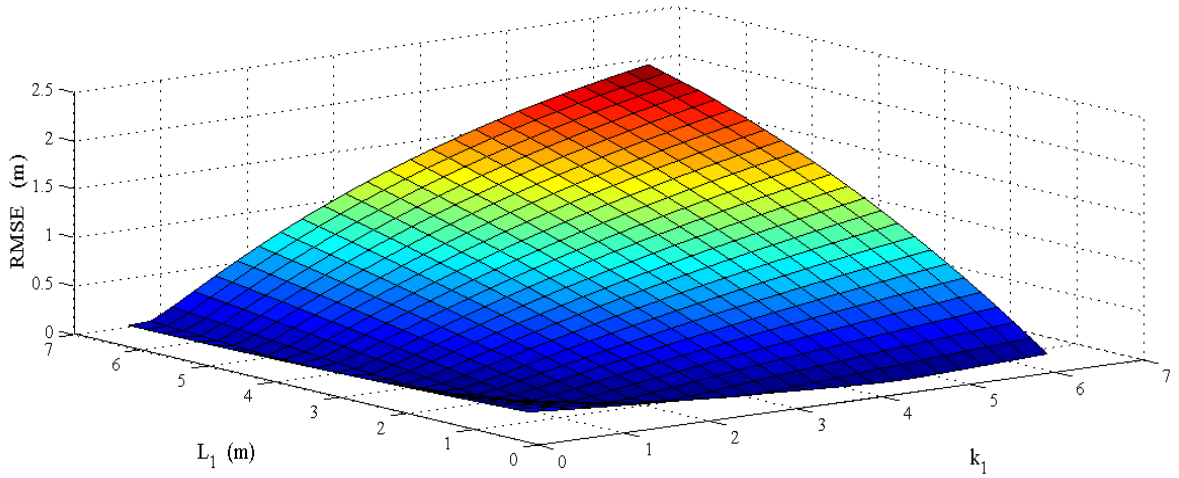


Figure 11: The relation between K_I and L_I with RMS error values

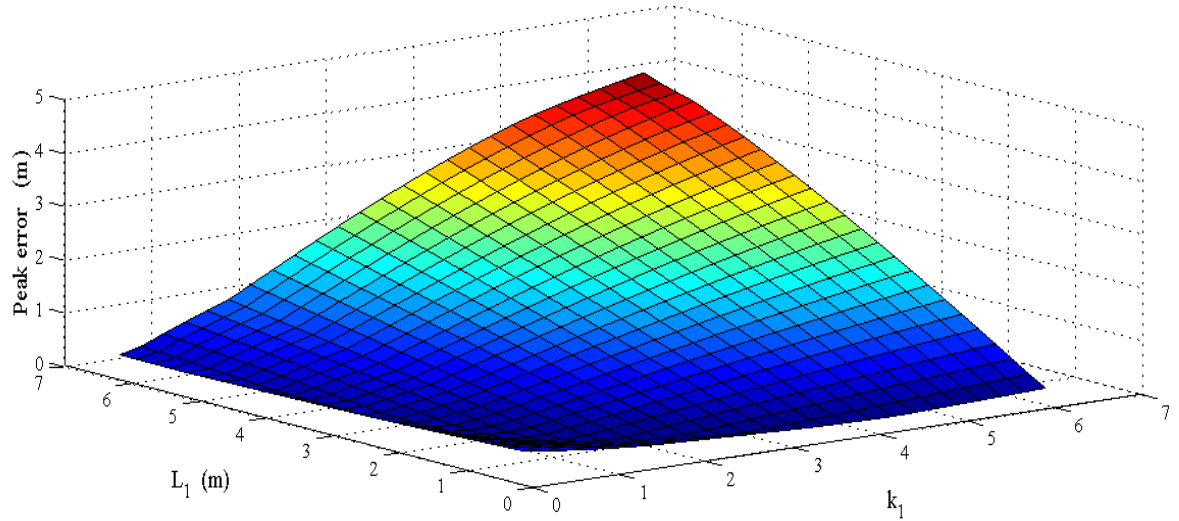


Figure 12: The relation between K_I and L_I with peak error values

4.5 Open loop transfer function on linear paths

The linear state space representation of the vehicle on a linear path is given by Gartley (2005, pages 10 and 11)

$$\dot{x}_p = A_g x_p + B_g \delta; \quad (15)$$

where $x_p = \begin{bmatrix} v_y \\ r \end{bmatrix};$

$$A_g = \begin{bmatrix} -2(C_r + C_f)/(m_{veh} v_x) & 2(l_r C_r - l_f C_f)/(m_{veh} v_x) - v_x \\ 2(l_r C_r - l_f C_f)/(I_z v_x) & -2(l_r^2 C_r + l_f^2 C_f)/(I_z v_x) \end{bmatrix};$$

$$B_g = \begin{bmatrix} 2C_f / m_{veh} \\ 2L_f C_f / I_z \end{bmatrix}.$$

For the complete plant model, the integral of v_y is necessary to obtain d_N , and an actuator model is necessary to drive the vehicle model. With the state $x = (v_y \ \Theta \ d_N)^T$ the coefficient matrices of the state space model $\dot{x} = Ax + B\delta$ is obtained as

$$A = \begin{bmatrix} \frac{-2(C_r + C_f)}{m_{veh} v_x} & \frac{2l_r C_r - 2l_f C_f - m_{veh} v_x^2 - 2C_f K_N v_x}{m_{veh} v_x} & -2C_f K_D / m_{veh} \\ \frac{-2(-l_r C_r + l_f C_f)}{I_z v_x} & \frac{-2(l_r^2 C_r + l_f^2 C_f + l_f C_f K_N v_x)}{I_z v_x} & -2l_f C_f K_D / I_z \\ 1 & 0 & 0 \end{bmatrix};$$

$$B = \begin{bmatrix} 2C_f / m_{veh} \\ 2L_f C_f / I_z \\ 0 \end{bmatrix} \quad (16)$$

With the parameters in Table 1 it corresponds to the transfer functions

$$\frac{d_N}{\delta} = \frac{24.2522 (s + 91.69)}{s (s + 86.74) (s + 20.03)}$$

and

$$\frac{\Theta_N}{\delta} = \frac{14.8659 (s + 75.79)}{s (s + 86.74) (s + 20.03)} \quad (17)$$

The transfer function of the simulated actuator has parameters specified by Derrick and Bevely (2008) as

$$\frac{\delta(s)}{\delta_{des}(s)} = \frac{3103}{(s + 4.694)(s^2 + 31.3s + 661.1)} \quad (18)$$

and the overall plant has the transfer functions

$$\frac{d_N}{\delta_{des}} = \frac{75254 (s+91.96)}{s(s+86.74)(s+20.03)(s+4.694)(s^2+31.3s+661.1)}$$

$$\frac{\Theta_N}{\delta_{des}} = \frac{46129 (s+75.79)}{(s+86.74)(s+20.03)(s+4.694)(s^2+31.3s+661.1)} \quad (19)$$

The stability analysis of the system on a linear or circular path is possible by using these 6th order transfer functions with the feedback control

$$\delta_{des} = K_d^l d_N + K_N^l \Theta_N. \quad (20)$$

Chapter 5

SIMULATION PLATFORM AND CONTROLLER PARAMETER OPTIMIZATION

5.1 Modern off-road operation and automation

Empirical field tests on farm applications are tedious, hazardous, and costly. Simulation tests are not only cost-effective but also precisely observable, and they provide rapid estimation of the efficiency of the proposed methods.

In addition to the simulations to optimise the control law parameters, extensive numerical simulations were conducted in MATLAB using the same set of parameters and field test data previously presented by Lenain et al. (2007), Rovira-Mas et al. (2010) and Fang et al. (2011), which are also similar to the parameters and constraints presented by Norremark et al. (2008) on a GPS-based system for weed control.

5.2 Simulation Platform and Agricultural Vehicle Parameters

The simulation platform used in this study is mainly used to optimize the control parameters, and then to examine the reliability, manoeuvrability, and tracking accuracy of an agricultural vehicle, along with testing the proposed control method on some path tracking scenarios. The dynamic equations (2-5), the deviations from the path (8-9) and the control law were numerically solved in MATLAB using 1ms time steps for the hydraulic actuator model, 10 ms time steps for the vehicle model, and 50 ms time steps

for the control action to simulate the vehicle kinetics and kinematics quantitatively and qualitatively.

The simulations are carried out using “CLAAS Renault *ARES* 640” and “John Deere 8420” farm tractor parameters listed in Table 1 and 2 which were also used in the field experiments by Lenain et al. (2007) and Derrick and Bevly (2008), respectively.

5.3 Test Path

In the simulations, a synthetic test path was used, which is comparable to the agricultural test paths used in the literature. It contains typical important path features of agricultural applications such as long linear regions followed by sharp circular turns. It comprises a U-turn with a 7 m radius in between two straight regions (Figure 13). Similar paths were used by Lenain et al. (2006). The verification of the simulation program and the determination of the settings for the disturbance parameters were carried out to determine the performance of their control law.

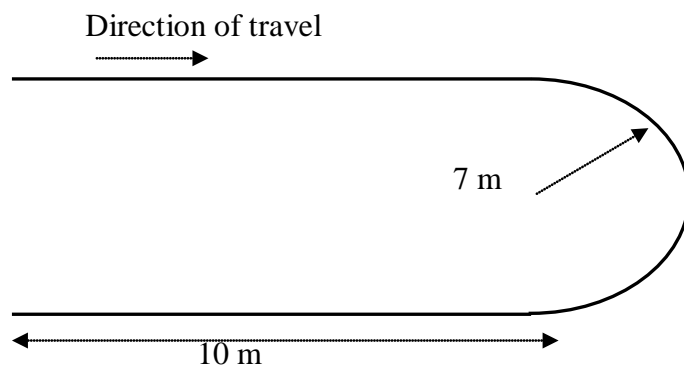


Figure 13. Top view of the test path to observe the performance of the controller. This path is similar to the path used by Lenain et al. (2006).

5.4 System Identification for the Dynamic Simulations

Using equations 1 – 7 the dynamic model was simulated over specific duration, times intervals and along desired arbitrary path. In order to get sufficient similarity within the bandwidths of agricultural vehicle, terrain and operation conditions the parameters are obtained and tuned. The detailed procedure will be discussed in section 6.2.

5.5 Optimization Method

The controller parameters of the proposed control law are L_1 , L_2 , K_N , K_d , K_1 , and K_2 . Design methodology based on linear models is not suitable because the system is highly nonlinear and number of parameters is large. Therefore it was preferred to search all practically possible values of these six parameters with the constraints (12) and (14) to satisfy the same stability conditions on the linear and circular paths. Among many brute-force search trials, the following four search steps may give insight on a possible systematic search to determine the best performing control parameter sets for 1 and 2-LARP cases. Figure 14 represents the overall algorithm behind the optimization used in this study.

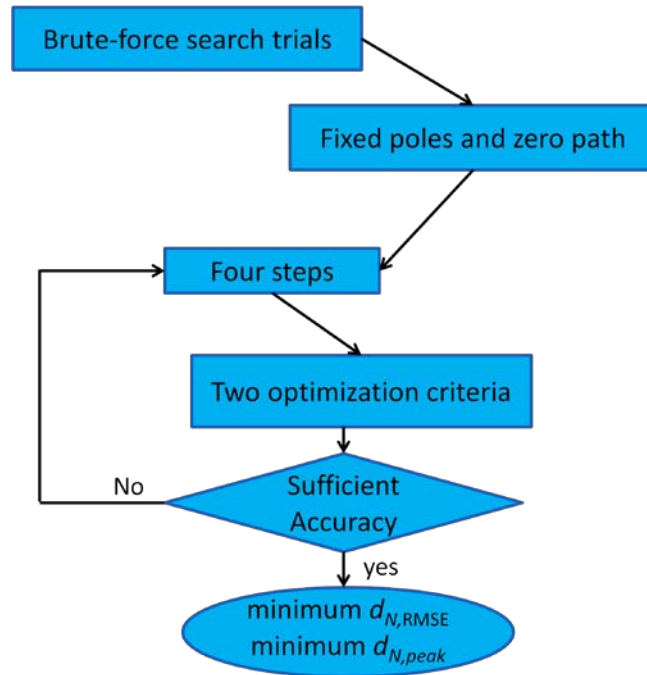


Figure 14. The overall algorithm of the optimization

a) Set $(L_1=0; L_2=0, K_1=0, K_2=0)$, and search for $\{K_N^l, K_d^l\}$ pairs that minimize $d_{N,RMSE}$ along the initial linear part of the test path starting with a 0.1 m initial d_N as a disturbance for the step responses. The best parameters $\{K_N^l=5.6, K_d^l=3.0\}$ were obtained by scanning both parameters in the range $[0, 20]$ in steps of 0.02. The lateral error of the resulting system is shown in Figure 15. Keeping $K_N^l=5.6$ constant, the root locus of the system for the feedback K_d is shown in Figure 16, and the linear system is stable in the range $0 < K_d < 20$.

b) Set $(L_1=0, K_1=0, K_d=3.0)$ and search for $L_2^c=L_2$ and $K_2^c=K_2$ under the constraint (12) that minimise $d_{N,RMSE}$ along the steady state part of the circular section. The

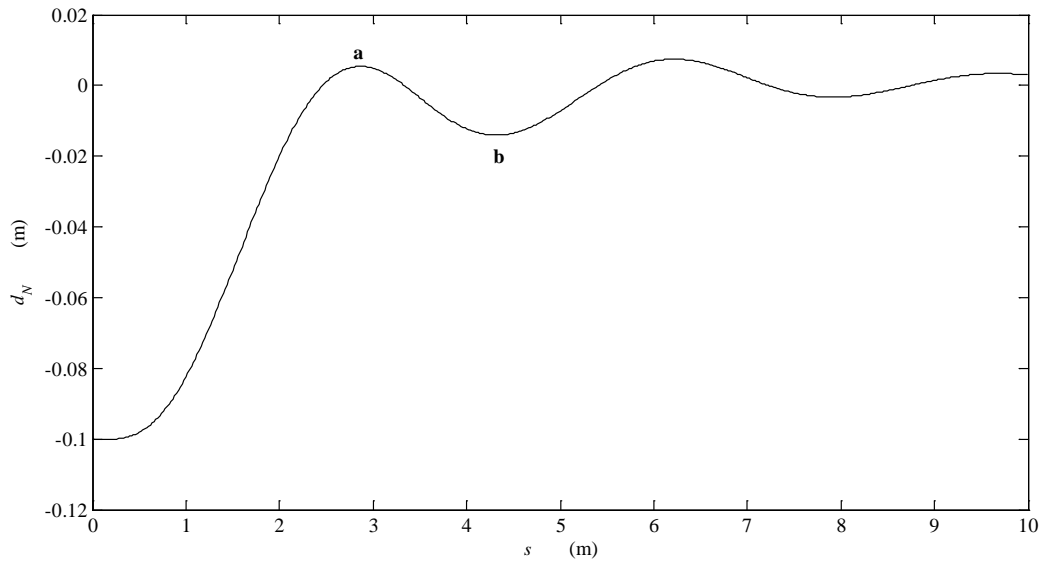


Figure 15. Step response of lateral error control for minimum $d_{N, RMSE}$ case without using LARP. The amplitude of the applied step is 0.1 m. The peak and opposite peak points are marked by a and b.

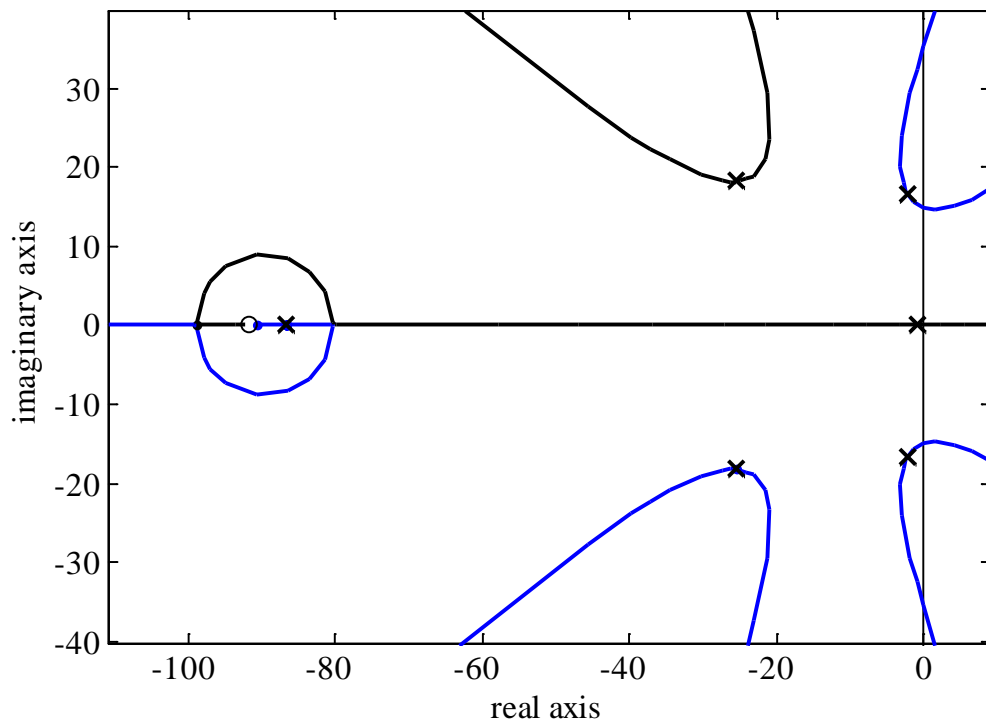


Figure 16. Root locus plot for the overall system. The circle marks the zero, and the crosses are the poles of the system with the minimum $d_{N, RMSE}$ along a 0.1 m step response.

minimum $d_{N, \text{RMSE}} = 1.2$ mm is obtained with the parameters $L_2 = 1.0$ m, $K_2 = 2.28$, and $K_N = 3.32$ giving $d_{N, \text{peak}} = 22.4$ mm. This test concludes that, under the simulation conditions, $K_2^c L_2^c = 2.28$. The poles ($p_1 = -86.6$, $p_{2,3} = -25.4 \pm 18.2i$, $p_{4,5} = -2.17 \pm 16.5i$, $p_6 = -0.8788$) of the closed loop system are marked in Figure 16. The linear system is stable since the real parts of all poles are in the negative half-plane.

c) Set ($L_1 = 0$, $K_1 = 0$), and search L_2 , K_N , and K_d , around the setting $L_2 = 1.4$, $K_N = 2.37$, $K_d = 2.2$, for minimum $d_{N, \text{peak}}$, using only constraint (14) to calculate K_2 , results in optimum parameters $L_2 = 1.4$, $K_N = 7.7$, $K_d = 0.44$, and $K_2 = 1.6286$ reducing $d_{N, \text{peak}}$ to 14.6 mm, as listed in Table 3 case (c). However the response tends to be sluggish and $d_{N, \text{RMSE}}$ increases to 2.5 mm. Releasing the constraint (12) shifts K_N^l to 9.33, and the poles of the controlled system to ($p_1 = -86.6$; $p_{2,3} = -28.4 \pm 19.7i$; $p_4 = -0.081$; $p_{5,6} = 0.33 \pm 19i$) (Figure 17 and Figure 18). The linear system becomes unstable because of the poles with positive real part. Most probably its effect is not fully observed in the simulation because of the limited linear and circular distances of the test path. Since the optimised result of (c) is unstable, it can be concluded that 1-LARP system with best RMSE performance is obtained in case (b) with 22.4 mm peak error (Figure 20).

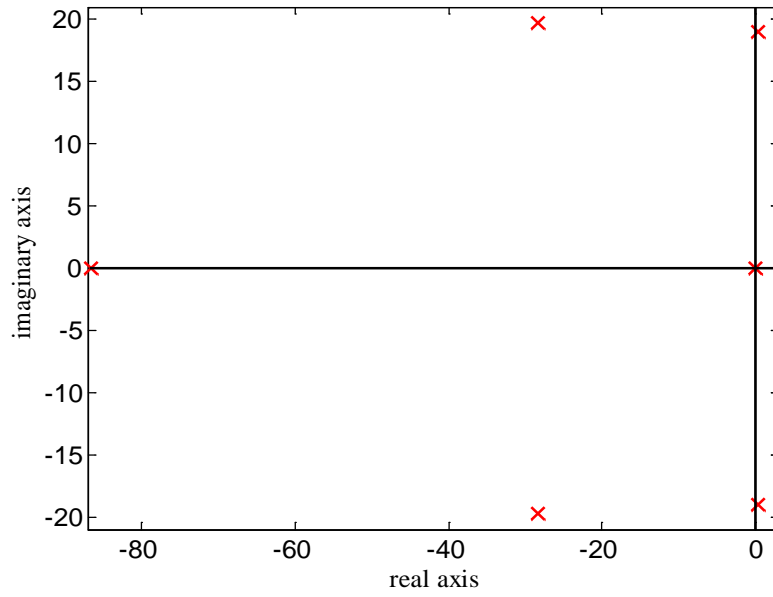


Figure 17. Root locus plot of the poles caused by the controller parameters found in the third step, non-constrained search for best peak lateral error.

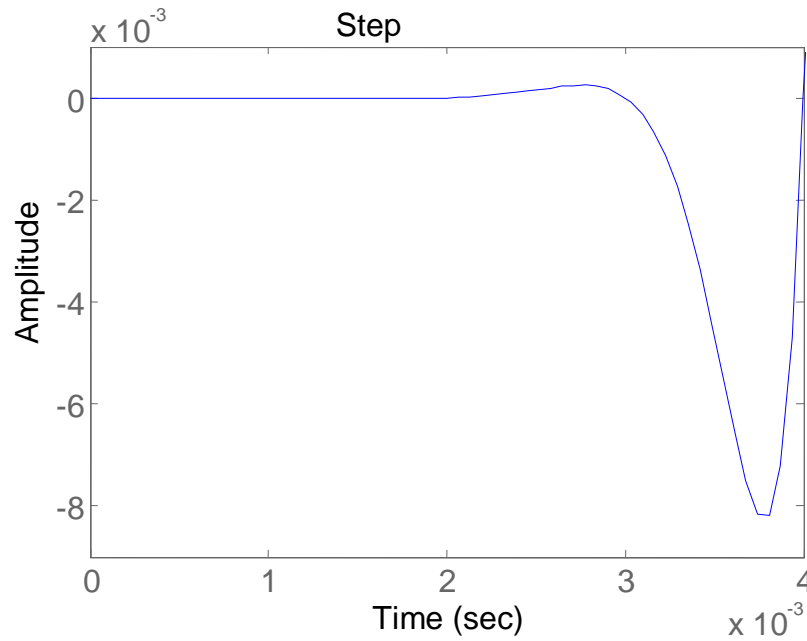


Figure 18. Step response of the linear system from the controller parameters found in the third step, non-constrained search for best peak lateral error.

d) Set $K_d=3$ and search L_1 , L_2 , and K_I values that minimise $d_{N,peak}$ with both constraints (12) and (14), i.e., $K_N=K_N^d -K_1-K_2$ and $K_2=(K_2^c L_2^c -K_1 L_1)/L_2$. The closed loop poles of the linear model remains unchanged because both constraints (12), and (14) are satisfied.

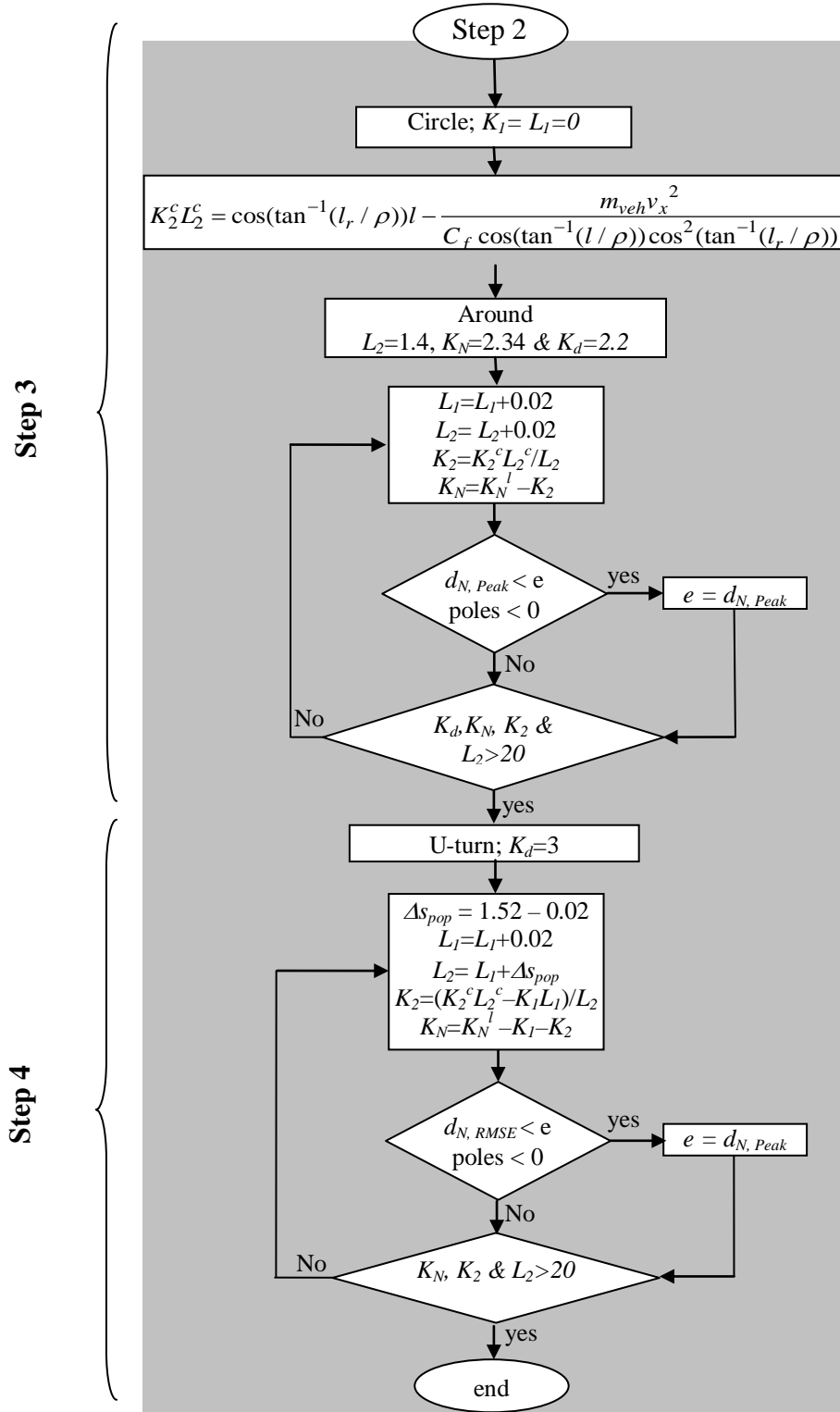


Figure 19. Schematic flowchart of the third and fourth steps of optimization algorithm (complete flowchart of all steps is brought in appendix A)

In Figure 15 and Figure 20, the curvilinear distance from the peak point (a) to the opposite peak (b) is $\Delta s_{pop}=1.5$ m. Accordingly two LARPs with a distance $L_2-L_1=\Delta s = 1.5$ m shall have opposite effects because of 180 degrees phase shifted actions. The 2-LARP parameters with minimum peak error satisfying both constraints are found $L_1=-0.7$; $L_2=0.73$; $K_N=0.90$; $K_D=3.0$; $K_1=1.644$; $K_2=4.7$; resulting in $d_{N,peak} =4.42$ mm and $d_{N,RMSE} =1.5$ mm. The distance $L_2-L_1=1.43$ m slightly deviates from the expected distance. It might be because the system is nonlinear. Indeed, in Figure 20, the response of 2-LARP control displays $\Delta s_{pop} =1.15$ m instead of 1.50m.

The resulting plots of lateral errors at the curvature transition are shown in Figure 20 to compare d_N of the 1-LARP (dotted line) and 2-LARP (solid line) control, and, the optimum parameters are listed in Table 3. Accordingly, using the second LARP contributes to the performance of the system by reducing the peak lateral deviations at the curvature-transition to one fifth of the 1-LARP case.

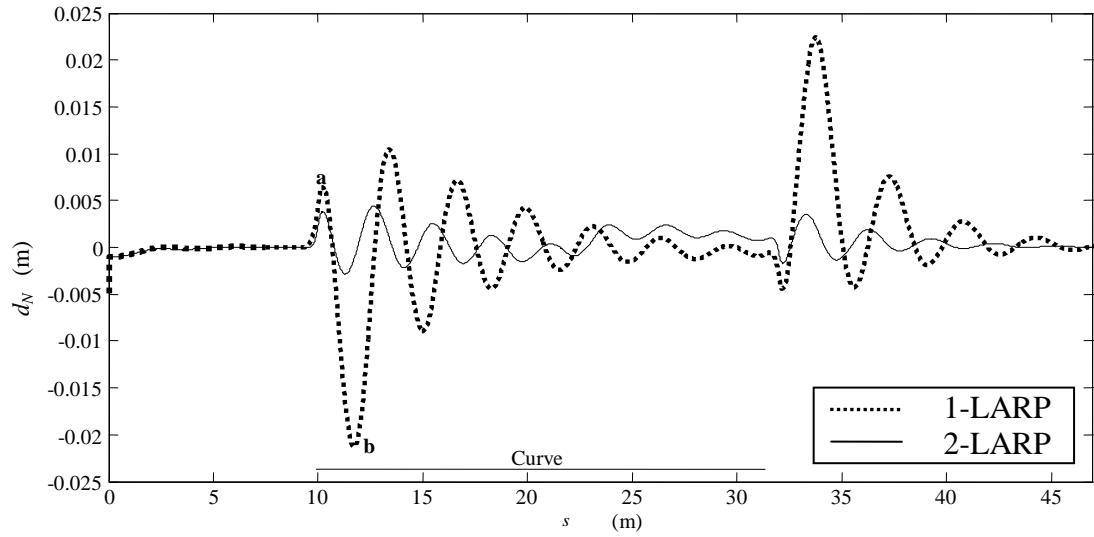


Figure 20. Lateral displacements of the systems with the best parameters for case b (dotted line) and for case (d) along the test path with 7 m circular section from $s=10$ to $s=32$. The peak and opposite peak points are marked by a and b.

Chapter 6

APPLICATIONS, RESULTS AND VALIDATION

6.1 Overview

In the modelling and control strategy chapters number of formulations has been presented. Indeed, the steering system possesses many parts and in each, variety of parameters which work collectively to serve the purpose of desired steering system behaviour in a fashion that the designer of the controller desires. Therefore, in this chapter, the accuracy, usefulness, effectiveness and importance of the presented formulations were demonstrated by the aid of numerous diagrams using the overall framework provided by Ozada (2008). The aim of representing the graphs in this section is to graphically evaluate the criteria in the following research questions;

- 1- Does the implementation of the proposed method feasible for typical land vehicle system?
- 2- Will the system exhibit similar behaviour if the same parameters values are applied?
- 3- How much non-linearity may be caused by introducing the new method to the conventional system?
- 4- Will the stability stay in the required thresholds by controlling the lateral error overshoot and decaying oscillations? In addition, does that limit the manoeuvrability?
- 5- Does the proposed method provide sufficient accuracy?

- 6- What is the effect of 2-LARP controller on the peak error value at curvature transition compared to the results obtained in similar studies?
- 7- Most importantly, how much improvement will be produced quantitatively, if a particular off-road application is addressed?

Hence, this chapter is devoted to visualizing the performance by graphically answering the above questions as well as the evaluation of steering parameters illustration within a full tracking of a single given path tracking test. In addition, it is attempted to show the relation among parameters more clearly. Furthermore, the approaches for parameters determination and stability concerns are further supported by the aid of diagrams. These diagrams show changes in the main parameters value and the system performance according to the variation of the corresponding parameters.

6.2 Verification of the dynamic simulation platform

The following control law stated by Lenain, et al. (2006) is coded into the dynamic simulator with the original system parameters, enlisted in Table 1 adopted from Lenain, et al. (2006),

$$\delta(y, \tilde{\theta}) = \arctan\left(L \left[\frac{\cos^3 \tilde{\theta}}{(1-c(s)y)^2} \left(\frac{dc(s)}{ds} y \tan \tilde{\theta} - K_d(1-c(s)y) \tan \tilde{\theta} - K_p y + c(s)(1-c(s)y) \tan^2 \tilde{\theta} \right) + \frac{c(s) \cos \tilde{\theta}}{(1-c(s)y)} \right] \right), \quad (21)$$

where, s is the curvilinear abscissa and $C(s)$ indicates the curvature at that abscissa and is equal to the one over the radius of curvature in this study. Moreover, $\tilde{\theta}$ represents the angular deviation of the vehicle with respect to the reference path and y represents the lateral deviation. Hence the state of the system can be represented as $(y, \tilde{\theta}, -s)$.

Table 1: Verification parameters of CLAAS Renault ARES 640

Parameter	Value	Parameter	Value
C_f	34378 N rad ⁻¹	l_f	1.88 m
C_r	71620 N rad ⁻¹	l_r	1 m
I_Z	11051 kg m	m_{veh}	8000 kg

Table 2: Simulation Parameters of John Deere 8420

Parameter	Value	Parameter	Value
C_f	137510 N rad-1	l_f	1 m
C_r	286479 N rad-1	l_r	2 m
I_Z	18500 kg m	m_{veh}	11340 kg

where $(y, \tilde{\theta}, -s)$ corresponds to $(-d_N, \Theta, s)$ of this study. K_d and K_p are 0.6 and 0.15, respectively, and $C(s) = 1/\rho$.

The dashed line in Figure 21 shows the lateral deviation obtained by Lenain et al. (2006), and the solid line is the result of simulated motion on the simulation platform by applying the control law (21) reported by Lenain et al. (2006) as a disturbance-free test. The minor deviation between the two traces can be explained by the differences in the

disturbances, which are effective in the field test, but neglected in the simulation model as well as absence of anti-roll bar (GPS sensor mounted on the top of cabin).

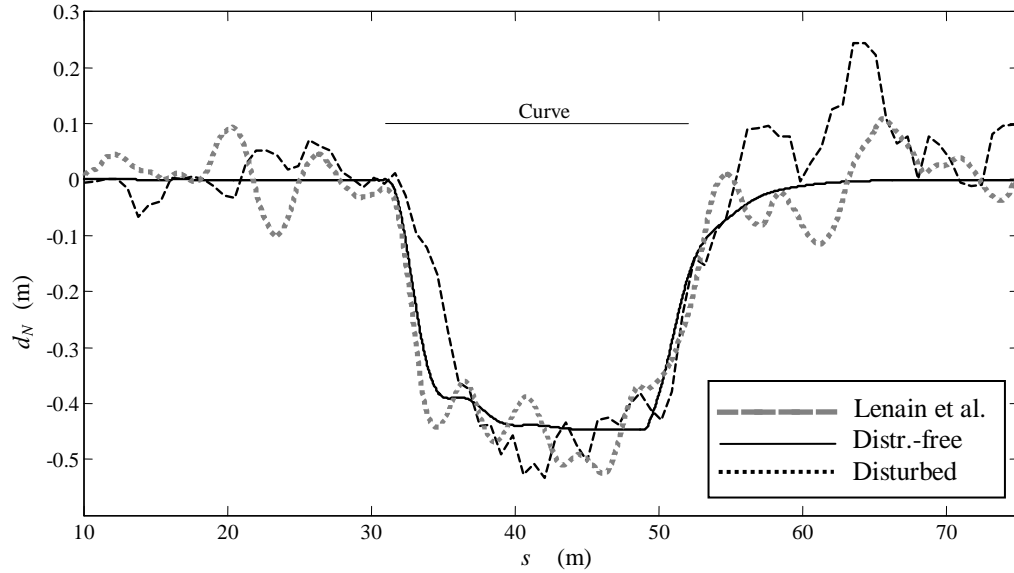


Figure 21. Comparison of the lateral errors reported by Lenain et al. (2006) (dashed line) and the tested platform with the control law (16). The solid line is obtained disturbance-free response and the dotted line is with the applied disturbances.

Obviously, the cited field test results have random deviations due to the nature of the terrain irregularities and GPS noise. The dotted line $d_{N,dis}$ is obtained according to (6) by injecting a soil disturbance into the simulated equation of motion using a disturbance function $a_{F,dis} = 0.9$ and $a_{M,dis} = 0.73$ and sample time of 0.1 s which corresponds to randomly sized soil clods distributed every 0.22 m for $v = 8 \text{ km h}^{-1}$ to approximate the amplitude and the pattern of the disturbances of the typical deviations observed by Lenain et al. (2006).

6.3 Nonlinearity Comparison in Controller Parameters Formulation

Steering system presented in this study is highly nonlinear and it uses six parameters. It is beneficial to observe the interrelation among parameters to observe the level of nonlinearity and compare it with similar studies represented in the literature.

Hence, for the sake of brief observation of the relation introduced by the steering system and interaction among steering parameters, it is required to fix four of the parameters and then continue on the relation of two of them with the lateral error.

Figure 22 and Figure 23 demonstrate the nonlinear relation between lateral deviation and orientation deviation gains with peak and RMSE value of the lateral error, respectively while $k_1 = l_1 = 1$ and $l_2 = k_2 = 0$.

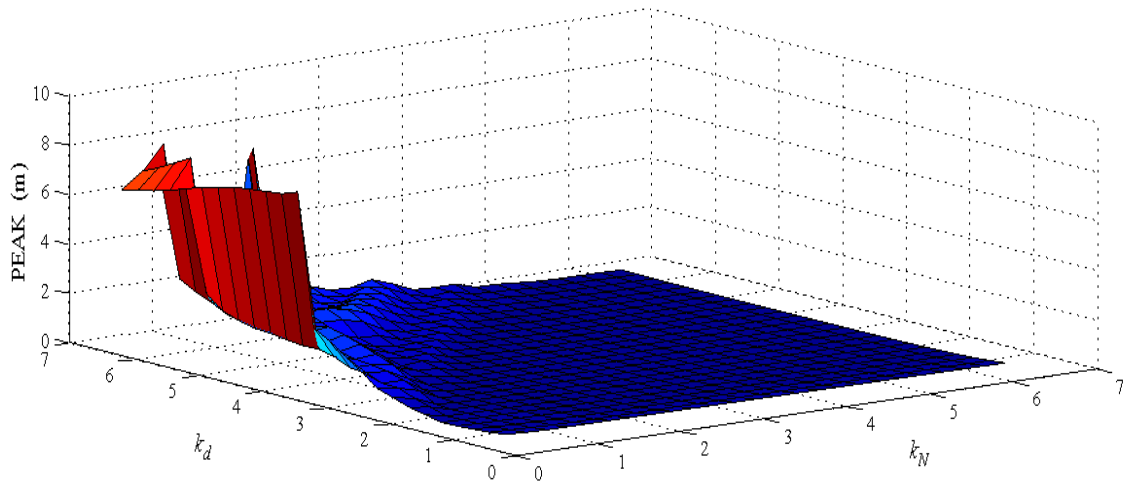


Figure 22. Relation between lateral deviation and orientation deviation gains with peak value of the lateral error.

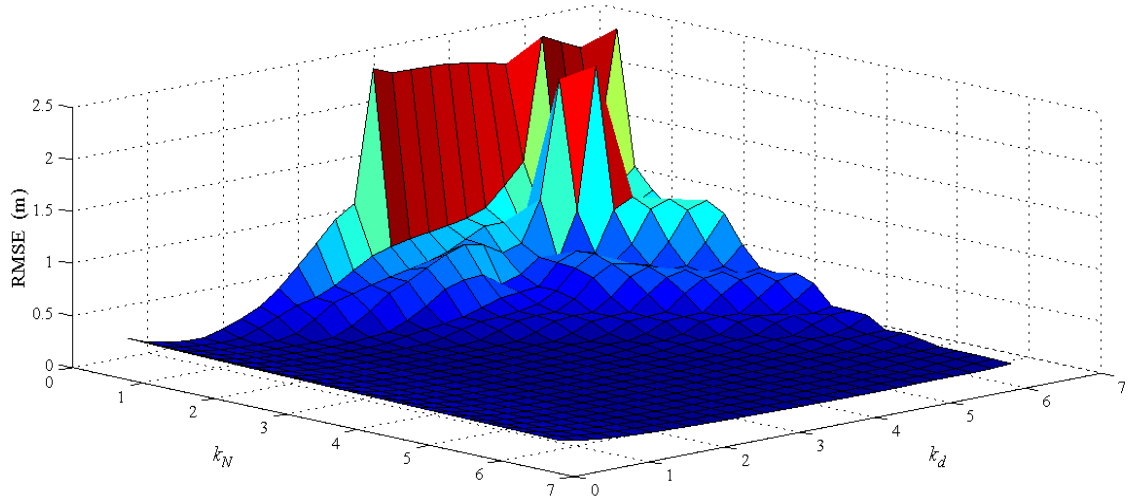


Figure 23. Relation between lateral deviation and orientation deviation gains with RMSE value of the lateral error.

The importance of parameters of k_d and k_N is defining constraints for the optimization of the rest of the parameters such as look ahead distances l_1 and l_2 . Tuning these look ahead reference points distances, l_1 and l_2 are very significant since if they are well set then the centrifugal force will remarkably reduces. Indeed, setting the above distances correctly means that two feedforwards from the look ahead reference points (LARPs) can cancel out mutual lateral undesired forces through sole control variable of δ (steer angle). Figure 24 and Figure 25 depict the relation between look ahead point distances, l_1 and l_2 with peak and RMSE values of the lateral error, respectively, while $k_d = k_N = k_1 = k_2 = 1$.

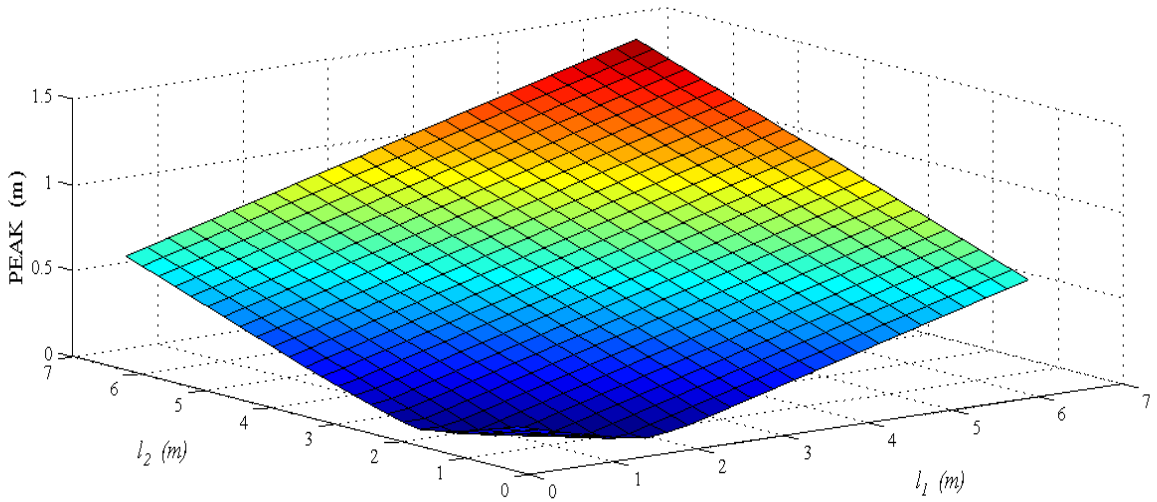


Figure 24. Relation between look ahead point distances, l_1 and l_2 with peak values of the lateral error, while $k_d = k_N = k_I = k_2 = 1$.

Comparing Figure 22 - Figure 25 with the controller parameters relation generated in studies done by Lenain et al. (2006), and Fang. et al. (2001) the level of nonlinearity is higher however the control law is much simpler.

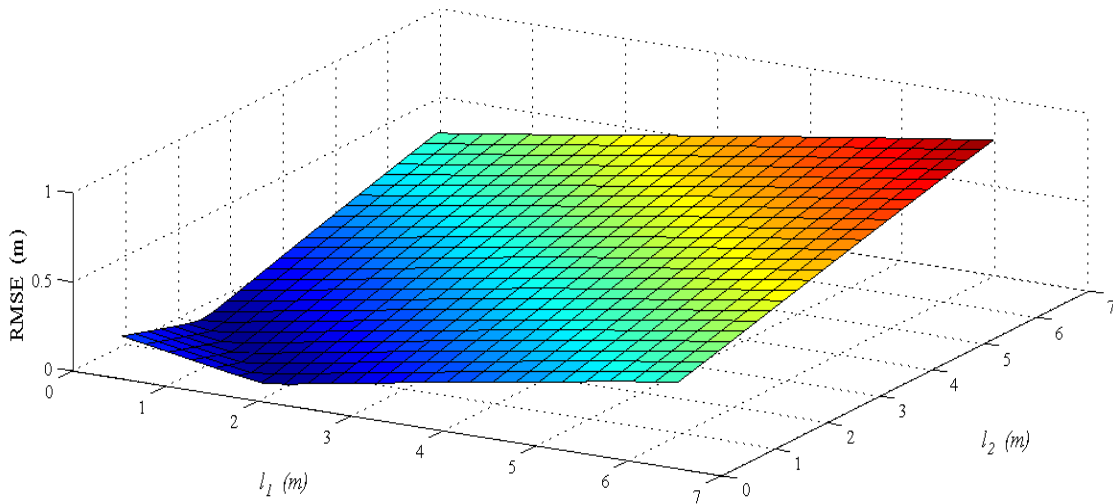


Figure 25. Relation between look ahead point distances, l_1 and l_2 with RMSE values of the lateral error, while $k_d = k_N = k_I = k_2 = 1$.

To observe the effect of each parameter variation on the system tracking accuracy response, Figure 26 - Figure 28 **Error! Reference source not found.** depict second LARP gain and distance variation in the control law. Comparing this figure with Thuilot, et al. (2002), it can be observed that 2-LARP is more sensitive even at linear system case.

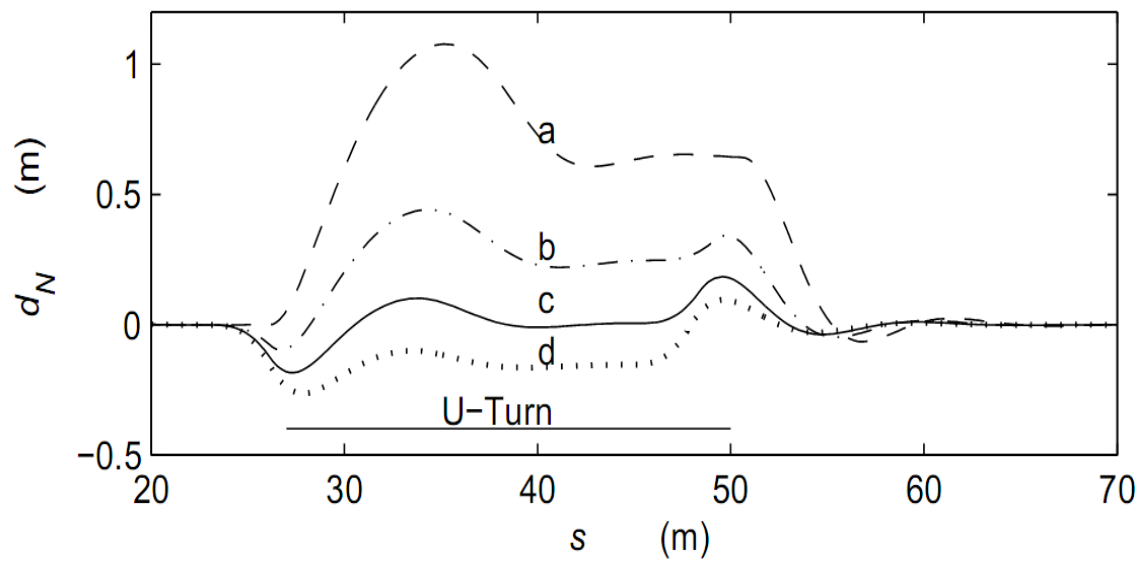


Figure 26. Centrifugal force compensation tests on a circular path of $\rho=7$ m, with $K_I=0$, $K_d=0.6$, and $K_0=2-K_2^c$, for four cases of K_2^c , (a) $K_2^c=0$, (b) $K_2^c=0.5$, (c) $K_2^c=0.8$, (d) $K_2^c=1.0$.

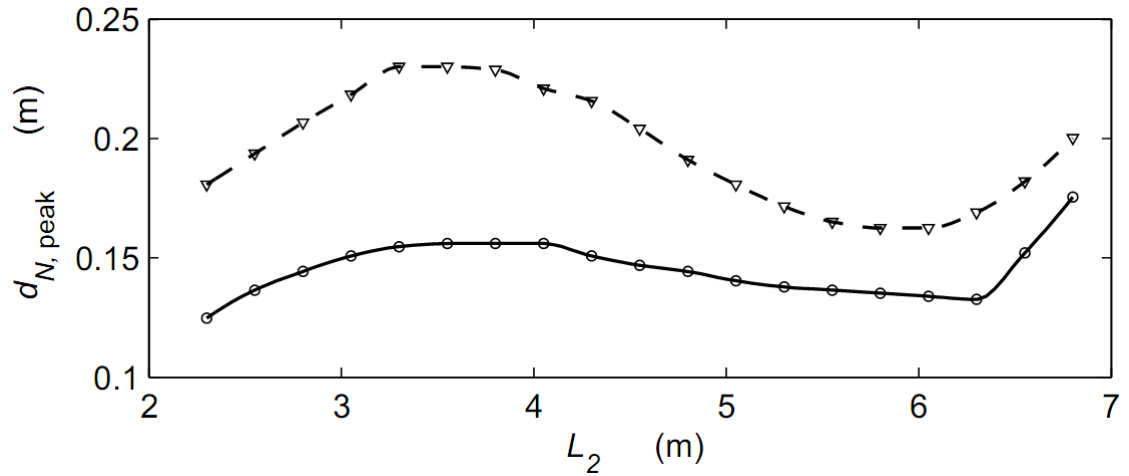


Figure 27. Effect of second LARP distance on the peak lateral deviation $d_{N, peak}$; the solid curve is for 8 kmh^{-1} and the dashed curve is for 11 kmh^{-1} forward speeds.

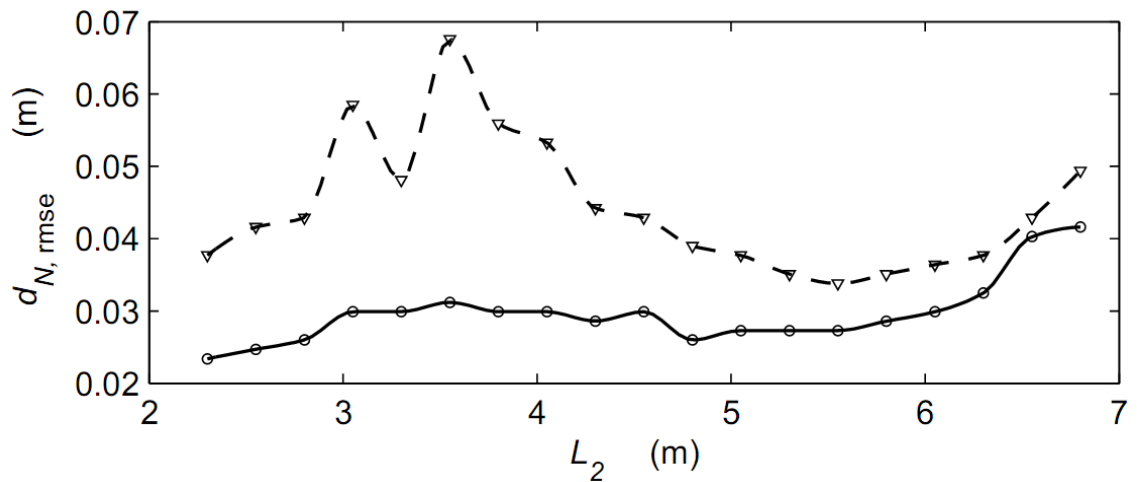


Figure 28. Effect of second LARP distance on the mean lateral deviation, $d_{N, RMSE}$; the solid line is for 8 kmh^{-1} , and the dashed line is for 11 kmh^{-1} forward speed.

6.4 Evaluation of Step Responses of the system

Step response of the system is very significant in system analysis since the error behaviour will be clearly observed and basically evaluated. Therefore, a set of simulation tests were designed for the simulation of the dynamic equations on a linear path with a 2.5 m initial lateral deviation to obtain the lateral step response of the system

with the equivalent control law (equation 20) having zero disturbance and soil grip conditions variation. Figure 29 displays the saturation of the system in response to such a large deviation under the chosen controller coefficients. Furthermore, while the systems parameters are time-varying, the stability can be verified via the response of the system to change in parameters and observing the performance. This response can be compared with no implement experiment presented by Derrick and Bevly (2008), to observe the tracking enhancement of angular corrective gain, K_N .

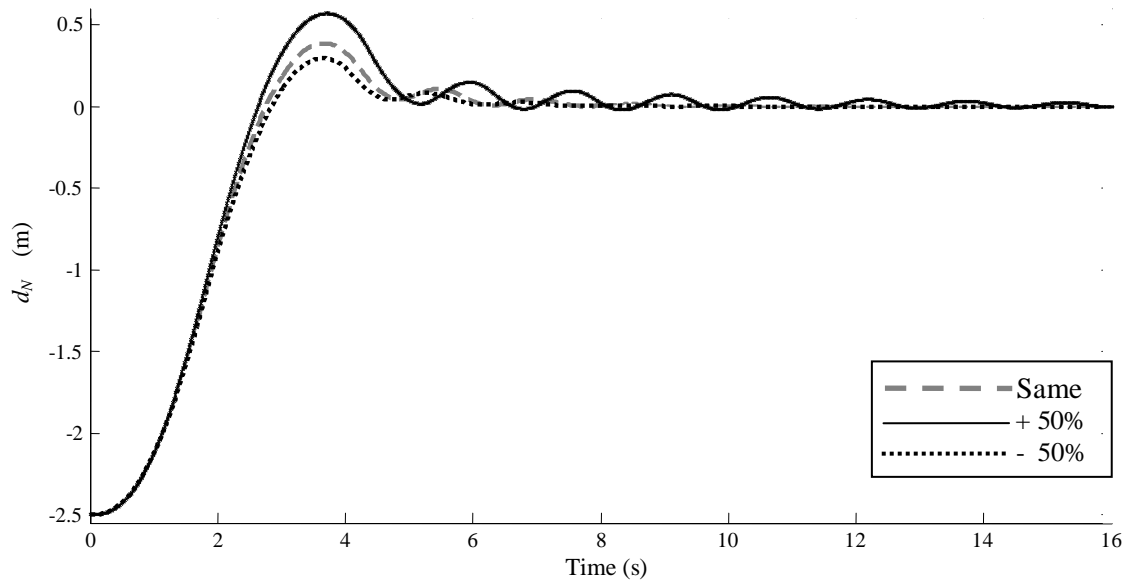


Figure 29. Step response of the disturbance-free system to 2.5 m initial deviation, travelling over soil profiles with different grip conditions. Comparable with no towed implement experiment of Derrick and Bevly (2008), with cornering stiffness of $(C_r, C_f) = (286479, 137510)$ N/rad. Grey dashes line: same coefficients. Dotted line: 30% increase in those coefficients. Thick black line: 30% decrease in those coefficients.

For the sake of basic comparison of the simulation bed of this study and the experimental setup of Lenain et al. (2005) along their linear part test, Figure 30 is provided which in brief represents the same system response applying the same parameter values.

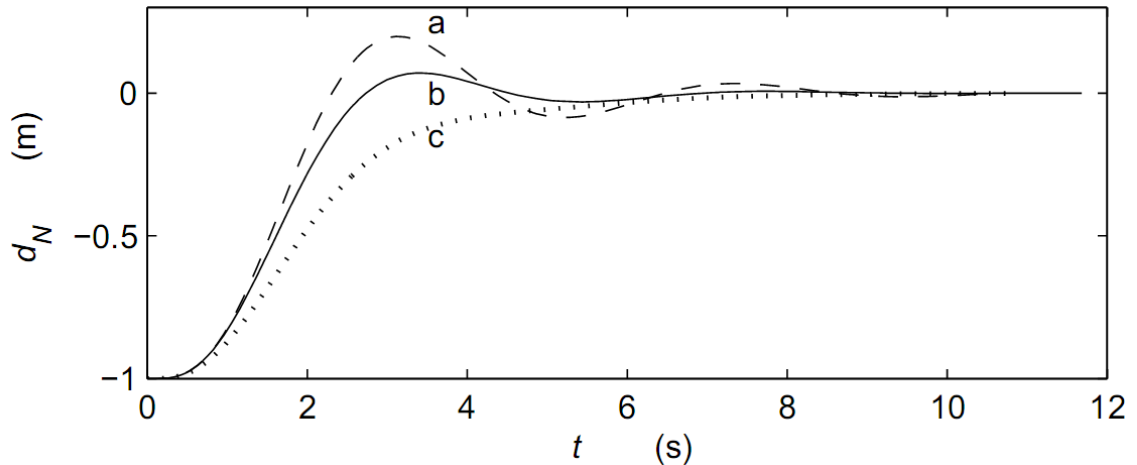


Figure 30. Step response of the closed loop system with $d_N = 1$ m initial lateral deviation for controller settings $K_N^l = 2.0$, ($K_1 = K_2 = 0$) and (a) $K_d^l = 0.4$, (b) $K_d^l = 0.6$ (c) $K_d^l = 0.8$.

6.5 Steer-Ability Evaluation for a Typical Farm Application

Using the test path of section 5.3 (Figure 13), two simulations, with and without disturbances, were carried out at 2 m s^{-1} constant forward velocity, parameters of Table 2 (adopted from Derrick and Bevly, 2008) and using the best LARP control parameters:

$$L_1 = -0.7 \text{ m } L_2 = 0.73 \text{ m}, K_d = 3.0, K_N = 0.9 K_1 = 1.64, \text{ and } K_2 = 4.7.$$

Table 3: Optimization conditions, optimum parameters, and resulted errors

Optimization Conditions: Path, LARP, Objective	L_1	L_2	K_N	K_D	K_1	K_2	$d_{N,peak}$ (mm)	$d_{N,RMSE}$ (mm)
a) Line, no-LARP, RMSE	-	-	5.6	3.0	-	-	-	-
b) Circle, 1-LARP, RMSE	-	1.0	3.32	3.0	-	2.28	22.4	1.2
c) Circle, 1-LARP, peak	-	1.4	7.7	0.44	-	1.63	14.6	2.5
d) Test, 2-LARP, peak	-0.7	0.73	0.9	3.0	1.64	4.7	4.42	1.5

6.6 Frequency Response Analysis

Linear system transfer function provides a good measure for perfect circumstances condition and by obeying the peak to the opposite peak relation with both LARP distances it is expected to obtain a response similar to the following illustrations. Since performance of the system is evaluated by two criteria of lateral and orientation errors. Figure 31 and Figure 32 display the frequency response of the linearized system along linear segment of the reference path. Furthermore, keeping $K_N = 1$ the variation of pole and zero location is presented by Figure 33. It should be noticed that although the actuator impact is taken into account, the timing samples were not applied since the schematic diagram were required to compare with similar studies in the literature. The performance is slightly different from Bell (1999) and Bevely (2001) however the basic curvatures in the same frequencies of lateral deviation are almost the same. That similarity is probably caused by applying same vehicle and terrain parameters.

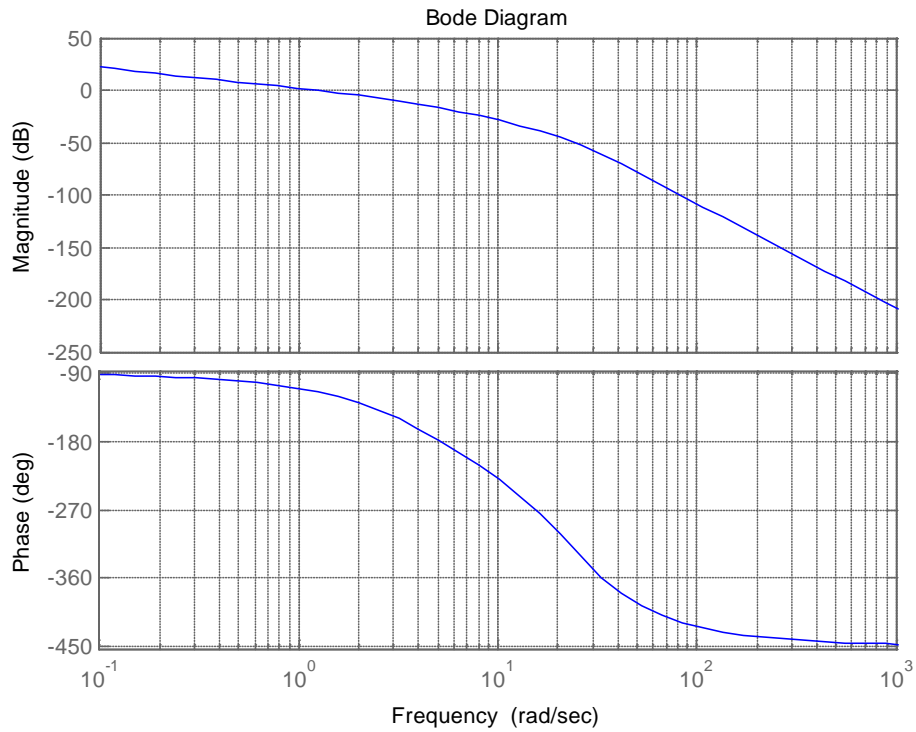


Figure 31. Schematic illustration for frequency response of lateral deviation in linear system transfer function

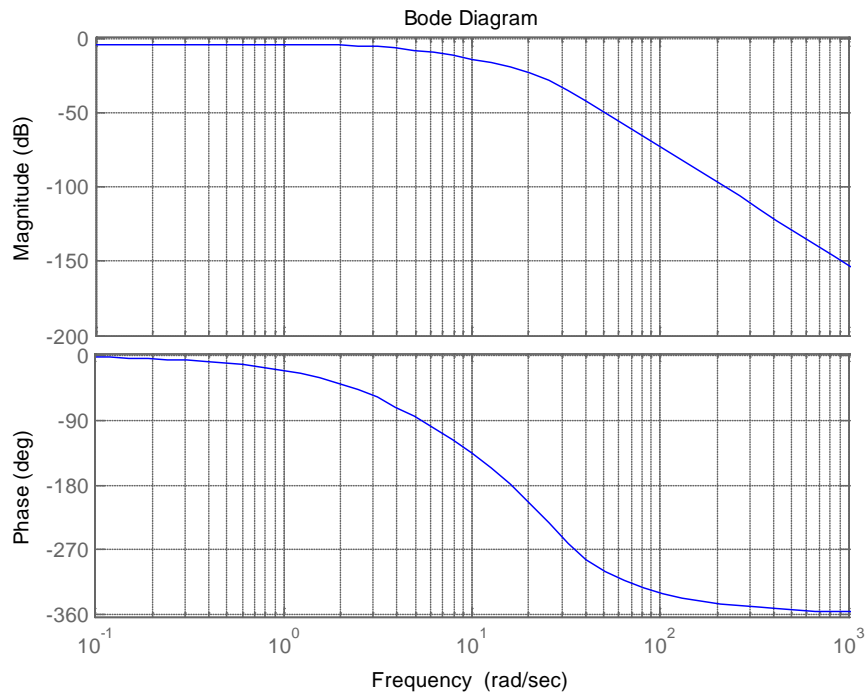


Figure 32. Schematic illustration for frequency response of orientation deviation in linear system transfer function

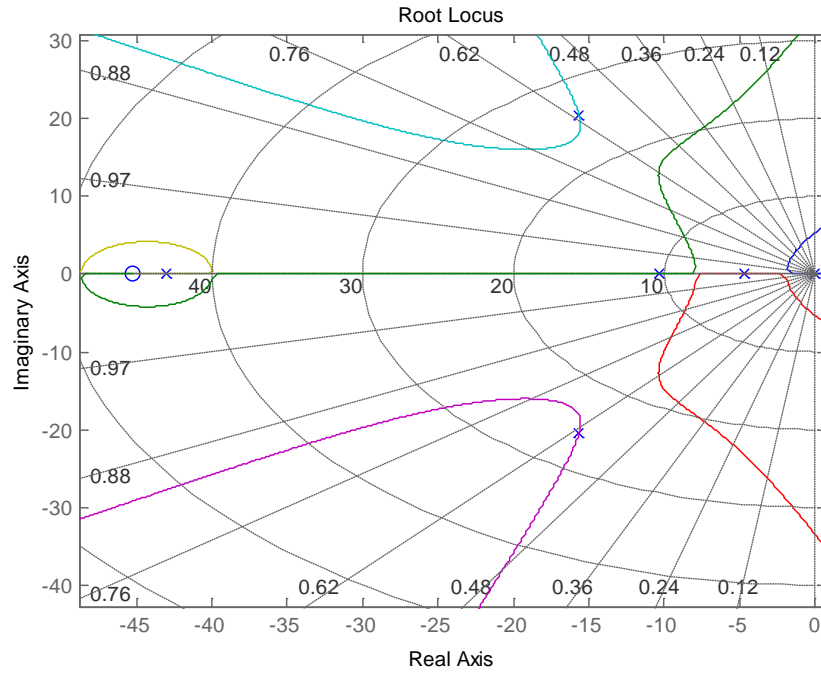


Figure 33. Root locus plot for lateral deviation gain variation along the linear path with $K_N=1$.

6.7 Steering Angle Outcomes and Steer-Ability

Figure 34 shows the steering angle, δ , and the lateral deviation, d_N , without disturbances (solid line) and with disturbances (dotted line). It was observed that the steering angle has almost 0.4 s lag in tracking δ_{des} with a negligible offset consistent with the experimental results of Derrick and Bevly (2008).

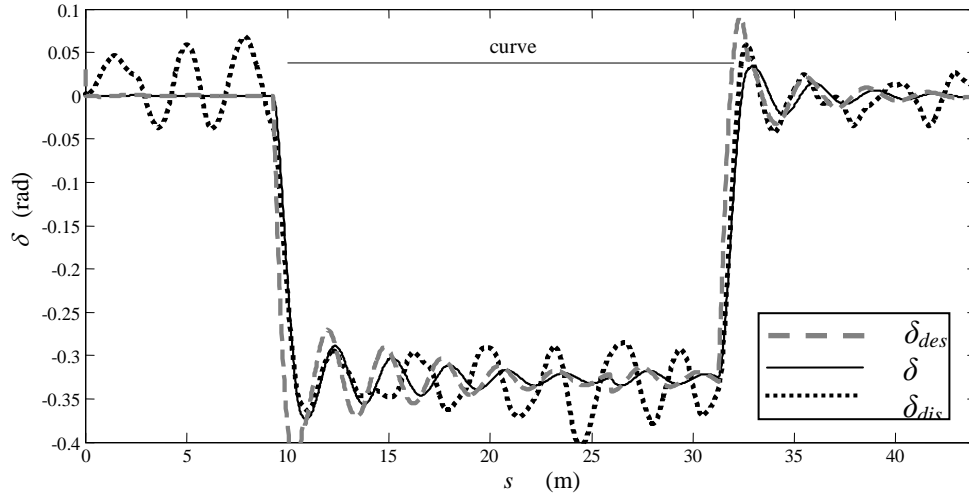


Figure 34. Steering angle δ (solid line), δ_{des} (dashed line), δ_{dis} (dotted line). Dotted lines are obtained with disturbance parameters used in the verification tests.

6.8 Tracking Accuracy performance comparison

The proposed control system results in $d_{N,peak} = 8.1$ mm and $d_{N,RMSE} = 2.6$ mm.

Comparison of the proposed 2-LARP controller lateral deviation results with Lenain et al. (2006) is provided graphically via Figure 36. The lateral deviation error results provided in this section will be used as the basis for the performance evaluation in Chapter 7.

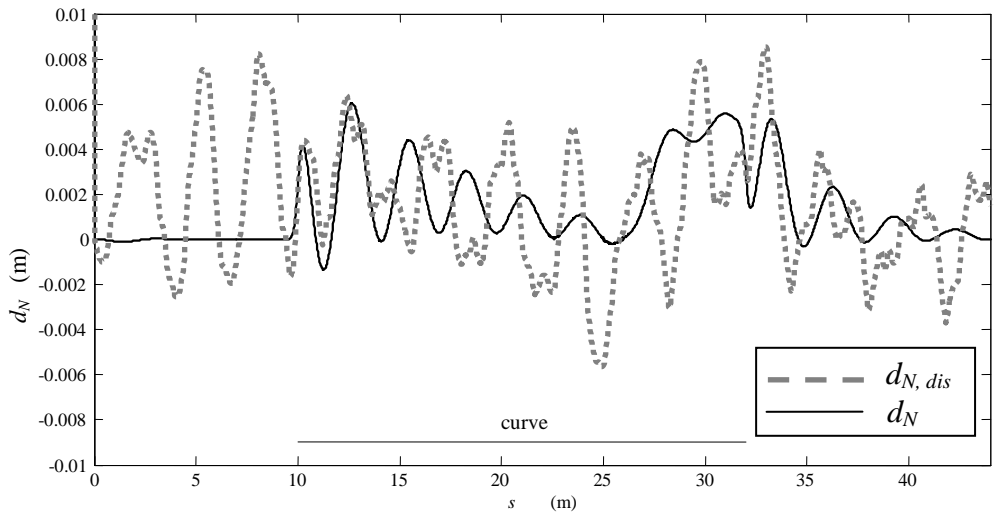


Figure 35. Lateral deviation d_N (solid line), $d_{N, dis}$ (dotted line) measured at 8 km h^{-1} . Dotted lines are obtained with disturbance parameters used in the verification tests.

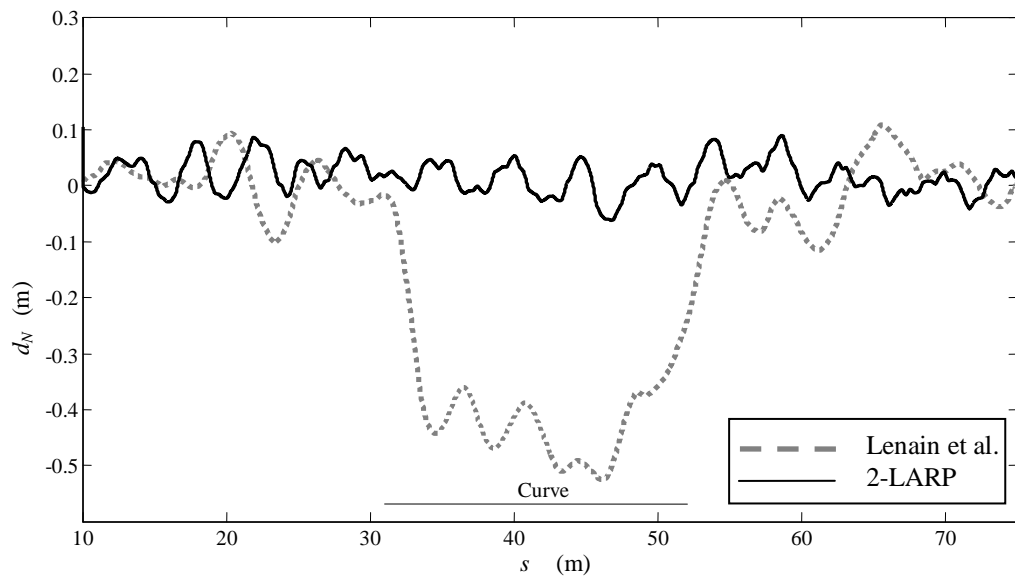


Figure 36. Tracking accuracy comparison of the Proposed 2-LARP method and results reported by Lenain et al. (2006).

6.9 Lateral Motion Enhancements

The lateral motion has been mostly characterized by the tire and vehicle side slip angles.

Therefore, Figure 37 shows the chassis side slip angle β , which is the angle between the

vehicle heading and the actual velocity. The dotted line β_{dis} shows the side slip angle with the disturbance parameters included.

Figure 37 and Figure 38 indicate that larger steering command, required for the curve, results in higher chassis and tyre slip angles, as well as larger lateral deviations. Peak deviation values are expected at the curvature transitions, i.e., where the path changes from a straight line to a circle or vice versa. The transition phase is observed starting from $s = 9.16$ m, where P_{L2} enters the curvature zone, while P_N remains in the linear zone. The observed magnitudes of the tyre and chassis slip angles do not exceed 4° and 16° , in the linear and transition phase, as recommended by Kiencke and Nielsen (2005).

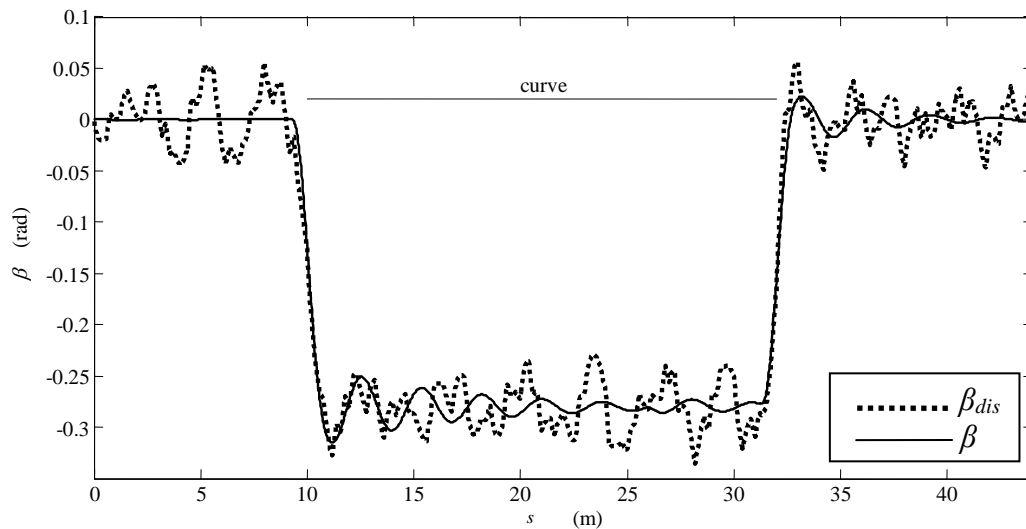


Figure 37. Vehicle side slip angle. β (solid line), β_{dis} (dotted line).

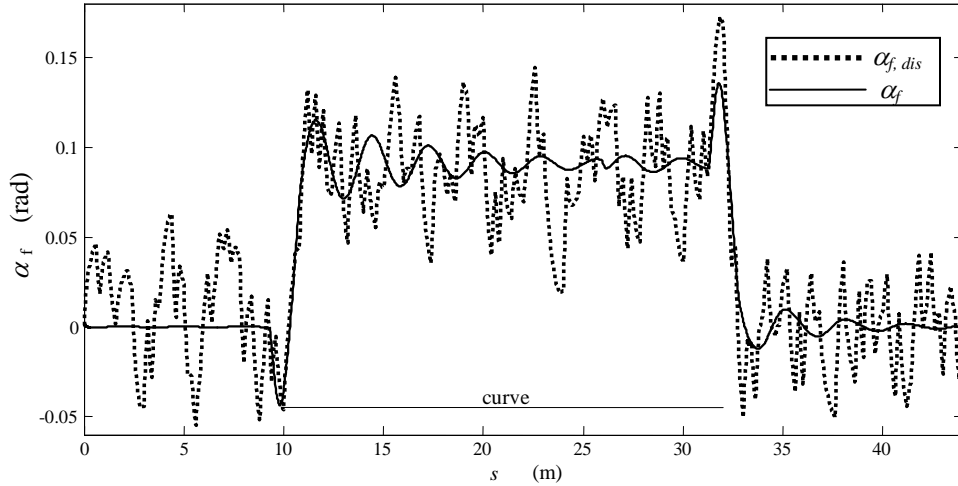


Figure 38. Front tyre slip angles α_f (solid) without disturbances, and $\alpha_{f,dis}$ (dotted) with disturbances.

6.10 Manoeuvrability Evaluation

A set of simulations were carried out to observe the effects of vehicle velocity on the lateral deviation along the U-turn. The lateral deviations, d_N , obtained with the set of constant vehicle velocities $\{5, 6.5, 8\}$ km h⁻¹ are shown in Figure 39. Due to the squared increase of the centrifugal forces, $F_c = mv^2 / \rho$, it is expected to have larger lateral deviations at higher vehicle velocities on the circular portion of U-turn (Figure 39). The observed lateral deviations for the forward speeds of $v = \{5, 6.5, 8\}$ km h⁻¹ are $d_{N,RMSE} = \{3.1, 1.9, 3.5\}$ mm, respectively. For higher velocities in the field, it is recommended to retune the controller gains which have been obtained for about 2 m s⁻¹, as applied by Derrick and Bevly (2008) and Lenain et al. (2006). The obtained results of this section are in consistency with the velocity effects results of Bevly (2001).

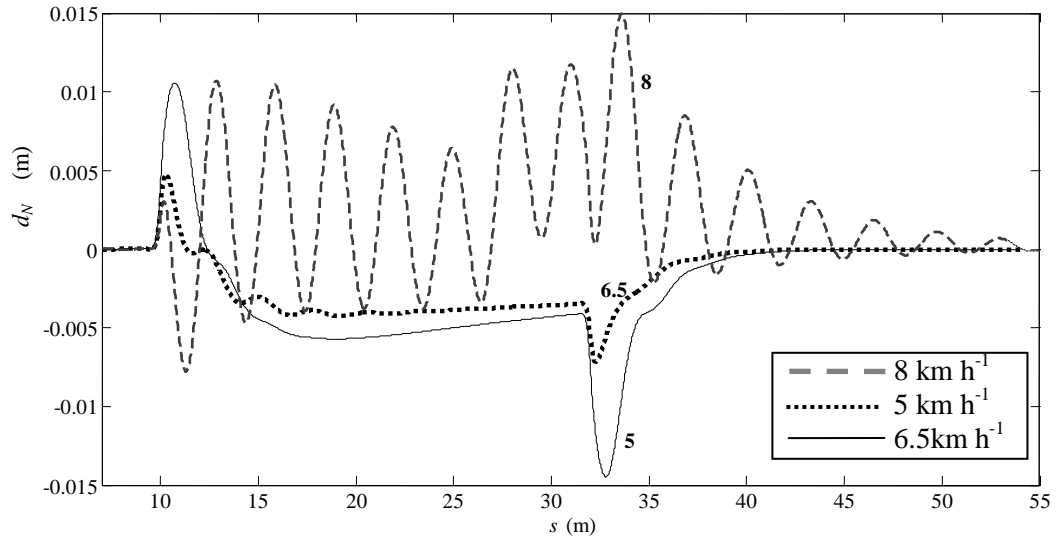


Figure 39. Lateral deviation, d_N , for velocities 5, 6.5 and 8 km h⁻¹.

More numerical experimentation on the platform to observe the interrelation among forward velocity, look ahead reference point distance and centrifugal force in order to compare with the lateral deviation based controller presented by Derrick and Bevely (2008). Figure 40 - Figure 43 illustrate how the feedforward centrifugal force and consequently lateral deviation error varies. Exterma are mostly observable easily in the disturbance applied simulations. Comparing these results with the results of Derrick and Bevely (2008) same level of sensitivity can be seen, however this study is initialized by the aforementioned values to come up with higher robustness.

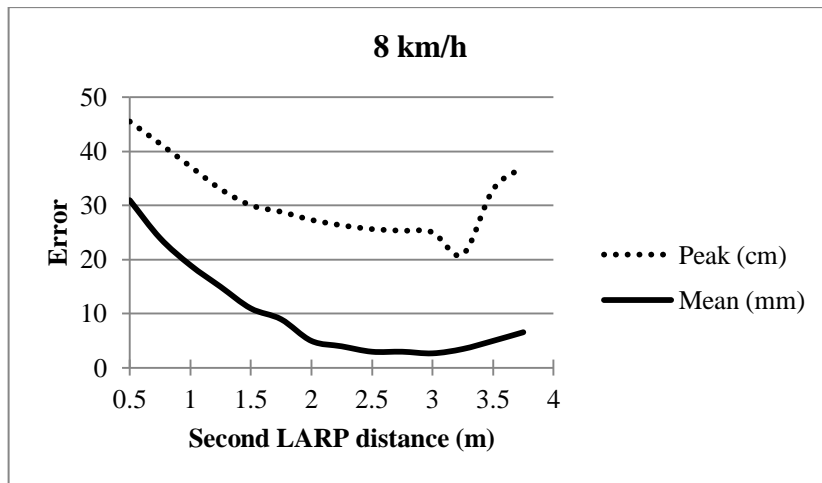


Figure 40. Lateral deviation error cause by change in second LARP distance having constant velocity of 8 km/h

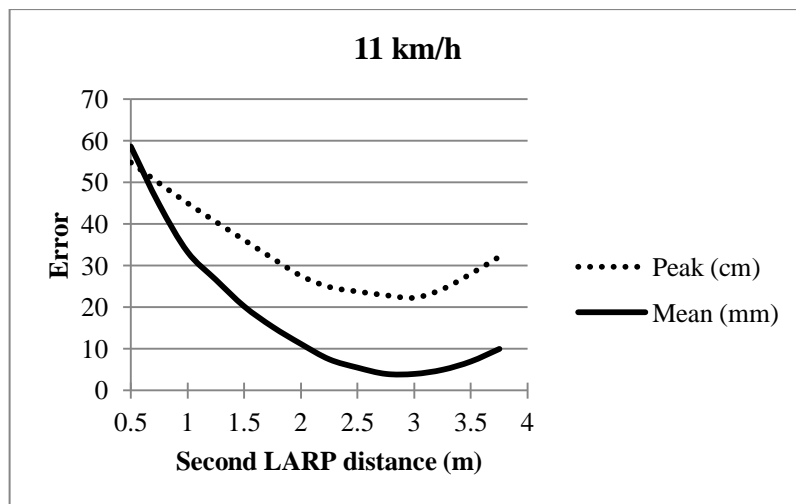


Figure 41. Lateral deviation error cause by change in second LARP distance having constant velocity of 11 km/h

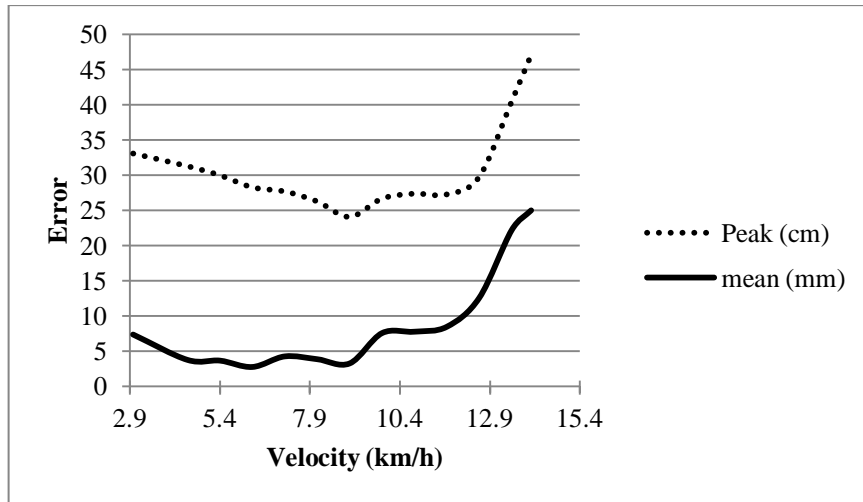


Figure 42. Lateral deviation error cause by change in 2-LARP forward velocity

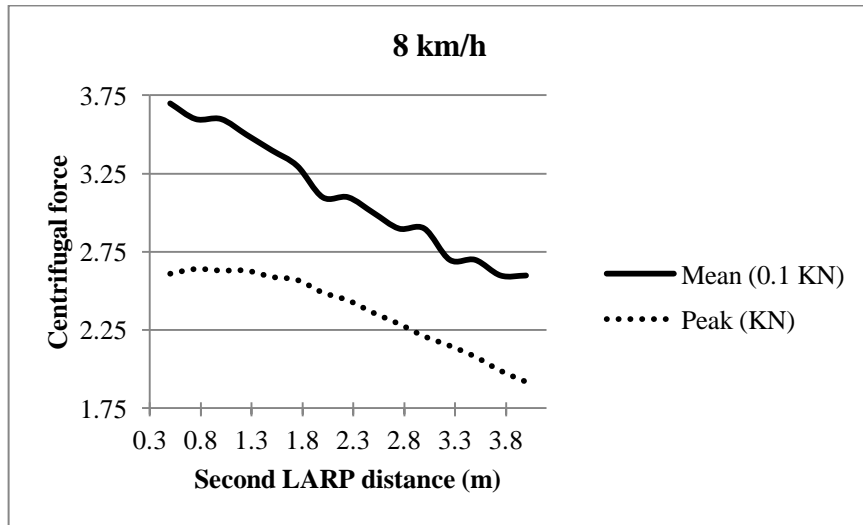


Figure 43. Centrifugal Force versus second LARP distance variation

6.11 Seeding, Spraying and Fertiliser-Spreading Efficiency

The estimated efficiency enhancement in seeding-harvesting η_{SH} by reducing the length of the seeder row has been discussed by Karayel et al. (2004), and in material spreading η_{MS} by increasing the uniformity across the spreading area by Tola et al. (2008).

Assuming the total path length as S_t , the formulas of $A = \int_0^{S_t} ds$ and $B = \int_0^{S_t} |d_N| ds$ are applied along the travelled path, where A and B represent the total travelled distance and

the covered area around the reference path, respectively. The reduction of the seeder row length, ΔA , is the difference between A of the proposed and that of the other approaches mentioned. Likewise, ΔB represents the reduction in spreading area. Consequently, the efficiency enhancements can be estimated $\Delta\eta_{SH} = \Delta A / A$ and $\Delta\eta_{MS} = \Delta B / B$.

Since the agricultural work is pursued often along the straight line segments of the path, one may notice that the comparison is made along linear segments. Comparing 2-LARP against to surface laid cable method by Aghkhani and Abbaspour-Fard (2009) along a straight line the decrease of lateral deviations corresponds to an estimate of efficiency increase about $\Delta\eta_{SH}, \Delta\eta_{MS} > 30\%$. Similarly, assuming that agriculture practiced on the curvatures, the efficiency improvement against to the predictive controller by Lenain et al. (2006) are estimated about $\Delta\eta_{SH} > 7\%$ and $\Delta\eta_{MS} > 3\%$. Finally, compared to the results of robust anti-sliding controller by Fang et al. (2011), 2-LARP controller indicates almost the same level of overall efficiencies, though 2-LARP control has an advantage by its simplicity. Figure 44 gives a visual measure for estimated agricultural performance comparison.

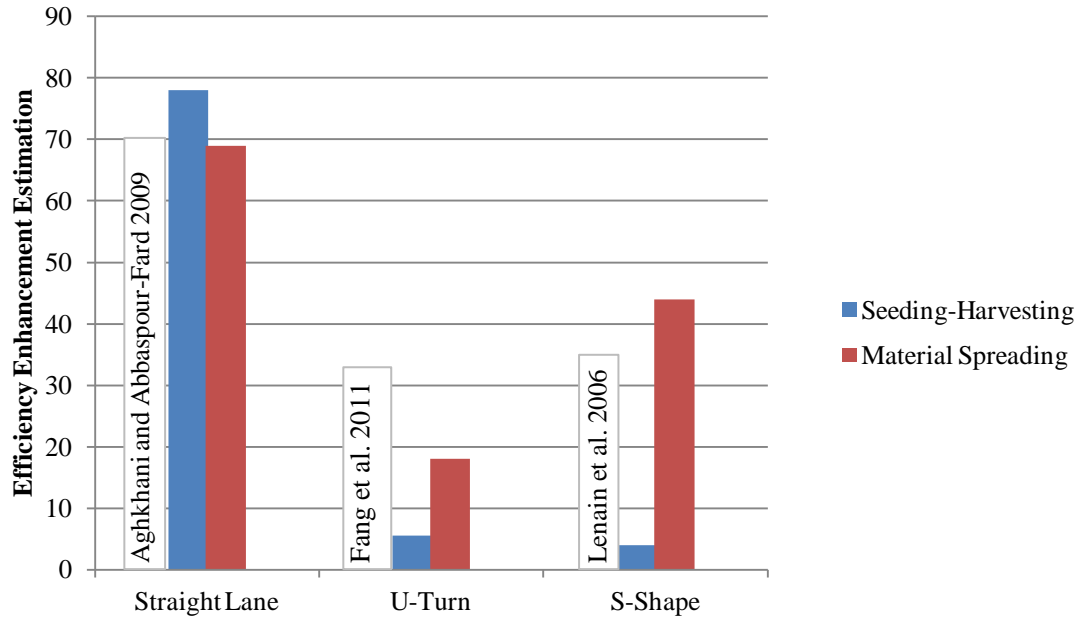


Figure 44. Graphical demonstration for estimated agricultural performance comparison

6.12 Overall Evaluation of the System Attributes

By scaling the prototype into real vehicle, disregarded of transient phase of Figure 21 and Figure 36, proposed system performs at least in the same level with Lingdgren et al. (2002) considering both slip-aware and unaware of Odometric model. In other words, controller needs some time to find correct orientation. Brief characteristics of the proposed system through applying variety of specifications are summarized in Table 4.

Table 4. Overall system characteristics and evaluation

Robustness	High sensitivity / instability	tracking failure
Vehicle shape and weight parameters	$WB + 2R/v < R < WB + 2R/v$	$R < WB + R/v$
Initial vehicle states (e.g. Fair orientation, location and velocity)	$15 \text{ km/h} < v < 19.5 \text{ km/h}$	$v > < 19.5 \text{ km/h}$
external disturbance due to unevenness or sinking into the soil	Poor contact patch characteristics (in particular, low soil friction coefficient)	

Chapter 7

DISCUSSION

7.1 Overview of 2-LARP Controller Significance Evaluation

The agricultural automation requires higher precision in tracking the crop rows and manoeuvring between them to increase the efficiency and safety of the agricultural processes. The precision of agricultural operation helps improve environmental protection and optimizes the usage resources. Even a few percentages improvement is very significant for farmers and manufacturers. Since the path shape of an agricultural operation strongly depends on the shape of the terrain, crop rows and surrounding environment, the path tracking accuracy should be improved for a typical farm pattern with some irregularity. Hence, tracking overshoot and decaying oscillations at curvature transition are common problems in agricultural path tracking control systems. Reduction of the lateral peak deviation error at curvature transitions was suggested by Lenain et al. (2006) and motivated this study to emphasis on the lateral peak error reduction.

In this study a feed forward control method has been developed based on lateral deviation controller and using look-ahead reference points to compensate the decaying oscillations at the curvature transients. These look ahead reference points compensate centrifugal force which is the main source of the large lateral error. The feedforward lines from two look ahead reference points reduce the lateral error significantly far better than the single look ahead reference point feedforward and also lateral control methods.

7.2 Discussion of Results

To achieve the above characteristics, a simple control law is proposed that consists of a lateral deviation feedback and two LARPs feedforward compensation that reduces the lateral tracking deviation significantly. The proposed control law is verified on a nonlinear model of vehicle dynamics using typical farm application conditions, i.e., the desired path consists of lines and arcs with 7 m radius which are represented by coordinates in x - y plane with 0.02 m curvilinear distances between the points and the forward speed of 2 m s^{-1} .

The simulator was validated by reproducing similar response curve for the same control law at the same operational parameters and desired paths compared to the response obtained by Lenain et al. (2006). The simulation results also verify that the tyre model remains in the valid range of linear region since the observed maximum slip angle is around 2.5° , and does not exceed 4° as recommended by Kiencke and Nielsen (2005).

A sixth order linear model of the system is developed to analyse the stability of the farming vehicle and proposed controller. Although the tyre model is expected to remain in the linear region, the steering system is expected to introduce significant nonlinearity because it has positional and rate restrictions. However, our observations on the simulation results indicate that once the system reaches to steady control condition, the control law does not produce sharp steering changes, and the system behaviour obeys the linear model.

Indeed, the deviation from the linear model is observable in measurements of peak to opposite peak curvilinear distances, where larger peak deviation results in larger peak to opposite peak distances. For the typical farming conditions, the dominant closed-loop poles in the root locus have always imaginary parts for the whole range of stable feedback gains, resulting to an overshoot and decaying oscillations at the curvature transitions. The introduced second LARP compensates the overshoot and decaying oscillations when the distance L_2-L_1 is tuned to Δs_{pop} , the curvilinear distance from the lateral peak deviation point to the opposite peak deviation point.

The non-constrained search for minimum $d_{N,peak}$ along the test path failed for the 1-LARP control, resulting in unstable controller parameters. Thus, in Section **Error! Reference source not found.**, constraints were applied on the controller parameters to keep the poles and zeros of the control at fixed positions of the root locus plot, which is determined on the linear test path. Existence of two optimization criteria, minimum $d_{N,RMSE}$ and minimum $d_{N,peak}$, indicates that this problem exhibits a multi-objective optimization problem character. The determined optimum 2-LARP parameters were considered as a reasonable sub-optimum, and expect future studies on determination of better control parameter sets.

Simulation results indicate that the lateral deviation based control has weakness against the changes in speed and cornering coefficients. On the root locus, decrease of C_f and C_r to 50% of their usual values shifts the zero from -90 to -45 , but system remains stable. Similar tests on root locus shows that with the determined set of controller parameters for $v = 2 \text{ m s}^{-1}$, the system remains stable up to $v=3.25 \text{ m s}^{-1}$. However, the simulation

tests indicates that the response is highly oscillatory even at $v=2.22 \text{ m s}^{-1}$, and needs tuning of K_d for a better performance.

It was tried to distinguish a specific relation as a formula or pathway among parameters for the sake of parameter value determination by the aid of an extensive search along each of six controller parameters. One may notice that the applied optimization algorithm brought desired millimetre tracking accuracy however there might be better algorithms. These control law parameters are gains of the lateral deviation, and orientation deviations as well as the look ahead distances.

Rather than observing a specific pathway for six-entry sets of the controller variable determination, the parameter search was ended up with discrete pathways of sets which are the basis for optimization process. But there were some major concerns within each parameter coordinate scanning that is worth to be further discussed as follows;

First, the error exhibits different characters during each test time interval. As stated previously, present study focused on the lateral peak error reduction. The error is deviation of the control point (midpoint of the rear wheels) with respect to the given waypoints. Indeed, the lateral error is provoked over curvature transitions which are in this study straight line section to circular in the U-turn that is commonly used by farmers to pursue the agricultural operation such as seeding. Hence, careful consideration must be taken into account in order to minimize the offset which occurs along the circular path segment. Then, on top of that, the peak lateral error will be

compensated. Thus in brief, RMSE value of the lateral error came first in the error computations for analysis.

Second, the parameters relations with error are highly nonlinear and thus within demonstrations, four parameters were fixed about an arbitrary value. Although fixing four parameters eases the observation by a clear three dimensional plot, it affected the entire system to exhibit 1-LARP relation rather than 2-LARP controller. It had limitations in showing the extrema locations, too.

Third, some points must be skipped carefully in scanning parameters. The reason is system resonances and thus produces large error at curvature transitions or even in the beginning by a small initial step. These points interrupted any detected pathway of optimum parameters.

Forth, a discrepancy always exists between the non-restricted and linearized systems. The degree of this discrepancy depends on the lateral error d_N . The more the lateral error the larger the systems discrepancy is. Controller parameters selection, system parameters variations such as cornering coefficients and forward velocity as well as the magnitude of the external disturbances seriously contributed the performance level of the system in as much as, in some cases demonstration of the results becomes unclear or nonsense.

In the present study, a third order delay was applied in the actuation part since in the actual application, a certain time delay always exists between the desired value computed by the controller, and the actual value produced by the actuator. This delay

associates with the disturbances or any other irregularity that might drastically change the final tracking results or even tracking failure.

Sensor noise and delay are significant. According to Derrick and Bevly (2008), sensor bias can damage the estimation and control algorithm. Therefore, in real time application they must be applied. Within the present study, the same assumptions were held, so that the simulations tests are noise and bias free, since the actuation delay for the specific case of Derrick and Bevly (2008) is far more effective than sensor typical bias in “John Deere farm tractor” experimental setup.

The $d_{N,\text{peak}}$ under 1-LARP control is stabilised to have a minimum RMSE for the transient of a step response. Introducing 2-LARP reduced $d_{N,\text{peak}}$ to one fifth compared to $d_{N,\text{peak}}$ of 1-LARP at the curvature transitions down to millimetres, without effecting $d_{N,\text{RMSE}}$ on any part of the desired path with a minimal computational complexity. It is expected the effect of the soil disturbances on $d_{N,\text{RMSE}}$ and $d_{N,\text{peak}}$ to be more significant than further reductions by more sophisticated control methods.

The provided simulation foundation is a useful tool to observe the effects of parameters variation of the test circumstances especially vehicle type, forward velocity and terrain grip condition. Tyre slip angle and in particular the front one, added to the terrain irregularities govern the dynamics and influence accuracy performance.

Large error gap observed at path curvature change between 1-LARP and 2-LARP controller under the best parameters. This fact supports the claim of advantage by

bringing preview information via employment of farther second LARP and thus an equilibrium point can never be found even with much heavier extensive optimization. Therefore, independency of effects of both above methods on lateral deviation error was observed in the results comparison of them. Indeed, mathematical proof of LARP effects on the error is a complicated problem and requires sophisticated techniques due to highly nonlinear nature of the system.

Although the offset error on the circular part always exists even at the best parameters controller recruitment, the offset can be minimised down to millimetre accuracy. This off-set in the simulation without positional and rate simplifications (which were carried out in the linearizing of the system), distinguishes the linear and nonlinear systems since it immediately affects the orientation deviation required to control law formula. Hence, the performance enhancement by tuning the controller parameters for stabilizing the linear six-order linear system transfer function dynamics deviates from the simulation progressively as the offset grows.

Degree of complexity or computational efficiency is obtained from a trade-off between the approach simplicity and the controller sensitivity to parameter variation. While the farm operations are being repeated over an agricultural field with certain terrain conditions and crop rows path, the proposed tracking accuracy approach of the present study loses certain amount of system variation sensitivity in order to gain more performance accuracy. For example, the system bears up to 30% change in soil grip conditions and loses millimetre tracking accuracy, in return.

According to the simulation results, disturbance of the random local terrain conditions in a stubble agricultural field has dominant effect on the lateral deviations, and must be considered in development of more advanced control methods to minimise the lateral deviation error.

The improvements of tracking accuracy were compared to the recent similar off-road vehicle tracking control methods and also the results reported in the literature. It was concluded that the proposed double look ahead reference (2-LARP) control strategy performs more satisfactory. The reason was reduction of the lateral error at the curvature transition of the reference path by compensation of lateral forces by optimizing the corresponding parameters in the controller.

In general, the proposed control law performs better than the previously presented control methods concerned with vehicle off-road applications for irregular path shapes and thus it boosts the reliability and precision to facilitate the agricultural automation. The industry can be benefited from the proposed method by manufacturing improved embedded control unit and processor for autonomous off-road vehicles. Finally, the market is interested in saving resources required for off-road operations will make the proposed method commercially available.

Chapter 8

CONCLUSION AND FUTURE WORKS

8.1 Concluding Remarks

In this thesis a novel off-road steering control strategy is developed to enhance the automatic land vehicle tracking accuracy by the reduction of lateral deviation error at curvature transitions. The proposed control strategy is mainly based on the properties of two look ahead points on the reference path that are added to a conventional lateral controller. This strategy eliminates the common undesired lateral deviation overshoots and stabilizes decaying oscillations to guarantee the accuracy and stability which are key factors for an automatic off-road operation.

Injection of the second LARP into the conventional lateral control law provides path preview information of upcoming changes in the radius of curvature that is the main source of lateral peak error. In addition, first LARP feedforward and the error feedback compensate centrifugal forces and guaranteeing the tracking accuracy, respectively. Therefore, the developed control law is a derivative control with simple arithmetic operations to provide computational efficiency.

Simulation results indicate that the overall performance of the system is at least in the same level with the results of similar methods reported in the literature. Controller keeps

the system within the desired tolerances around the reference path and reduces the peak lateral error to one fifth of the conventional lateral controller. Hence, farmers will be benefited from the implementation of the proposed method into an agricultural tractor by efficiency increments in resources consumption and products quantity.

Large discrepancy in accuracy outcomes of 1-LARP and 2-LARP control strategies numerically proved that each LARP affects the lateral behaviour of the system independently and thus an equilibrium point does not exist.

Simplicity as a secondary controller key aspect rises by arithmetic complexity reduction and hence desired performance is held as long as the certain system parameters are invariant such as velocity, soil grip conditions and magnitude of terrain disturbances.

The advent of new technology and also modern market and industry demands have increased the competition in agricultural operation control strategy performance enhancement, especially regarding automation, precision and ease of strategy implementation. Therefore, the proposed method can facilitate the aforementioned objectives to take a milestone towards fully autonomous agricultural technology.

8.2 Future works

The optimization algorithm introduced within this study exhibits multi-objective optimization character. Since the results obtained by the optimization were considered as a reasonable sub-optimum parameter sets, further study to reduce the lateral error in

order to improve the tracking accuracy is suggested. Utilising the program code of Appendix B as an optimization test bed, better results can be possibly reached.

The mathematical proof for independency of each LARP effect on the lateral tracking error can be studied. The problem can be simply stated as the necessity of the second LARP and minor contributions of further LARPs employment. System constant velocity abandons high sophistications in mathematical determination of the formula among parameters.

Further lateral error reduction should take into account the domination effect of disturbances on the lateral error. Therefore, compensation of external disturbances due to the random local terrain conditions requires an advanced control method integrated with 2-LARP control method.

The provided simulation test bed (Appendix B) gives a useful platform for performance evaluation of future proposed controller algorithms.

Finally, the proposed controller and developed steering simulation system can be implemented in real time application and benefited the steering system in the case of GPS outage. 2-LARP control and the software code of Appendix B can hold the system tracking accuracy by dead reckoning of automatically steered farm tractors.

REFERENCES

Aghkhani, M. H., & Abbaspour-Fard, M. H. (2009). Automatic o-road vehicle steering system with a surface laid cable: concept and preliminary tests. *Biosystems Engineering* 103, 265-270.

Backman, J. Oksanen, T., & Visala, A. (2012). Navigation system for agricultural machines: Nonlinear Model Predictive path tracking. *Journal of Computers and Electronics in Agriculture*. 82, 32–43.

Bakker, E., Nyborg, L., & Pacejka, H. B. (1987). Tire modelling for use in vehicle dynamics studies. *SAE Transaction*. 870421, 2190-2204.

Barton, M. J. (2001). Controller development and implementation for path planning and following in an autonomous urban vehicle. *Undergraduate Thesis*, School of Aerospace, Mechanical and Mechatronic Engineering, The University of Sydney.

Behrouzi Lar, D. (2006). Tractors and Agricultural Machinery. In Persian, *Abu-Ali Sina University Publications*. Hamedan. Iran.

Bell, T. (2000). Automatic tractor guidance using carrier-phase differential GPS. *Journal of Computers and Electronics in Agriculture*, 25, pp. 53 - 66.

Bell, Th. (1999). Precision Robotic Control of Agricultural Vehicles on Realistic Farm Trajectories. *PhD Thesis*, Stanford University

Bevly, D.M. (2001). High speed dead reckoning and towed implement control for automatically steered farm tractors using GPS. *PhD dissertation*, Stanford University.

Bevly, D.M., Cobb, S. (2010). GNSS for vehicle control. *Artech house*. Boston, USA.

Bodur, M., Kiani E. And Hacisevki, H. (2012). Double look-ahead reference point control for autonomous agricultural vehicles. *Journal of Biosystems Engineering*. In Press.

Daily, R., & Bevly, D. M. (2004). The Use of GPS for Vehicle Stability Control Systems. *IEEE Transactions on Industrial Electronics*. 51(2).

Day, W., Field, E.M., & Jarvis, A.L., (Eds). (2009). *Chapter 3 Tractors and vehicles. Biosystems Engineering*. The Wrest Park Story 1924-2006. 103 (Supplement 1), 36-47.

Derrick, J. B. (2008). Adaptive Control of a Farm Tractor with Varying Yaw Properties Accounting for Actuator Dynamics and Nonlinearities. *Master thesis*. Auburn University. Auburn. USA.

Derrick, J. B., & Bevly, D. M. (2008). Adaptive control of a farm tractor with varying yaw dynamics accounting for actuator dynamics and saturations. *Control Applications*. CCA. IEEE International Conference on. 547 -552.

Derrick, J. B., & Bevly, D. M. (2009). Adaptive Steering Control of a Farm Tractor with Varying Yaw Rate Properties. *Journal of Field Robotics*. 26(6-7), 519-536.

Eaton, R., Katupitiya, J., Siew, K. W., & Dang, K. S. (2008). Precision Guidance of Agricultural Tractors for Autonomous Farming. *IEEE International Systems Conference*. Montreal, Canada.

Fang, H., Dou, L., Chen, J., Lenain, R., Thuilot, B., & Martinet, P. (2011). Robust anti-sliding control of autonomous vehicles in presence of lateral disturbances. *Journal of Control Engineering Practice*. 19 (5), 468 - 478.

Fang, H., Lenain, R., Thuilot, B., & Martinet, P. (2005). Trajectory Tracking Control of Farm Vehicles in Presence of Sliding. *Proceedings of the IEEE/RSJ International Conference on Intelligent Robots and Systems, IROS'05*. Edmonton, Canada.

Fateh, M. M., & Alavai, S. S. (2009). Impedance control of an active suspension system. *Journal of Mechatronics*. 19, 134 – 140.

Gartley, E. R. (2005). On-Line Estimation of Implement Dynamics for Adaptive Steering Control of Farm Tractors. *Master of Science Thesis*. Auburn University.

Gartley, E. R., & Bevly, D. M. (2008). Online Estimation of Implement Dynamics for Adaptive Steering Control of Farm Tractors. *IEEE/ASME Transactions on Mechatronics*. 13(4), 429 – 440.

Hellstrom, T., & Ringdahl, O. (2006). Follow the past: a path-tracking algorithm for autonomous vehicles. *International Journal of Vehicle Autonomous Systems*. 4 (2-4), 216 - 224.

Hemmat, A., Tahmasebi, M., Vafaeian, M., & Mosaddeghi, M. (2009). Relationship between pre-compaction stress and shear strength under confined and semi-confined loadings for a sandy loam soil. *Journal of Biosystems Engineering*. 102 (2), 219 - 226.

Karayel, D., Barut, Z. B., & Özmerzi, A. (2004). Mathematical modelling of vacuum pressure on a precision seeder. *Journal of Biosystems Engineering*. 87 (4), 437-444.

Keicher, R. And Seufert, H. (2000). Automatic guidance for agricultural vehicles in Europe. *Journal of Computer and Electronics in Agriculture*. 25, 169–194.

Karkee, M., & Steward, B.L. (2010). Local and global sensitivity analysis of a tractor and single axle grain cart dynamic system model. *Journal of Biosystems Engineering*. Vol.106, 352 – 366.

Kiencke, U., & Nielsen, L. (2005). Automotive control systems: for engine, driveline, and vehicle. *Springer*. Berlin. Germany.

Lenain, R., Thuilot, B., Cariou, C., & Martinet, P. (2006). High accuracy path tracking for vehicles in presence of sliding: Application to farm vehicle automatic guidance for agricultural tasks. *Journal of Autonomous Robots*. 21, 79-97.

Lenain, R., Thuilot, B., Cariou, C., & Martinet, P. (2007). Adaptive and predicative path tracking control for off-road mobile robots. *European journal of control*. 4, 1-21.

Li, M., Imou K., Wakabayashi, K., & Yokoyama, Sh. (2009). Review of research on agricultural vehicle autonomous guidance. *International Journal of Agricultural & Biological Engineering*. 2(3), 1- 16.

Lingdren DR, Hague T, Smith P and Marchant PJ. (2002). Relating torque and slip in an odometric model for an autonomous agricultural vehicle. *Journal of Autonomous robots*. 13, 73-86.

Lundgren, M. (2003). Path tracking for a miniature robot. *Master's thesis*. Department of Computing Science, Umea University, Sweden.

Moustris, G., & Tzafestas, S. G. (2005). A robust fuzzy logic path tracker for non-holonomic mobile robots. *International Journal on Artificial Intelligence Tools*. 14, 935-966.

Norremark, M., Griepentrog, H., Nielsen, J., & Sagaard, H. (2008). The development and assessment of the accuracy of an autonomous GPS-based system for intra-row mechanical weed control in row crops. *Journal of Biosystems Engineering*. 101 (4), 396-410.

Oscar C., Barawid J., Mizushima A., Ishii K., Noguchi N. (2007). Development of an Autonomous Navigation System using a Two-dimensional Laser Scanner in an Orchard Application. *Journal of Biosystems Engineering*. 96(2), 139-149.

Owen, G. M. (1982). A Tractor Handling Study. *Journal of Vehicle System Dynamics*. 11, 215–240,.

Ozada, N. (2008). A Novel Musculoskeletal Joint Modeling For Orthopaedic Applications. PhD Thesis. Brunel University. UK.

Ozguner, U., Unyelioglu, K., & Hatipoglu, C. (1995). An analytical study of vehicle steering control. In: Control Applications. *Proceedings of the 4th IEEE*. Conference on. 125 -130.

Reid, J. F., Zhang, Q., Noguchi, N., & Dickson, M. (2000). Agricultural automatic guidance research in North America. *Journal of Computers and Electronics in Agriculture*. 25, 155–16.

Rovira-Mas, F., & Zhang, Q. (2008). Fuzzy logic control of an electrohydraulic valve for auto-steering off-road vehicles. *Proceedings of the Institution of Mechanical Engineers Part D-Journal of Automobile Engineering*. 222 (D6), 917-934.

Rovira-Mas, F., Zhang, Q., & Hansen, A. (2007). Dynamics behaviour of an electrohydraulic valve: typology of characteristic curves. *Journal of Mechatronics*. 17, 551-561.

Rovira-Mas, F., Zhang, Q., & Hansen, A. (2010). *Mechatronics and Intelligent Systems for Off-road Vehicles*. Springer, New York.

Senatore, C. and Sandu, C. (2011). Off-road tire modelling and the multi-pass effect for vehicle dynamics simulation. *Journal of Terramechanics*. 48, 265–276.

Solmaz, S. And Baslamisli, C. (2010). A Nonlinear Sideslip Observer Design Methodology for Automotive Vehicles Based on a Rational Tire Model. Proceeding of Otekon, Bursa, Turkey.

Thuilot, B., Cariou, C., Martinet, P., & Berducat, M. (2002). Automatic guidance of a farm tractor relying on a single cp-dgps. *Journal of Autonomous Robots*. 71, 13-53.

Tola, E., Kataoka, T., Burce, M., Okamoto, H., & Hata, S. (2008). Granular fertiliser application rate control system with integrated output volume measurement. *Journal of Biosystems Engineering*. 101 (4), 411-416.

Torii, T. (2000). Research in autonomous agriculture vehicles in Japan. *International Journal of Computers and Electronics in Agriculture*. 25, 133–153.

Wang, Q., Zhang, Q., Rovira-Mas, F., & Tian, L. (2011). Stereovision-based lateral offset measurement for vehicle navigation in cultivated stubble fields. . *Journal of Biosystems Engineering*. 109(4), 258-265.

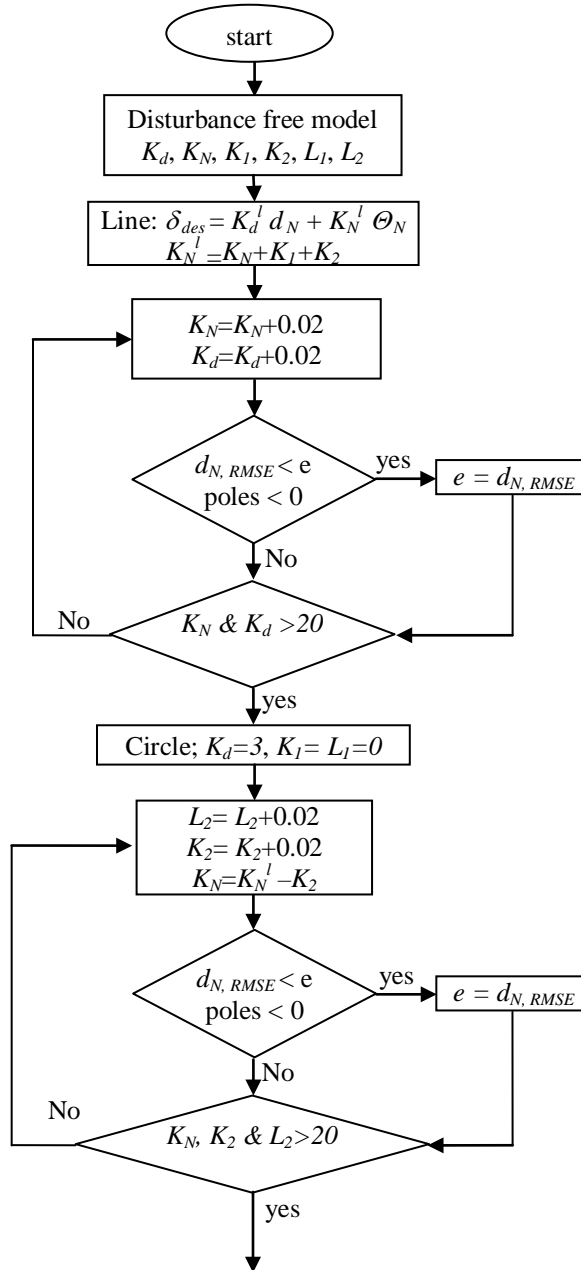
Wong, J. Y. (2009). Terramechanics and Off-Road Vehicle Engineering; Terrain Behaviour, Off-Road Vehicle Performance and Design. *Elsevier*. Second Edition. Ottawa. Canada.

Zhang, Q., & Qiu, H. (2004). A dynamic path search algorithm for tractor automatic navigation. *Transactions of the ASABE*. 47 (2), 639-646.

APPENDICES

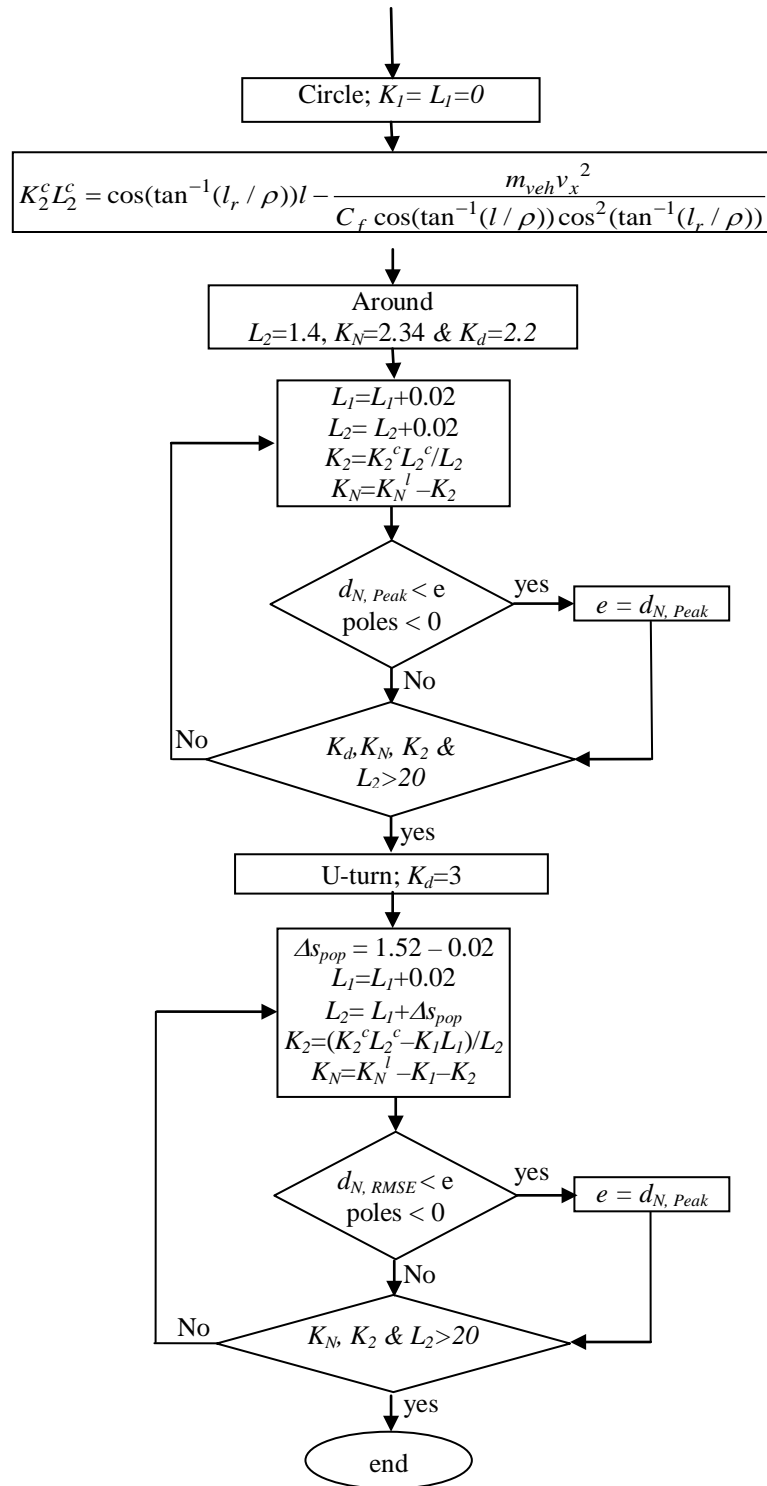
Appendix A: Optimization Algorithm Flowchart

The algorithm used in this study for optimization of control parameters is as follows:



Continued in next page

Continued from previous page



Appendix B: Simulation Program

B.1 MatLab Code Used in the Simulation Test Bed

The MatLab code used for the numerical simulation of the control algorithm and the present modeling of steering system of this study is given within the following lines. The source code is c

ompletely brought without any change so that applying the code below requires copying the program into a specified directory defined for this purpose. Moreover, the additional files must be executed to generate an individual file that will be read by the main simulation file as the reference path.

```
function 2LARP
clear all; close all;
fclose all; format compact; Tclk=clock;
fns=sprintf('mdhm%02i%02i%02i%02i.txt',Tclk(2),Tclk(3),Tclk(4),Tclk(5));
dispvectitle='%[ iter L1 L2 kN KD k1 k2 peakd rmsd poff
tcomp]';
pfs(-1,fns);
pfs(fns, ['\r\n' dispvectitle '\r\n']);
clc; tic;
path=pathdef; len_path=size(path,1); plotgrA=0; plotgrB=0;
plotgrM=1;
% CTRL Coefficients
x=1; y=2; w=3; % Positional terms
s=0; b=0; v=2.0; smax=0.5585; smin=-smax; % Steering
parameter
R=abs(path(1,2)); % Path parameters L2>L1
% Bevly & Derrick (2008) coefficients
m=11340; I=18500; Lf=1; Lr=2.0; L=Lf+Lr; Cr=286479;
Cf=137510; Fr=0;
dt=0.01; dtc=0.05; dts=0.001;
ds=path(2,1); equit=0.1; most=equit-1e-4; ibest=1;
vbest=[]; iter=0; tcalc=0;

LKbest=2.27;
```

```

startstep=0.01;

%-----
t=0; j=0; tf=22;
ts=t; s1=0; s2=0; s3=0; % actuator time and states
tc=t+dt; % controller time
pv=[-R-startstep Lr-10 pi/2]; % Initial position and
heading pv=[R -Lr+25 -pi/2];
vv=[0 v 0]; % Initial velocities
av=[0 0 0]; % Initial acceleration
xr=pv(x)-Lr*cos(pv(w)); yr=pv(y)-Lr*sin(pv(w));
clear ov ;
idN=2; dsign=1;dsigna=1; plotgraph=0;
while( t<tf)
    t=t+dt; j=j+1; %time & iteration
    %program notation simplification
    Cw= cos(pv(w)); Sw= sin(pv(w)); Cs= cos(s); Cb= cos(b);
    %Path tracking controller
    % CoG Coordinates (x,y) converted into rear wheels
    point (xr,yr)
    xrp=xr; yrp=yr; xr=pv(x) - Lr*Cw; yr=pv(y) - Lr*Sw;
    if(t==dt), xrp=xr; yrp=yr; end % debug

    if tc>=t, tc=tc+dtc; % control part
    % control starts with finding pN
    % inputs idN, xr, yr,thetar, path outputs idN, dN, d
    idNs=idN; idNend=idN+200;
    xk=path(idN-1,2); yk= path(idN-1,3);
    ddNp= (xk-xr)*(xk-xr)+(yk-yr)*(yk-yr); ddNpp=ddNp;
    for kdN=idNs:idNend,
        xk=path(kdN,2); yk= path(kdN,3);
        ddN=(xk-xr)*(xk-xr)+(yk-yr)*(yk-yr);
        idN=max(kdN-1,2);
        if(ddNp<ddN), break; end
        ddNpp=ddNp; ddNp=ddN;
    end
    dNbest=sqrt(ddNp); dNfw=sqrt(ddN); dNbw=sqrt(ddNpp);
    if(dNfw<dNbw), dNnext=dNfw; else dNnext=dNbw; end
    dN=nearestdist(dNbest,dNnext,ds); dN=abs(dN);
    thetaP=path(idN,4); thetaN=thetaP-pv(w);
    thetaP1=path(max(idN+round(L1/ds),1),4);
theta1=thetaP1-pv(w);
    thetaP2=path(max(idN+round(L2/ds),1),4);
theta2=thetaP2-pv(w);
    ca=path(idN,1); xn=path(idN,2); yn=path(idN,3);
    % determine sign of distance

```

```

xNd=-xn+path(idN+1,2); yNd=-yn+path(idN+1,3);
dsign= -sign(xNd*(yr-yn)-yNd*(xr-xn));
xnp=path(max(idN-1,1),2); ynp=path(max(idN-1,1),3);
dsign= sign(+thetaP -atan2(yr-ynp,xr-xnp) );
dsignp=dsign; d= dsign*abs(dN);

% Control Law for steer angle
sd=kD*d + kN*thetaN + k1*theta1 + k2*theta2;
end
%--control part is over, vehicle simulation starts here--
-----

% Vehicle equations of motion
if s>=0, Ff= -Cf*(s-b- vv(w)*Lf*Cb/v); % Friction
force is normal to tires
else Ff= Cf*(b + vv(w)*Lf*Cb/v-s); end
Fc=m*(v*cos(b))^2*tan(s)*sign(b)/L; Fwf=27e3*sin(s);
ddy=(-Fr-Ff*Cs-Fc+Fwf)/m+v*vv(w);
av(w)= (-Ff*Cs*Lf + Fr*Lr+Fwf*Lf)/I; av(x)=-ddy*Sw;
av(y)= ddy*Cw;
% Absolute Velocities
vv(x)=vv(x)+av(x)*dt; vv(y)=vv(y)+av(y)*dt;
vv(w)=vv(w)+av(w)*dt;
% Constant Forward Velocity
vyy=-vv(x)*Sw+vv(y)*Cw; % Lateral y velocity
vv(x)=-vyy*Sw + v*Cw; vv(y)= vyy*Cw + v*Sw;
% Side slip angle
b= atan2(vv(y),vv(x))-pv(w);
Fr= Cr*(b - vv(w)*Lr*Cb/v); % Friction force is normal
to tires
% Vehicle positions and orientation
pv(x)=pv(x) + vv(x)*dt; pv(y)=pv(y) + vv(y)*dt;
pv(w)=pv(w) + vv(w)*dt;

%=====
=====
%          1 2 3  4  5  6  7  8  9      10
Observation Vector
%          t s Xn Yn d  xr yr  dN thetaN dsign ca
ov(j,:)= [t s xn yn d  xr yr  dN thetaN dsign ca];
end % case run completed
% Postprocessing of the case observations
L_ov=size(ov,1); if L_ov>2100,
    [peaka,ipeak]=max(ov(100:2100,8)); peakd =
ov(ipeak+100,5);
    rmsd = sqrt(ov(:,5)'*ov(:,5)/len_path ); iter=iter+1;
tcomp=toc;

```

```

poff=ov(900,5);
dispvec=[ iter  L1 L2 kN kD k1 k2 ...
          peakd*1000 rmsd*1000 poff*1000 tcomp];
if plotgrB, plotthem(ov); end; tcalc=tcalc+tcomp;
if(mod(iter,100)==0), disp( sprintf('%i %f',iter,
tcalc)); tcalc=0; end
if peaka < most,
    most=peaka; disp(dispvectitle); disp(dispvec);
dispvec(1)=-iter;
if plotgrM, plotthem(ov); pause(2); end
vbest(ibest,:)=dispvec; ibest=ibest+1; end;
pf(fns,dispvec); end
%end; end; end; end; end;
% all cases are over
pfs(fns,'Best Values List\r\n');pfs(fns,[dispvectitle 13
10]);
for i=1:ibest-1; pf(fns,vbest(i,:) );end
disp('Run is completed\r\n');
end

function pf(fns,v)
fh=fopen(fns,'a'); s='';
for i=1:length(v), s=[s num2str(v(i)) '\t']; end; s=[s
'\r\n'];
fprintf(fh, s); fclose(fh); pause(0.1);
end

function A=distlist(c,d,n)
% L=distlist(c,d,n), L=[n c c+d c-d c+2d c-2d ...] total n
centers
if n<2, A=[1 c]; else
    if n<5, A=[3 c c+d c-d]; else
        dp=d; nd=round(n/2-0.5); dd=d/nd;
        A=zeros(1,n+1); A(1)=nd*2+1; A(2)=c;
        for i=1:nd, A(3+(i-1)*2)=A(2)+i*dd; A(4+(i-
1)*2)=A(2)-i*dd; end
    end
end
end

```

Appendix C: Program Code of 2-LARP Control Law

```

function [delta,Xm,Ym,yy,v,Tn,TR] = fcn(x,y,yaw,t)
R=6;
% time needed for first and second and third straight paths
L1=3;
L2=6;
Ky=-0; Kn=0; K1=0; K2=3;
%closest point
if (y<100)&&(t<57.5)
    Tn=pi/2-yaw;          %Tc:reference tangent angle
    s=y;                 %s: curvilinear absissa
    Xm=R;                %coordinate of closest point
    Ym=y;
    yy=R-x;
    v=1.8;
    TR=0;
%    delta=0;
elseif (y>100)
%    delta=0.3;
    TR=atan2((y-100),x);
    yy=R-sqrt(x^2+(y-100)^2);
    s=100+R*(TR);
    Xm=R*cos(TR);
    Ym=100+R*sin(TR);
    Tn=TR-yaw + pi/2;
    v=1;
else

    Tn=3*pi/2-yaw;
    Tn=Tn;
    s=200+pi*R -y;
    Xm=-6;
    Ym=y;
    yy=-R-x;
    YY=-YY;
    v=1.8;
    TR=0;
%    delta=0;
end
%coordinate of first ahead point
if (s<100-L1)
    T1=pi/2-yaw;        %T1:look ahead tangent angle
elseif s<(100+pi*R-L1) %first turn
    TR1=(s-100+L1)/R;
    T1=pi/2+TR1-yaw;

```



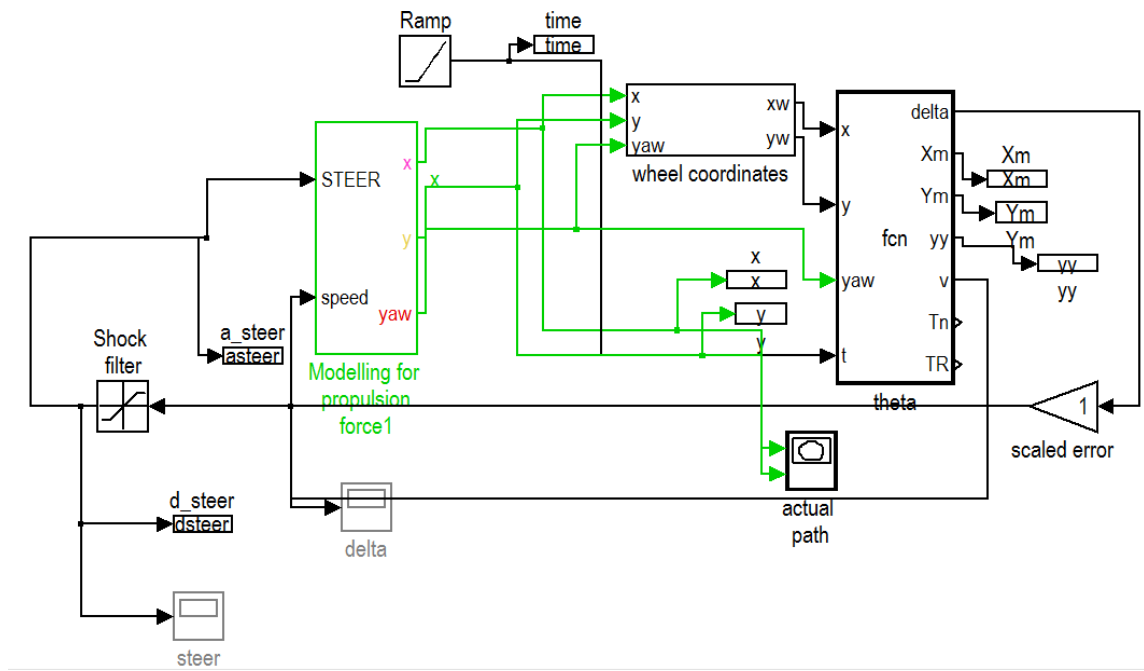
```

else
    T1=3*pi/2-yaw;
    T1=T1;
end

if (s<100-(L1+L2))
    T2=pi/2-yaw;           %T1:look ahead tangent angle
elseif s<(100+pi*R-(L1+L2)) %first turn
    TR2=(s-100+L1+L2)/R;
    T2=pi/2+TR2-yaw;
else
    T2=3*pi/2-yaw;
    T2=T2;
end
delta=Ky*yy+Kn*Tn+K1*T1+K2*T2;
% delta=0.1;
end

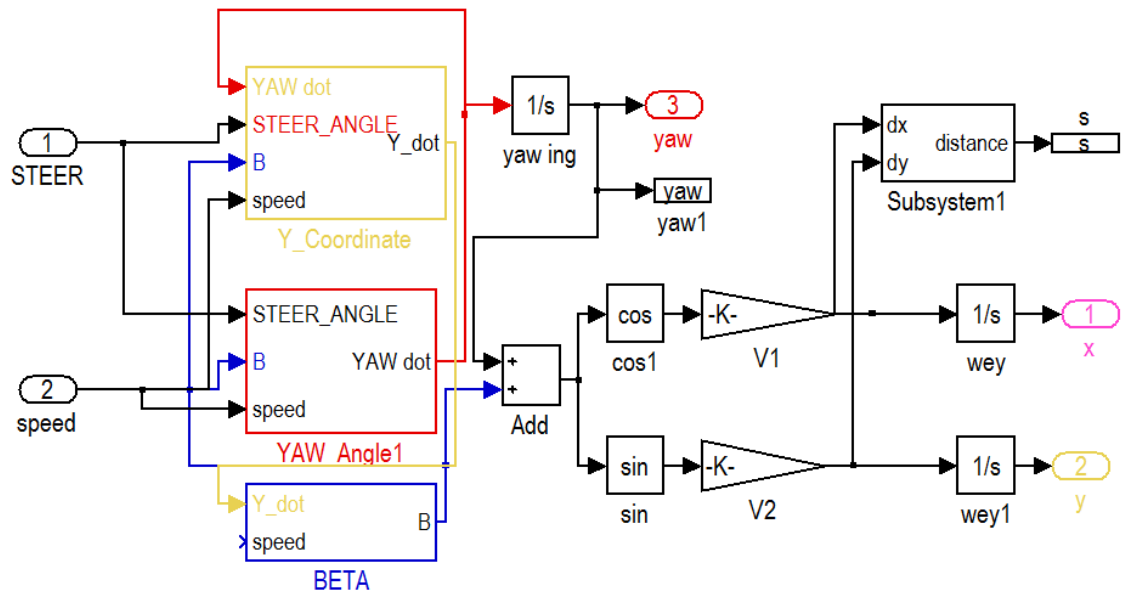
```

Appendix D: Control Loop Used in Simulations

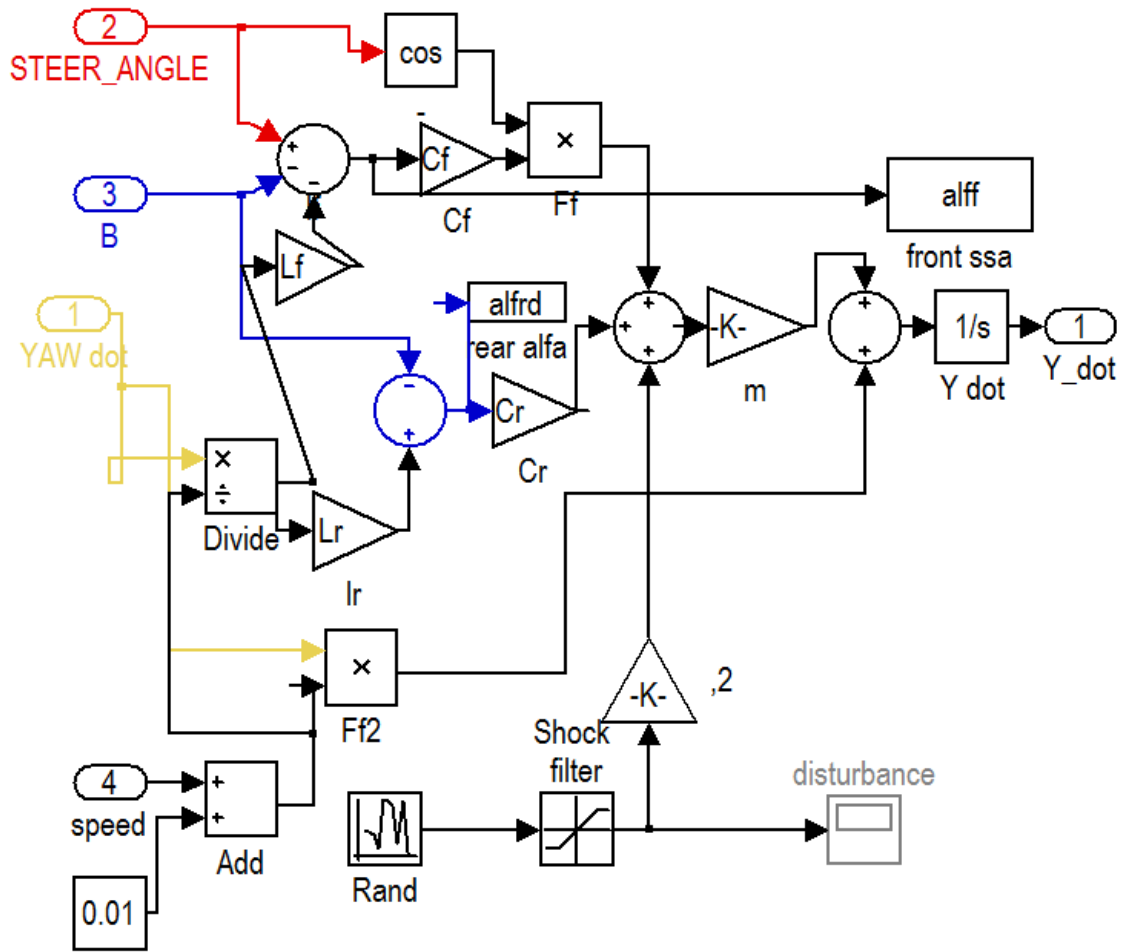


Appendix E: Dynamics Modelling in Simulation Software

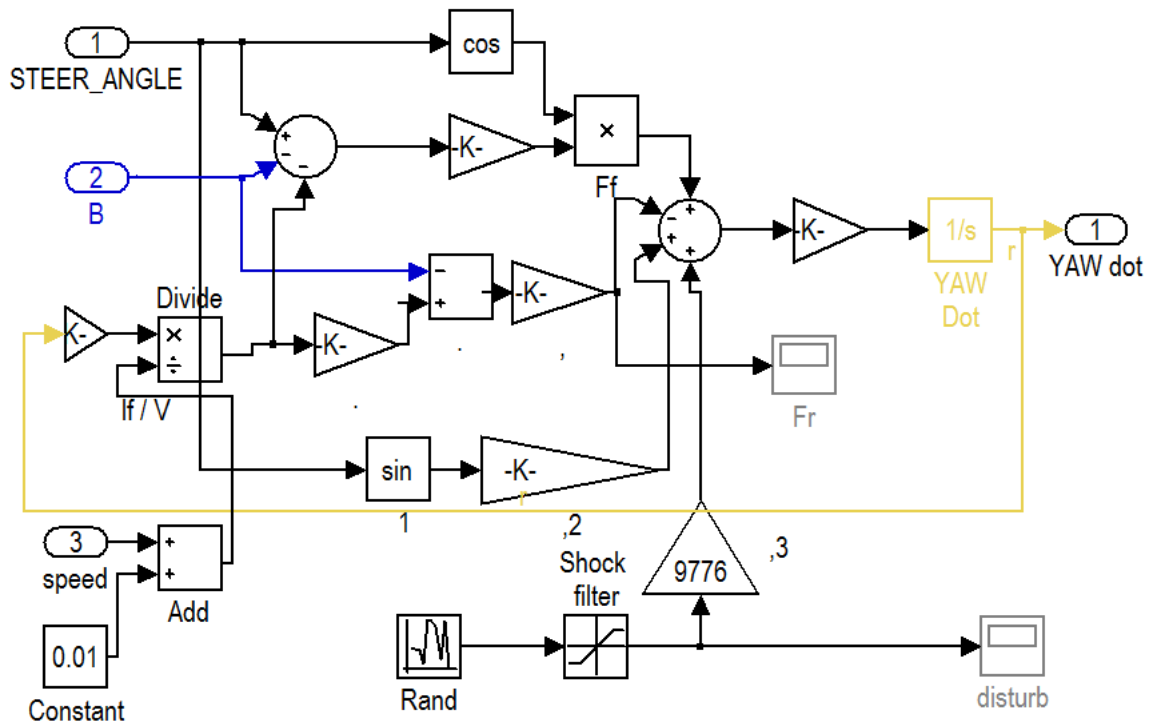
E.1 Simulink Configuration of Two DOF Model Equations



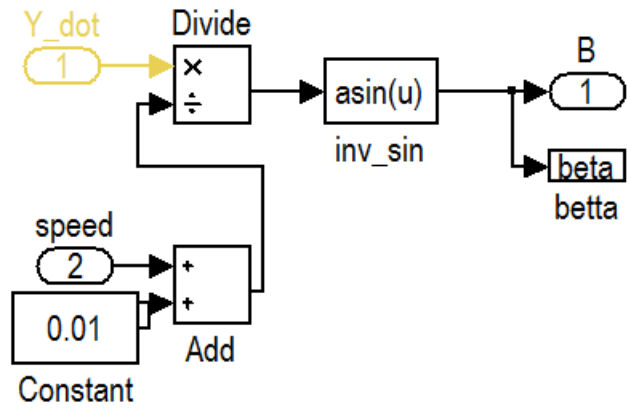
E.2 Modelling of Y-Coordinate Dynamics



E.3 Modelling of ψ -Coordinate Dynamics



E.4 Modelling of Side Slip Angle (β)



E.5 A Model of Actuator Used for Simulation Tests

